



SCHOOL OF MINES AND ENGINEERING

**MAPPING AND CHARACTERIZATION OF SOLID IRON ORE MINING WASTES
IN KISHUSHE AREA, TAITA TAVETA COUNTY, KENYA**

FRANCIS GITAU

(TU01-EM331-0021/2018)

**A THESIS SUBMITTED IN PARTIAL FULFILMENT FOR THE DEGREE OF
MASTER OF SCIENCE IN MINING ENGINEERING IN THE DEPARTMENT OF
MINING AND MINERAL PROCESSING ENGINEERING OF TAITA TAVETA
UNIVERSITY**

MAY, 2022

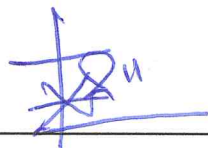
DECLARATION

This thesis is my original work and has not been presented for a Degree in any other University.

Candidate:

Francis Gitau

Signature: _____



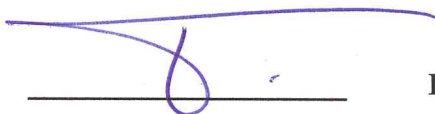
Date: _____

07/JULY/2022

Supervisors:

This thesis has been submitted to Taita Taveta University for examination with our approval as University supervisors.

Signature: _____



Date: _____

25th July, 2022

Dr. Justin Maghanga

Taita Taveta University (TTU),

P.O. Box 635 – 80300,

Voi, Kenya

Signature: _____



Date: _____

19/07/2022

Dr. Nelima Ondiaka

Taita Taveta University (TTU),

P.O. Box 635 – 80300,

Voi, Kenya

ABSTRACT

Solid mine waste management is a continuous and systematic assessment of the potential hazards, disposal, and proper utilization of waste produced in a mining company during the mining and mineral processing stages. In the mining industry, solid mine waste is generated at every stage of operation and must be disposed of properly. There is a need to understand the solid mine waste composition in depth and know the extents they cover at a mine. Solid mine wastes can affect the environment through their intrinsic properties. Therefore, proper assessment of these solid wastes is essential in waste management. This study was done at Samruddha Resources Limited Iron Ore Mines in Taita Taveta County, Kenya. The main objective of this research was to map and determine the environmental pollutants in the solid mine waste produced during iron ore mining and processing. This was achieved by utilizing geochemistry, mineralogy, Geographical Information Systems (GIS), and Remote Sensing techniques. Geochemistry and mineralogy of the solid mine wastes were determined by X-ray Fluorescence (XRF), X-ray Diffraction (XRD), and Petrographic Analysis. The extent and the volumes of the solid mine waste were mapped using GIS and Remote Sensing techniques utilizing the surface volume differencing method and Maximum Likelihood Classification (MLC) at an accuracy of 74%. XRD studies revealed Magnetite Fe_3O_4 and Hematite Fe_2O_3 were highest at 29% and 21%, respectively, with subordinate amounts of Quarts and Calcite in stockpile samples. Quartz concentration was high (43%) in waste dump samples and Berlinite (33%) and Quartz (31%) in high concentrations in the overburden samples. XRF studies indicated high amounts of iron in the stockpile (80%) and waste dump (36%). Silica was in excess of (41%). Potentially toxic elements such as Zinc, Lead, Chromium, Titanium,

Manganese, and Copper were in considerable amounts in all the samples. Petrography analysis results indicated the major minerals in the solid mine wastes to be magnetite, hematite, and quartz with traces of mica, feldspar, and biotite and intrusions of pyro garnets and olivine. The minerals are characterized by a lamellar structure with grains boundaries between individuals being mutual. It was observed that the solid mine wastes covered an estimated total area of $591,100 M^2$ with a volume of $523,237.11 M^3$. This research pointed out pollutants in the solid mine wastes and the unregulated dumping of solid mine wastes. Therefore, proper solid mine waste management can be improved by improving mining and processing methods to mitigate waste and subsequently exploit the value of these wastes.

DEDICATION

I dedicate this thesis to my parents, Mr. Henry Gitau and Mrs Zipporah Gitau, and my lovely sisters, Mary Gitau, Sally Gitau, and Liz Gitau.

ACKNOWLEDGEMENT

First and foremost, I am thankful to Almighty God for the divine grace, enablement, and endurance to complete this thesis. This research would not have been achieved without God's divine intervention and provision. All the Glory to Jesus Christ, my (our) Lord and Savior, for seeing me through to the end.

I want to extend my sincere and deserved gratitude to my supervisors, Dr. Justin Maghanga and Dr. Nelima Ondiaka, for their valuable advice, ideas, corrections, suggestions, and time at my disposal, during every step of the research. I am also indebted to the other lecturers, such as Dr. Benard Alunda and Geologist Odhiambo Ochieng, who contributed to the development of my research.

My deep appreciation goes to the Ministry of Petroleum and Mining, Madini House, Kenya, led by Madam Magdalene Wangui and Mr. Vincent Osebe, for their reception and guidance during my sample analysis.

Finally, I would like to salute Oscar Mwakughu, the former Geologist at Samruddha Resources Kenya Limited. He took time off his busy schedule to travel to the study area and walked me through the entire data collection phase and geological interpretations.

May God bless you and all the other people who were part of this journey.

TABLE OF CONTENT

| | |
|---|-------|
| Declaration..... | i |
| Abstract..... | ii |
| Dedication..... | iv |
| Acknowledgement | v |
| Table of Content | vi |
| List of Figures..... | xi |
| List of Tables | xv |
| Acronyms and Abbreviations | xvii |
| Symbols | xviii |
| CHAPTER ONE..... | 1 |
| 1. INTRODUCTION | 1 |
| 1.1. Background Information..... | 1 |
| 1.2. Problem Statement..... | 4 |
| 1.3. Justification of the Study | 5 |
| 1.4. Research Questions..... | 7 |
| 1.5. Objectives of the Study..... | 7 |
| 1.5.1. General Objective | 7 |
| 1.5.2. Specific Objectives | 7 |
| 1.6. Scope and Limitations of the Study..... | 8 |
| CHAPTER TWO..... | 9 |
| 2. LITERATURE REVIEW | 9 |
| 2.1. Global and Local Iron Ore Deposits | 9 |

| | |
|---|----|
| 2.2. Iron Ore in Kishushe | 10 |
| 2.3. Waste Generated from the Mining Life Cycle..... | 10 |
| 2.4. Iron Ore Mining and Processing | 12 |
| 2.4.1. Ore Extraction..... | 13 |
| 2.4.2. Ore Beneficiation..... | 13 |
| 2.5. Iron Ore Processing Methods..... | 14 |
| 2.6. Mining and Exploitation of Minerals in Kenya | 15 |
| 2.7. Mine Wastes..... | 16 |
| 2.8. Characterization of Iron Ores..... | 18 |
| 2.9. Analytical Techniques..... | 19 |
| 2.9.1. Geochemistry and Mineralogy Techniques | 19 |
| 2.9.2. Mine Wastes Geochemistry and Mineralogy | 19 |
| 2.10. GIS and Remote Sensing Techniques..... | 21 |
| 2.10.1. Volumes and Areal Extent Estimate of Solid Waste Dumps using GIS and Remote Sensing Methods..... | 21 |
| CHAPTER THREE | 24 |
| 3. METHODOLOGY | 24 |

| | |
|--|----|
| 3.1. Study Area | 24 |
| 3.1.1. Methodology Workflow | 26 |
| 3.2. Determination of Environmental Pollutants due to Iron Ore Mining and Processing Operations at the Samruddha Resources Kenya Limited Iron Ore Mine | 27 |
| 3.2.1. Identification of Solid Iron Ore Mining Wastes | 27 |
| 3.3. Quantification of the Extent and Volume of Solid Mine Wastes from Samruddha Resources Kenya Limited Mine..... | 32 |
| 3.3.1. Data Extraction | 32 |
| 3.3.2. Data Processing | 33 |
| 3.3.3. Solid Mine Waste Extents Mapping | 35 |
| 3.3.4. Waste Volume Quantification | 35 |
| 3.4. Determination of the Geochemistry and Mineralogy of Solid Mine Wastes from the Study Mine..... | 37 |
| 3.4.1. Collection of Samples..... | 37 |
| 3.4.2. Preparation Of Samples | 40 |
| 3.4.3. Properties of Solid Mining Wastes | 43 |
| CHAPTER FOUR | 46 |
| 4. RESULTS AND DISCUSSION..... | 46 |

| | |
|--|----|
| 4.1. Environmental Pollutants Resulting from Iron Ore Mining and Processing Operations at the Study Mine | 46 |
| 4.1.1. Secondary Data on Environmental Pollutants from Iron Ore Mining Activities in Kishushe Area | 46 |
| 4.1.2. Mining Activities At Samruddha Resources Kenya Limited Mine..... | 49 |
| 4.2. The Extent and Volume of Dumps and Stockpiles of Solid Mining Wastes at the Study Mine | 57 |
| 4.2.1. Solid Mine Waste Extents | 57 |
| 4.2.2. Accuracy Assessment..... | 61 |
| 4.2.3. Volumes of Solid Mine Waste Dumped..... | 62 |
| 4.3. Properties Of Solid Mine Wastes From The Study Mine | 66 |
| 4.3.1. Chemical Elements And Compounds..... | 66 |
| 4.3.2. Mineral Composition..... | 72 |
| 4.3.3. Mineral Crystallization..... | 82 |
| CHAPTER FIVE | 90 |
| 5. CONCLUSION AND RECOMMENDATIONS | 90 |
| 5.1. Conclusion | 90 |

| | |
|---|----|
| 5.1.1. Environmental Pollutants Resulting From Iron Ore Mining and Processing Operations at the Study Mine..... | 90 |
| 5.1.2. The Extent and Volume of Dumps and Stockpiles of Solid Mining Wastes at the Study Mine | 91 |
| 5.1.3. Properties of Solid Mining Wastes | 91 |
| 5.2. Recommendations..... | 92 |
| 5.3. Recommendations for Further Study..... | 93 |
| References..... | 94 |
| Appendices | I |

LIST OF FIGURES

| | |
|---|----|
| Figure 2-1: Wet screening | 14 |
| Figure 2-2: Dry screening..... | 15 |
| Figure 2-3: Waste stream in mining industry | 17 |
| Figure 3-1: Map of the study area..... | 25 |
| Figure 3-2: Complete workflow | 26 |
| Figure 3-3: Flowsheet for systematic literature review | 28 |
| Figure 3-4: Elevation profile of iron ore stockpile in google earth | 33 |
| Figure 3-5: Data processing workflow | 33 |
| Figure 3-6: Model for volume computation | 36 |
| Figure 3-7: Stratified sampling design | 38 |
| Figure 3-8: Location where samples were collected. Source: image; (google earth)..... | 39 |
| Figure 3-9: Solid waste samples preparation..... | 40 |
| Figure 3-10: XRF equipment..... | 41 |
| Figure 3-11: Diamond saw cutter | 42 |
| Figure 3-12: Sectioning plate (30 microns)..... | 43 |

| | |
|---|----|
| Figure 3-13: Polished sample ready for analysis | 43 |
| Figure 3-14: XRD equipment | 44 |
| Figure 3-15: Photograph of the fein optic polarized light microscope r40pol-rt..... | 45 |
| Figure 4-1: Systematic literature review procedures | 47 |
| Figure 4-2: Literature reviewed..... | 49 |
| Figure 4-3: Relief map of the area surrounding the study area | 50 |
| Figure 4-4: Overburden material from blasting operation piled near the open pit..... | 52 |
| Figure 4-5: Overburden material as a result of the extraction of alluvial iron ore | 53 |
| Figure 4-6: Screened non-magnetic material both from the alluvial and reef..... | 53 |
| Figure 4-7: Screened iron ore ready for shipping | 54 |
| Figure 4-8: Iron ore fines (circled in red) stockpiled near the plant..... | 54 |
| Figure 4-9: Map of the sample location in the study area | 56 |
| Figure 4-10: Mine wastes at samruddha resources kenya limited iron ore mine; a. Overburden material, b. Waste dump, c. Stockpiled iron ore fines, and d. Waste rock dump..... | 60 |
| Figure 4-11: Overburden material at the sides of the active open pit..... | 60 |
| Figure 4-12: GPX point features overlaying stockpiles | 61 |

| | |
|---|----|
| Figure 4-13: Solid mine waste map | 64 |
| Figure 4-14: Graph of major elements and error bars of the s.e for waste dump samples | 67 |
| Figure 4-15: Graph of minor elements and error bars of the s.e for waste dump samples | 67 |
| Figure 4-16: Graph of major elements and error bars of the s.e for stockpile samples | 69 |
| Figure 4-17: Graph of minor elements and error bars of the s.e for stockpile samples | 69 |
| Figure 4-18: Graph of major elements and error bars of the s.e for overburden samples | 71 |
| Figure 4-19: Graph of minor elements and error bars of the s.e for overburden samples | 71 |
| Figure 4-20: Phase graph of waste dump sample 1 | 73 |
| Figure 4-21: Phase graph of waste dump sample 2 | 74 |
| Figure 4-22: Phase graph of waste dump sample 3 | 75 |
| Figure 4-23: Phase graph of stockpile (sp 1) sample 1 | 76 |
| Figure 4-24: Phase graph of stockpile (sp 2) sample 2 | 77 |
| Figure 4-25: Phase graph of stockpile (sp 4) sample 4 | 78 |
| Figure 4-26: Phase graph of overburden material (ob2) sample 2 | 79 |
| Figure 4-27: Phase graph of overburden material (ob3) sample 3 | 80 |
| Figure 4-28: Phase graph of overburden material (ob4) sample 4 | 81 |

| | |
|---|----|
| Figure 4-29: Thin section of waste dump sample in ppl | 83 |
| Figure 4-30: Thin section of stockpile sample 2 in x.p.l | 84 |
| Figure 4-31: Thin section of stockpile sample 3 in x.p.l | 85 |
| Figure 4-32: Thin section of stockpile 1 (s.p. 1) in ppl | 85 |
| Figure 4-33: Thin section of overburden material (o.b. 4) in x.p.l..... | 86 |

LIST OF TABLES

| | |
|--|----|
| Table 3-1: Search criteria..... | 29 |
| Table 3-2: article selection criteria | 30 |
| . Table 3-3: Rating criteria of kappa statistics | 35 |
| Table 3-4: Summary of samples collected..... | 39 |
| Table 4-1: Summary of information on iron ore mining activities..... | 48 |
| Table 4-2: Attribute table for par pixel areal coverage..... | 58 |
| Table 4-3: Areas of solid mine waste extents..... | 58 |
| Table 4-4: confusion matrix..... | 62 |
| Table 4-5: Volumes of solid mining wastes | 62 |
| Table 4-6: Area and volume of solid mine waste | 63 |
| Table 4-7: Elements and compounds in the solid waste dumps samples | 66 |
| Table 4-8: Elements and compounds in the stockpiles samples..... | 68 |
| Table 4-9: Elements and compounds in the overburden samples..... | 70 |
| Table 4-10: Mineralogical composition of wd 1 | 73 |
| Table 4-11: Mineralogical composition of wd 2 | 74 |

| | |
|---|----|
| Table 4-12: Mineralogical composition of wd 3 | 75 |
| Table 4-13: Mineralogical composition of sp 1..... | 76 |
| Table 4-14: Mineralogical composition of sp 2..... | 77 |
| Table 4-15: Mineralogical composition of sp 4..... | 78 |
| Table 4-16: Mineralogical composition of ob | 79 |
| Table 4-17: Mineralogical composition of ob 3 | 80 |
| Table 4-18: Mineralogical composition of ob 4 | 81 |

ACRONYMS AND ABBREVIATIONS

| | |
|------|-------------------------------------|
| AAS | Atomic Absorption Spectrophotometer |
| GIS | Geographic information system |
| GPS | Global positioning system |
| Km | Kilometers |
| LULC | Land use land cover change |
| M | Meters |
| MLC | Maximum likelihood classification |
| PPL | Plane polarized light |
| RS | Remote sensing |
| SLR | Systematic literature review |
| SRKL | Samruddha resources kenya limited |
| UAV | Unmanned aerial vehicle |
| UTM | Universal transverse mercator |
| XPL | Cross polarized light |
| XRD | X-ray powder diffraction |
| XRF | X-ray fluorescence |

SYMBOLS

β

Beta

θ

Theta

CHAPTER ONE

1. INTRODUCTION

1.1. Background Information

Mining is an extractive industry that plays a significant role in world economic development (Wilson, 2019). Iron ore deposits, which provide raw materials for iron making, are widely scattered worldwide under diverse geological settings (Festin et al., 2019). Among iron oxides mined, magnetite and hematite are primary inputs in iron making (Singh et al., 2018). The consumption of steel globally shows an exponential increase, whereby 98% of iron consumed globally is used to produce steel products (Roy et al., 2020). Iron ore deposits worldwide are estimated at 800 billion tons of raw ore containing around 200 billion tonnes (Kuranchie, 2015). The highest iron ore producers are Australia, Brazil, China, and India, producing 70% of the world, with South Africa the leading iron ore producer in Africa at 4% (U.S. Geological Survey, 2021). China consumes 25% of all iron ore produced globally, approximately 800 million tonnes (Ericsson et al., 2021). The most significant Africa iron ore consumers are the United States of America, China, India, and Japan accounting for 80% of total iron ore produced (U.S. Geological Survey, 2021). According to Ericsson et al. (2021), Kenya's iron ore exports totaled 7.93 million dollars, and the main market is China. 80% of iron ore produced in Kenya goes to the export market, whereas the remaining 20% is locally used to produce cement, pigments, and other chemicals (Cheneket, 2018).

There are three broad stages of mining operations for metallic minerals. The first operation is the exploitation of a mineral resource or ore deposit to extract minerals from in-situ locations

of the earth (Vajda et al., 2016). The second operation is mineral processing, the beneficiation of the ore dressing process that separates minerals from rock and other fragment materials to concentrate a mineral of interest (Dauce et al., 2019). The third operation is the metallurgical extraction process to recover refined products from mineral concentrates (Lottermoser, 2011).

The mining industry is known to cause significant environmental degradation and pollution (Kakaie et al., 2019). This is due to various wastes produced at the different stages of mining operations. At active mine sites, mining and mineral processing operations such as drilling, blasting, crushing, grinding, magnetic or gravity separation, and flotation (Ferreira and Leite, 2015) and metallurgical operations, such as roasting and leaching (Lottermoser, 2011) result in the generation of gaseous, liquid, and solid mining wastes. During iron ore beneficiation in the blast furnace, carbon dioxide is produced as waste during the reduction process. Effluent from processing plants forms the liquid wastes produced, and solid wastes emerge from iron ore mining and processing, such as dust, sludge, slags, mill scale, and waste rock and soil (Dutta, 2020).

Iron, an abundant earth element, averages 3% in sedimentary rocks and 8.5 % in gabbro and basalt, ranking as the fourth most abundant element in the earth's crust (Yellishetty et al., 2010a). Iron ore occurs as Magnetite (Fe_3O_4), Goethite ($FeO(OH)$), and Hematite (Fe_2O_3) (Shrimali et al., 2016). Globally, iron ore is a crucial commodity in industrialization that has been continuously sought through mining (Ferreira and Leite, 2015). In the recent past, iron ore has been extracted from sedimentary rocks in different parts of the world over a long period (Lascelles, 2011).

The mining and extraction of iron ores from deposits generate tons of waste, occupying large tracts of land worldwide (Assawincharoenkij et al., 2017); (Wu et al., 2019)). The wastes produced during iron ore mining and processing contain various gangue minerals such as carbonates, hydroxides, silicates, and sulphates (Lottermoser, 2011; (Bastos et al., 2016); (Assawincharoenkij et al., 2017); (Joseph et al., 2018); (Akoto and Anning, 2021)).

Iron Ore mining activities have been linked and associated with the enrichment of various chemical elements in soils, water resources contamination, and environmental degradation (Gleekia, 2016). The minerals' surface area increases during iron processing, increasing and accelerating chemical weathering and oxidation, mobilizing various metals and contaminants to the environment (Colburn and Thorntorn, 2014). The dumping of iron tailings poses a significant risk whereby the increased concentration of these toxic chemical elements in these wastes end up in the environment (Ochieng et al., 2010).

Mining is also an apparent cause of land cover degradation (Munyao et al., 2012). To eliminate and possibly mitigate the environmental effects of mining different mineral resources, very close analysis and evaluation of the degree of hazards and extent based on constant assessment within a spatial framework are essential (Mwakumanya et al., 2016).

Kenya is well endowed with iron ore deposits (Cheneket, 2018). Bett et al. (2016) opine that significant iron ore deposits have been found in Tharaka Nithi County at Marimanti, Kitui County at Ikutha, Homa Bay, and Kishushe area in Taita Taveta County. Mining iron ore in the Kishushe area of Taita Taveta County has resulted in environmental degradation and pollution, posing a threat to air and water quality, affecting soil composition, and changing the land cover due to mining wastes produced (Cheneket, 2018). Moreover, the enrichment of

agricultural soils with metal elements and other chemical compounds directly affects the ecosystem and negatively impacts humans and wildlife (Maranga et al., 2013).

This study was carried out at an iron ore mine operated by Samruddha Resources Kenya Limited in Kishushe area of Taita Taveta County. This research investigated the environmental pollutants resulting from iron ore mining and mineral processing at SRKL mine. Thereafter the extent and the volumes of these solid mine waste were determined. Finally, the geochemistry and the mineralogy of the solid wastes resulting from mining and processing operations were determined using analytical techniques.

1.2. Problem Statement

Open-pit mining and mine development operations generate mine wastes such as waste rocks, spoils, overburden, atmospheric particulate emissions, and mine water (Ferreira and Leite, 2015). Moreover, mineral processing activities produce various processing wastes such as tailings, stockpiles of low-grade materials, sludge, milling water, and atmospheric emissions (Meehan, 2012).

The physical and chemical properties of mine wastes might vary owing to the geochemistry of the iron ore, the size of the crushed mineral particles, materials handling method, drilling and blasting techniques utilized, and the processing technology used (Amos et al., 2015; Jamieson et al., 2015; Jelenová et al., 2018). Seventy percent of material handled at active mines is waste whose geochemical properties are equivalent to the mined ore (Heather E Jamieson, 2011). Most environmental challenges from mining activities are associated with the capability of waste to react chemically with water and air (Heather E Jamieson, 2011). The most significant

sulfide minerals produced during iron ore mining include pyrite (FeS_2), galena (PbS), sphalerite (ZnS), and chalcopyrite ($CuFeS_2$) (Wu et al., 2019). According to Nordstrom, (2011), drainage chemistry is influenced by oxidative reactions of iron sulfide minerals such as pyrite, which generate acid and various sulfate compounds. Mining activities are one of the major drivers of land use and land cover changes resulting in large tracts of land being converted from vegetation covers to open pits, overburden dumps, and wastelands, leading to biodiversity loss (Khan, 2016). Studies by Basommi et al. (2015) revealed a decrease in normalized difference vegetation index for a mining area in Wa East in Ghana attributed to the reduction of vegetation cover.

Therefore, the characterization of solid mine waste produced during iron ore mining and processing for any mine is critical to predicting and monitoring various environmental impacts and coming up with remediation plans. This research aims at mapping and characterizing the solid mine wastes produced during iron ore mining and processing operations at the study mine.

1.3. Justification of the Study

Overman and Overman (2011) opine those rapid global changes introduce new challenges in protecting and conserving the environment. Thus, there is a need for scientific data to understand pollutants from mining wastes that contaminate environmental partitions: soil, water, and air.

The tendency of solid mine wastes to produce pollutants that affect the environment motivated this study. According to Jamieson (2011), the characterization of solid mine waste from

various mine sites in Nova Scotia, Canada, utilizing their geochemistry and mineralogical properties, provided essential knowledge to predict environmental impacts. Mineralogical and geochemical properties of tailings from a mine in Thailand were evaluated to determine the potential of acid mine drainage (AMD) and toxic elements to be released into the environment. Studies done by Finders Mines (2012) on solid mine waste and tailings utilizing geochemical characterization using the XRF method revealed infiltration of toxic elements into the soil and water, resulting in acid mine drainage. Kiptarus et al. (2015) performed a characterization on selected samples of iron ore at Mwingi in Kenya to gain knowledge on their status: their detailed studies were done using XRD, XRF, AAS, and Petrographic microscopic techniques. However, the studies on the characterization of various minerals and wastes have limitations. Rarely is one method enough to deeply characterize minerals in the solid mine wastes in instances where multiple hosts are present. Various techniques to perform characterization need to be done at a micrometer scale, usually using analytical methods.

With the increase in Iron ore mining at SRKL Iron Ore Mine, the production of solid mine wastes has increased immensely. However, there are many studies on these solid mine wastes produced during iron ore mining and processing. Therefore, this research sought to map the extents, estimate the volumes, and characterize the solid mine waste produced at the study mine.

1.4. Research Questions

1. What are the environmental pollutants resulting from iron ore mining and processing at SRKL mine?
2. What are the extents and volume of solid mine waste at SRKL mine?
3. What are the geochemistry and mineralogical properties of solid mine waste at SRKL mine?

1.5. Objectives of the Study

1.5.1. General Objective

The overall objective is to determine the environmental pollutants in solid mining wastes generated from iron ore mining and processing at Samruddha Resources Kenya Limited Iron Ore Mine, Kishushe in Taita Taveta County.

1.5.2. Specific Objectives

1. To establish the environmental pollutants from iron ore mining and processing operations at Samruddha Resources Kenya Limited Iron Ore Mine.
2. To quantify the extent and the volume of solid mine wastes generated from iron ore mining and processing activities at the study mine.
3. To determine the geochemistry and mineralogy of the solid mine wastes from the study mine.

1.6. Scope and Limitations of the Study

This research mainly focused on mapping and characterizing solid mine wastes produced during iron ore mining and processing at the Samruddha Resources Kenya Limited Iron Ore Mine (SRKL). The mine is located in Kishushe Area, Wundanyi Sub County. This research aimed to determine the areal extents, volume estimates, geochemistry, and mineralogy of these solid mine wastes.

Due to the unavailability of resources, dust and water samples were not sampled for analysis. Only solid mine wastes were considered in this research.

CHAPTER TWO

2. LITERATURE REVIEW

This chapter contains literature that is pertinent to this research. It gives a perspective of iron ore mining globally and locally, including the wastes that are likely to be produced during the mining and processing of the iron ore. Finally, it presents various analytical methods that have been used to determine both the elemental composition and the structure of the elements present in the waste. Additional areas covered in this section include various GIS and Remote Sensing methods used to quantify the areal extents and volumes of stockpiles.

2.1. Global and Local Iron Ore Deposits

Iron ores are rocks and minerals from which iron is economically extracted (Kuranchie, 2015). These ores are usually rich in iron oxide and vary in color from rusty red, deep purple, and dark grey and are generally found in the form of goethite, magnetite, and or hematite. (Yellishetty et al., 2010b). Iron ores mainly occur as magmatic and banded iron formations consisting of alternating layers of iron oxides and iron-poor chert (Bett et al., 2014). Iron ore consumed in the steel industry needs to have more than 60% iron content, whereas those with less concentration need to be beneficiated (Dutta, 2020). The most mined iron ore globally is magnetite, currently mined extensively in Brazil and China providing raw materials for iron-ore industries majorly in Australia (Mohr et al., 2015). Notable iron ore deposits are present in Chile formed from volcanic flows with significant phenocrysts and some alluvially accumulated deposits (Sadeghi et al., 2015). With notable exceptions of countries such as Brazil and Australia, most iron ore produced by the other countries are low grade and requires

to be beneficiated to be usable (Kuranchie, 2015). China is the world-leading producer and consumer of iron ore at 19% in a market that is not well fulfilled, thereby creating a high demand for iron ore globally (National Minerals Information Center, 2017). In Kenya, intensive exploration of iron ore is taking place, with active mining of iron ore being done on large and small scales at Kishushe and Ikutha (Kiptarus et al., 2015). Iron ore deposits have been discovered in various places, with viable economic deposits existing as alluvial deposits and banded iron formations (Bett et al., 2014). However, the Iron ore deposits at Taita Taveta County are associated with the geological zone rich in industrial minerals, the Mozambique Belt (Bett et al., 2016). The iron ore deposits found at Kishushe, Taita Taveta County, are mainly magnetite and hematite, occurring as magmatic intrusive and alluvial deposits (Maranga et al., 2013).

2.2. Iron Ore in Kishushe

The iron ore mined by SRKL in Kishushe is a medium grade (<65% *Fe*) deposit, which occurs basically in two forms, alluvial deposits and reef form (G. Bett et al., 2014). The alluvial deposits result from collisional tectonics, including uplifting, shearing, folding, and brecciation (Peter et al., 2015). As a result of large forces due to tectonics, the iron ore-rich veins were fragmented, creating the brecciated segments on the mineral veins, and iron ore upthrowing resulted in the alluvial deposit of iron ores (Peter et al., 2015).

2.3. Waste Generated from the Mining Life Cycle

Different phases define any mining project (Ferreira and Leite, 2015). The stages include minerals prospecting, exploration, mine development, mineral exploitation, and mine

reclamation (Vajda et al., 2016). Mineral prospecting and exploration are usually combined as related precursor phases to actual mining (Vajda et al., 2016). Likewise, mine development and minerals exploitation phases are closely related and constitute the actual mining of minerals (Vajda et al., 2016). Mining activities in the various phases significantly contribute to the production of solid mine wastes (Lottermoser, 2003). If not well managed, these may result in various environmental degradation (Lottermoser, 2003). Thus, reclamation is a post-closure phase after the mine life where the degraded land is restored to a natural and economically usable state (Mwakumanya et al., 2016). Each of the mining phases is associated with waste production and may result in environmental impacts.

The method used during prospecting may favorably contribute to waste production. During mineral exploration, the ecosystem is altered, water and soil are polluted, and emission of various gasses are released into the atmosphere (Harraz, 2009).

During mine development, various wastes from overburden stripping are produced. Air quality is also compromised by the release of particulate matter and toxic gases during blasting operations and fuel combustion in mining machinery.

At the exploitation stage, characteristics of the mineral deposit and constraints of technology, safety, economics, and environmental concerns determine the most appropriate mining method (Harraz, 2009). The main mining methods utilized in extracting minerals are surface, including mechanical excavation using an open cast, and underground mining methods (Groves and Santosh, 2015). Environmental impacts from mineral exploitation include contamination from mining waste, fuel combustion emissions, sound pollution from drilling and blasting

explosions, transportation, and mineral processing. Chemical contaminants are leached from the mining wastes and affect the soil and water resources.

Reclamation is the final phase of mining where a mine is decommissioned, closed, mined areas recontoured and revegetated, and the water quality restored. This important mining phase requires careful pre-planning before mining operations commence (Bassi, 2015). Solid waste from opencast mines is treated and restored, recontoured, and various drainage control measures and landscaping (Geelani et al., 2016).

2.4. Iron Ore Mining and Processing

Iron ore is mined almost exclusively using surface operations, with the surface mining methods predominantly being open pit and open cut mining methods (Festin et al., 2019). However, there are also various cases of iron mining utilizing underground mining methods (Maranga et al., 2013). Either the proximity of the ore body and geology is one of the ways the decision to use underground or surface mining method is reached (Lindsay et al., 2015).

Surface mining methods are designed to extract minerals from the surface where the overburden is removed to expose the ore deposit sought (Peter et al., 2015). The ore is mined progressively in open pits along with benches (Sikaundi, 2015). Depending on the hardness of the ore, drilling and blasting may be done. Following drilling and blasting, the fractured ore is loaded by front-end loaders onto large dumper trucks for further processing. The open pits in the surface mines are gradually enlarged until the ore is exhausted or until the stripping ratio changes (Overman, 2011). When the situation happens, the mines with depleted resources may

be abandoned or converted to landfills, where solid waste from the mine is disposed of (Suleman and Baffoe, 2017).

The high impacts of surface mining methods on the environment make it debatable and controversial due to the massive amounts of mine waste produced. There are evident issues of biodiversity loss, land degradation, and various pollution forms, including soils and water sources.

2.4.1. Ore Extraction

After the overburden has been removed, mineral extraction begins using various mechanical equipment that hauls and transports the ore to the processing plants. Considerable amounts of solid waste are generated during this process. During this process, various felt environmental impacts such as particulate matter emissions and environmental pollution should be carefully evaluated and assessed (Liu et al., 2019).

2.4.2. Ore Beneficiation

Though the ores contain high levels of required mineral metals, a large quantity of waste is generated. Most ores, such as copper, have a tiny percentage of the metal needed in the ore, requiring careful separation of the small amounts of the wanted metal from the unwanted metallic or non-metallic material (Liu et al., 2019). Beneficiation, where ore is reduced in size and gangue separated from the ore, does this (Rea et al., 2015).

Milling is one of the most common methods utilized in beneficiation though it is very costly (Ferreira and Leite, 2015). However, contaminants are released and become tailings.

Beneficiation includes physicochemical techniques such as; magnetic separation, electrostatic separation, chemical separation, leaching, flotation, amalgamation, and precipitation (Chen et al., 2015). Various waste generated from these methods include tailings, waste rock dumps, dump leach, and heap leaches (Wei et al., 2018).

2.5. Iron Ore Processing Methods

Iron ore processing mainly depends on the optimum product and the type of runoff mine ore feed (Sarvamangala et al., 2012). For high flaky ores and iron dust, dry screening into fines and lumps are utilized because if wet processing was used, and good quality iron minerals are rejected in the form of slime (Sarvamangala et al., 2012). Dry screening also allows for sintering at a later stage in processing, which is a crucial advantage (Sarvamangala et al., 2012).

Iron ores have gangue materials that adhere strictly to the valuable minerals to be subjected to classification or wet screening, as shown in Figure 2-1. This separation produces waste.

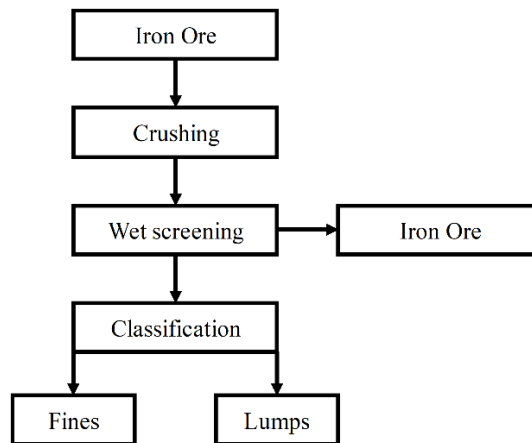


Figure 2-1: Wet screening

Dry screening shown in Figure 2-2 is also utilized for ores directly mined from the mine pit and benches (Sarvamangala et al., 2012).

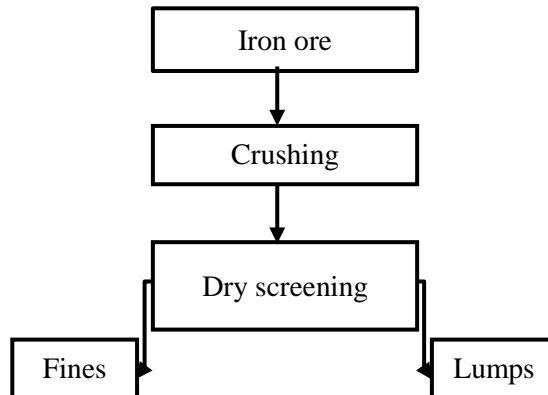


Figure 2-2: Dry screening

Dry screening contributes mainly to most of the mine wastes and harmful emissions in the form of solid wastes, dust, and particulate matter.

For iron ore to be further processed or used in blast furnaces, the ores should be grades above 65% of iron (Maranga et al., 2013). The resulting ore grades of iron ore below 65% are usually upgraded and beneficiated to maximally achieve the desired grade to produce very standard products (Krumbein, 2016). During both wet and dry screening, different processes produce wastes, which have become an enormous menace to the environment due to waste produced.

2.6. Mining and Exploitation of Minerals in Kenya

Ores and minerals play a significant role in the economic stability of the world (Muwanguzi et al., 2012). Specifically, iron ranks first among the metals in worldwide consumption (Maranga et al., 2013). There is a need for industrialization in Kenya as stipulated in the Vision 2030, sustainable development goals (SDGs), and the recently adopted Big Four Agenda

(Government of Kenya - GoK, 2019). The extractives sector contributes approximately 1% to Kenya's GDP, with base metals taking the lion's share; however, with the increase in exploration of minerals such as iron ore and rare earth metals, this is estimated to grow as much as 10% (IHRB, 2019). Although industrialization plays a key and strategic role in all countries' economic development, these industries pose a significant threat to the environment in terms of emissions and pollution. Mineral ores require extraction and processing to separate them from other gangue minerals and impurities (Bett et al., 2014).

SRKL operates the mine that Wanjala Mining Company Limited previously owned (Bett, 2018). After clearing the vegetation and removing the overburden, the deposit is blasted and hauled to the processing plant. The blasted ore is then introduced into a jaw crusher through a hopper. The jaw crusher reduces the iron ore to sizes less than 100 millimeters, fed to the vibrating screen. The 10 mm to 0 mm iron ores are conveyed directly to the magnetic separators. Iron ores above 50 mm ores are fed into the cone crusher, while ores less than 10 mm in size are separated magnetically using magnetic drums where iron ore fines are collected (Maranga et al., 2013). Highly magnetic iron ore is transported to the port of Mombasa for export. The non-magnetic rocks (mainly quartz and calcite) are dumped as waste. The iron ore fines are stockpiled near the processing plant (Cheneket, 2018). During the iron ore beneficiation cycle, the non-magnetic fines and boulders are moved to waste dumps.

2.7. Mine Wastes

Mine wastes constitute the largest percentage of waste produced by various industrial activities (Lottermoser, 2011). Mining wastes are sub-economic materials containing low cutoff grades or no ore mineral in mining and mineral processing operations.

Mining operations, metallurgical extractions, and mineral processing produce solid wastes. These may be generated in different processes during mining, mineral processing, and metallurgical operations, as shown in Figure 2-3.

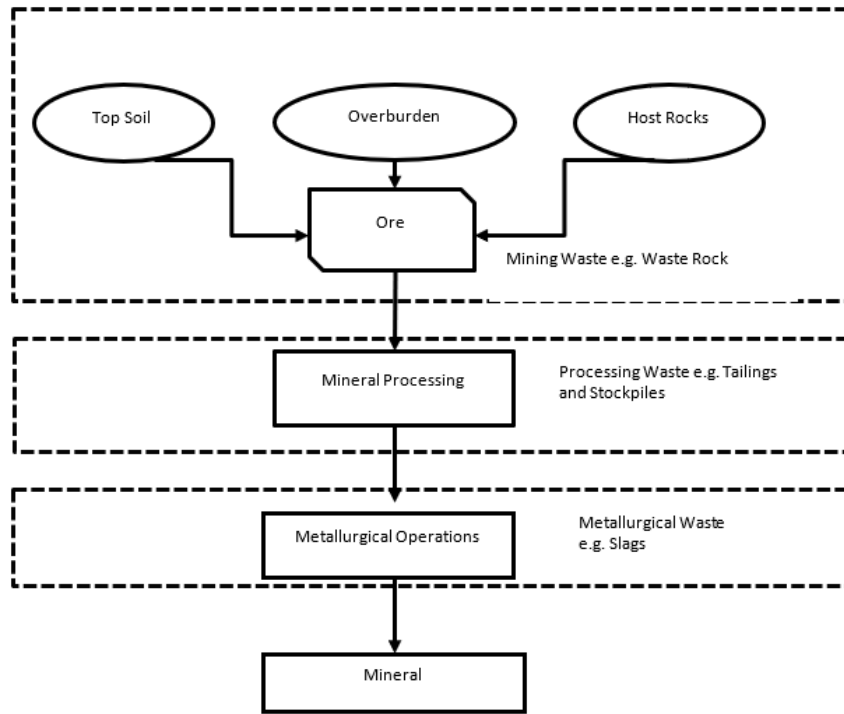


Figure 2-3: Waste stream in mining industry

During open pit mining and development, various mine wastes such as waste rocks, spoils, overburden, atmospheric emissions, and mine water may be generated. Mineral processing activities produce various processing wastes such as tailings, stockpiles of lower grade materials, sludges, milling water, and emissions. Consequently, metallurgical wastes such as leached ores, processing water, emissions, flue dust, and roasted ores may be produced during the last phase of metallurgical operations.

The chemical and physical characteristics of mine wastes may vary in relation to the geochemistry and mineralogy of the resource, the size of the crushed mineral particles, processing chemicals, materials handling method, method and type of blasting techniques utilized, and the processing technology used.

2.8. Characterization of Iron Ores

Iron oxide ores are the primary source of most iron, whereas some ores are a mixture of various minerals rich in iron (Aznar-Sánchez et al., 2018).

Characterization of ores includes but is not limited to the quantity, grade, quality, densities, shape, mineralogy, and physical and chemical properties. Muwanguzi et al. (2012) highlight that it is crucial to understand an ore or mineral's main inherent properties and composition as they determine their behavior during processing. Furthermore, the characteristics of minerals also often determine the economic aspect of commercial exploitation and processing of deposits. Significantly, the characterization of the ores differs from the location of the deposits.

Three broad types of oxidic iron ores occur naturally, dependent on the concentration of iron and oxygen in the given compound. The types are as follows

- i. Iron II oxide (FeO) – its mineral ore form is known as wustite
- ii. Iron III oxide (Fe_2O_3) - naturally, as the mineral hematite
- iii. Iron II, III oxide (Fe_3O_4) – its mineral form is called magnetite

2.9. Analytical Techniques

2.9.1. Geochemistry and Mineralogy Techniques

Geochemistry and mineralogy techniques utilizing methods such as atomic absorption spectrometry, optical petrography, X-Ray Fluorescence, X-ray diffractometry, and scanning electron microscopy with energy dispersive spectroscopy are used to assess and determine solid waste characteristics (Roller, 2011; Assawincharoenkij et al., 2017; Aznar-Sánchez et al., 2018; Modabberi, 2018)

The X-ray diffraction (XRD) is used to evaluate and analyze powdered solid materials through a diffraction pattern developed after electrons oscillate in the alternating electromagnetic field of the same frequency in the field. The diffracted beam composed of scattered rays that reinforce one another plays the role of analyzing the elements in a sample (Roller, 2011). XRD analysis was done to analyze the structure of the samples to give the mineralogical constituents in the samples. An X-ray fluorescence (XRF) spectrometer is an x-ray instrument used for non-destructive chemical analyses of minerals, rocks, or sediments working on wavelength-dispersive spectroscopic principles (Brouwer, 2010).

2.9.2. Mine Wastes Geochemistry and Mineralogy

Large volumes of solid waste and mine tailings are dumped at the mine site (Jamieson, 2011). Prediction and determination of the environmental impacts of these mine wastes require an in-depth understanding of the characteristics of the material (Jamieson, 2011). Studies were done at a Gold mine in Thailand by Assawincharoenkij et al. (2017) in mine waste characterization using XRF. XRD analysis revealed the crystalline structure of the minerals present in the solid

waste had the potential to generate acid mine drainage (AMD). According to Nordstrom (2011), drainage chemistry results from iron sulfide minerals oxidation such as pyrite, whose reaction generates acidity and various sulfates to release metal elements such as Copper, Cadmium, Lead, and Zinc. Nordstrom (2011) further explained that carbonate minerals neutralize the drainage, but toxic elements such as selenium and arsenic may be available in very high amounts.

Mineralogy and XRF analysis done on waste samples at Muteh Gold Deposit in Iran to investigate mineralogical and geochemical characteristics of waste revealed high concentrations of Zinc & Copper and high amounts of pyrite minerals that were an environmental concern (Modabberi, 2018).

Geochemistry and mineralogical studies done at a metal mine in Mexico revealed that mobility of the chemical elements in the mineral grains and redox reactions on the waste contributed production of environmental pollutants (Carrillo-Chávez et al., 2014).

Characterization of iron ore tailings using optical petrography at an iron ore mine in Brazil revealed hematite to be the dominant mineral existing as a lamellar and granular structure where kaolinite and amphibolite minerals were identified (Dauce et al., 2019).

Chemical and mineralogy properties of mine waste and leachate in a sulfide ore mine waste were studied by optical petrography and XRF and revealed the presence of secondary minerals consisting of goethite with sulfur Copper and Zinc compounds that included their oxides and hydroxides (Yang et al., 2015).

2.10. GIS and Remote Sensing Techniques

GIS and Remote Sensing methods have been used during various mining stages (Rwanga and Ndambuki, 2017). Mining, mineral exploration, and mineral extraction are spatial, covering large land spans in geographical space (Blachowski, 2015). Mining engineers require access to the reserves and volume of location-based information during mineral exploitation to guide the mining operation. Given the frequency in data collection for volumetric calculation and considering accuracy and safety, there is a need to employ Geographic information systems (GIS) and remote sensing techniques for areal changes and volume calculation (Rahman et al., 2017). This enhances efficiency in production, planning, and materials handling during mining operations.

2.10.1. Volumes and Areal Extent Estimate of Solid Waste Dumps using GIS and Remote Sensing Methods

GIS and Remote Sensing technology plays a crucial part in mining and has vast applications, including mineral predictive mapping, area calculation using land use and land cover classification (LULC) methods, and volume measurements (Rahman et al., 2017). Various Remote Sensing and GIS software are used to stitch together, and process geotagged photographs and remotely sensed images with high overlap captured from multiple angles for various applications such as waste dump mapping (Tucci et al., 2019). This photogrammetry software creates dense cloud points in 3D, and the result after processing is a rasterized 3D model that can be used for high accuracy volumetric calculations (Sang, 2020).

The Maximum Likelihood Classification (MLC) method utilizing machine learning has become popular in the recent past in identifying various land use and land cover classes at a higher accuracy (Verma et al., 2020). The statistics of these classes play a significant role in area calculation (Jamali, 2019). Land use and land cover are spatial-temporal and crucial in determining where various mine wastes are dumped. Land use and land cover (LULC) class area calculations have become vital in the current sustainability and environmental monitoring tools (Hosseini et al., 2019). Remotely sensed data, GIS, and Remote sensing techniques are used to detect land use and land cover classes whose classes are statistically computed to give the exact areas of specific classes (Hosseini et al., 2019). Accuracy is essential and needs apparent understating and due diligence in selecting and validating the classes and algorithms (Verma et al., 2020).

GIS and Remote sensing can be used to successfully estimate the volumes and extent of solid waste produced due to mining. This is done by utilizing various methods such as land per pixel computation statistics in classification dynamics (Robertson and King, 2011) to estimate the areas of the solid waste dumped. This uses remote sensing methods and involves classifying the remotely sensed image (Siljander et al., 2019). The surface differencing method in ArcGIS is used to estimate volumes from created 3D surfaces (Alrashidi, 2016).

Studies done by Orimoloye and Ololade (2020) at a Gold Mining Area using GIS and Remote Sensing revealed high par pixel areas for tailings dumped, which have increased due to increased operations between the year 1984 and 2019. Weighted overlay and par pixel computation methods done at Damang Mine in Ghana revealed the areas in Km² which were suitable for waste dumping (Suleman and Baffoe, 2017).

GIS has been used to quantify volumes and amounts of ore and waste in mines, including reserves estimation (Choi et al., 2020). GIS and Remote sensing has also been used to estimate the areas where rehabilitation activities are to occur for planning purposes (Choi et al., 2020).

UAV technology which utilizes geographical information systems and remote sensing plays a crucial part in mining and has been used in volume measurements (Rhodes, 2017). The volumes calculated and the extent generated play a vital part in the decision support to the design of tailings dams and waste dumps (Yilmaz, 2010).

The accuracy of volumetric calculations depends on the object size in question, resolution, the quality of the images, the operator's measurement ability, and the ground control points (Raeva et al., 2016). According to Raeva et al. (2016), mining engineering legislation outlines that volume calculations should present accuracy of $\pm 3\%$ of the whole amount. A study done by Rhodes (2017) showed a 2.5% increase in the volume estimated compared to what was hauled while assessing the accuracy of estimating stockpile volumes using GIS and Remote Sensing Methods.

ArcGIS Model Builder has been widely used to automate volume computation processes (Raju, 2020). This comes in handy due to the many iterations for each class under consideration for the volume computation. Raju (2020) highlights that automating processes and workflows in ArcGIS Model Builder has proven effective time management and improve user accuracy.

CHAPTER THREE

3. METHODOLOGY

This Chapter presents the procedures undertaken to investigate environmental pollution in the Kishushe area due to iron ore mining and processing operations. Both desktop research and site investigation techniques were used. The study mine is an iron ore mine operated by Samruddha Resources Kenya Limited Iron Ore Mine, in this study referred to as SRKL Mine.

3.1. Study Area

This study was conducted within the iron ore mining area in Kishushe region, Wundanyi Sub-County, Taita Taveta County, Kenya. The site lies within the Mozambique Belt, which is rich in industrial minerals and gemstones (Mwakumanya *et al.*, 2016). The area is approximately 450 km southeast of Nairobi and 250 km northwest of Mombasa, at between 3.1° S and 3.3° S and 38.1° E and 38.3° E, as shown in Figure 3-1.

Small-scale iron ore mining began in 1972; however, large-scale exploration commenced in 1997 by Wanjala Mining Company (Madini, 2013; Muriuki, 2020). From 2000 to 2018, the Wanjala Mining Company operated and managed an iron ore mine covering 30 km² at Oza Ranch, a community wildlife conservation area in the Kishushe Area. The ore was exported to countries mainly in Asia and sold locally in cement manufacturing (Mwandawiro, 2011; Cheneket, 2018a). Also, artisanal iron ore mining is also reported in the Kishushe area (Mwandawiro, 2011). Samruddha Resources Kenya Limited (SRKL) currently operates and manages the mine, semi-processes the iron ore before exportation, and performs mining

explorations. Mining is done in subdivided blocks or cadastral units of 0.21 km² as specified by the Mining Act 2016 (Government of Kenya - GoK, 2016).

The SRKL Mine neighbors Tsavo National Park on the east and farmlands on the west. The primary land use and land cover changes have been attributed to the agricultural and mining activities in the area.

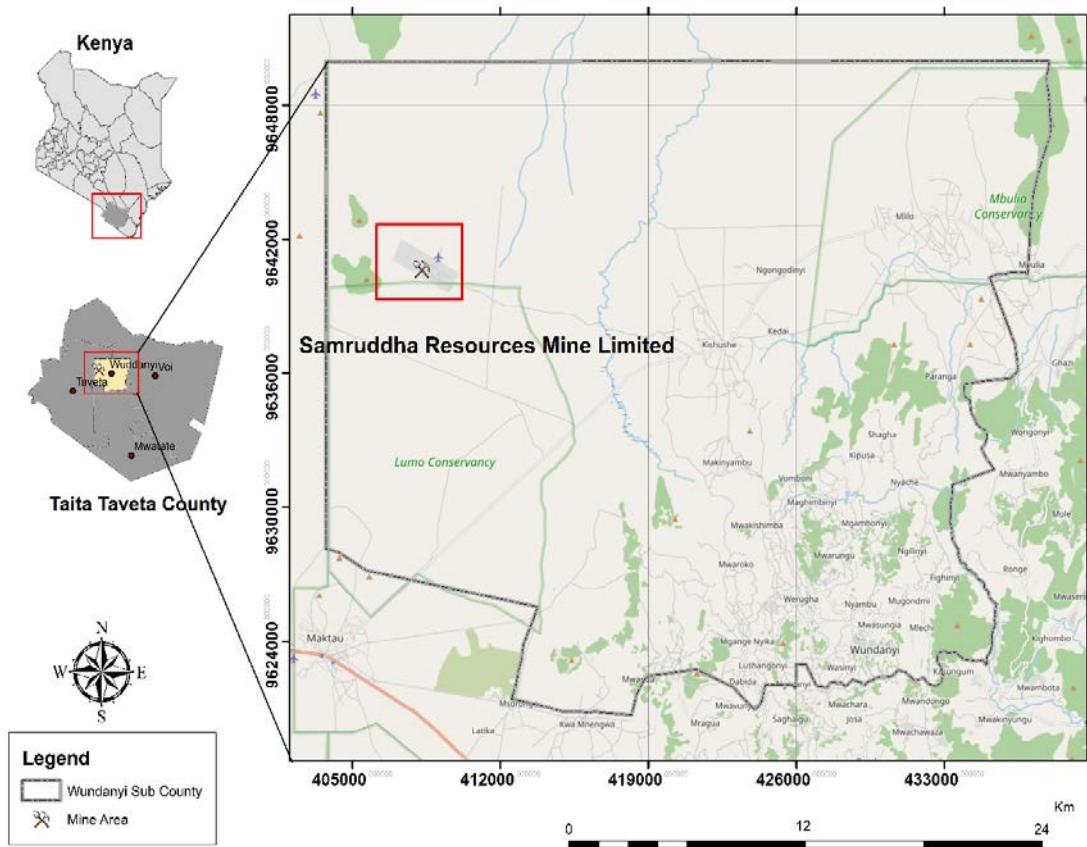


Figure 3-1: Map of the study area

3.1.1. Methodology Workflow

The first part is the workflow to determine the environmental pollutants due to the mining and processing of iron ore at SRKL mine. Secondly, the workflow for quantification of the areal extents and volumes of solid mine wastes at the study mine and finally, the analytical techniques that helped determine the geochemistry and the mineralogical properties of the solid mine waste at the SRKL mine. The complete workflow is presented in Figure 3-2.

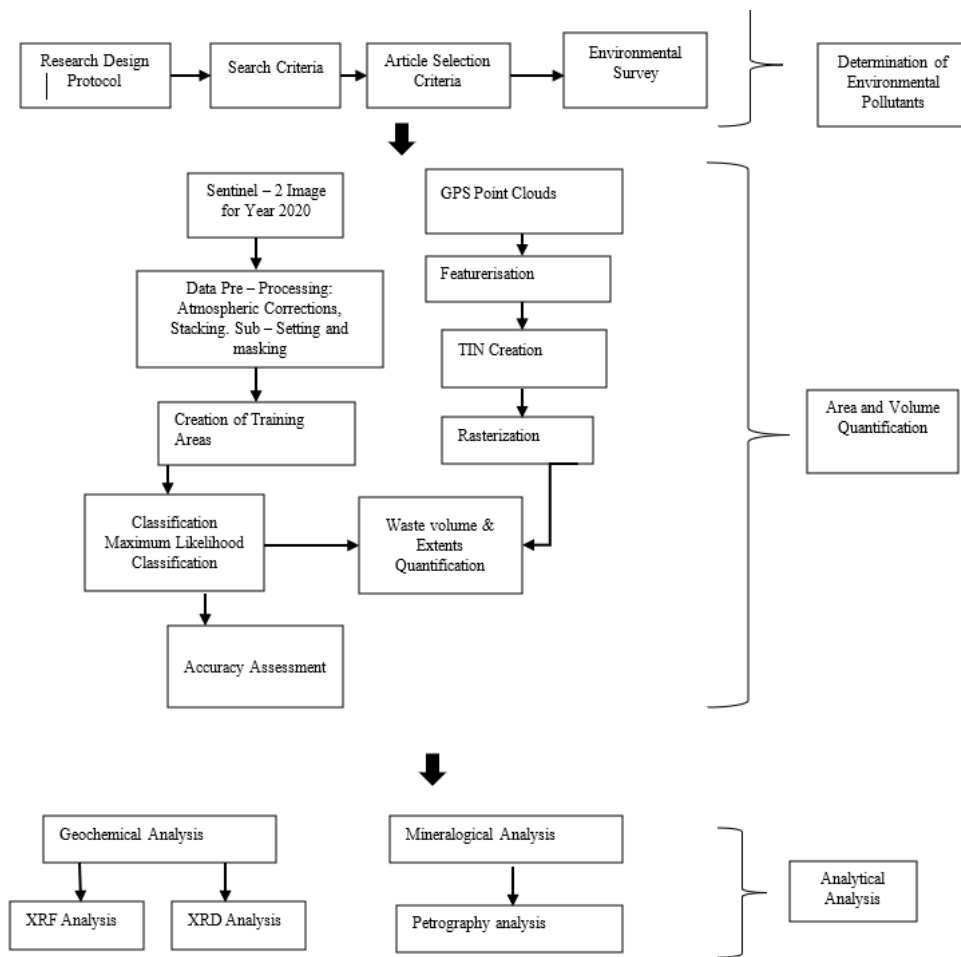


Figure 3-2: Complete workflow

3.2. Determination of Environmental Pollutants due to Iron Ore Mining and Processing Operations at the Samruddha Resources Kenya Limited Iron Ore Mine

3.2.1. Identification of Solid Iron Ore Mining Wastes

The systematic literature review (SLR) method, a desktop research method commonly used in environmental studies (Mengist & Soromessa, 2020), was used in this study to establish potential solid wastes generated from iron ore mining and processing operations at the SRKL mine. Information about solid wastes from iron ore mining was extracted from the published literature. Figure 3-3 summarizes the steps to carry out the SLR that helped identify all related published reports that fit the inclusion criteria used. The procedure assisted in minimizing bias during searching, synthesizing, identifying, analyzing, and summarizing scientific reports on solid mining wastes.

A research design protocol was set for desktop research objectives by developing the under-listed refined research questions.

- i. What is the geology of the Kishushe region?
- ii. Which iron ore mining methods are used at the SRKL Mine?
- iii. What types of solid wastes are generated from iron ore mining and processing activities?
- iv. Are the solid mining wastes potential environmental pollutants in Kishushe region?

- v. What are the environmental effects of iron ore mining and processing operations in Kishushe region?

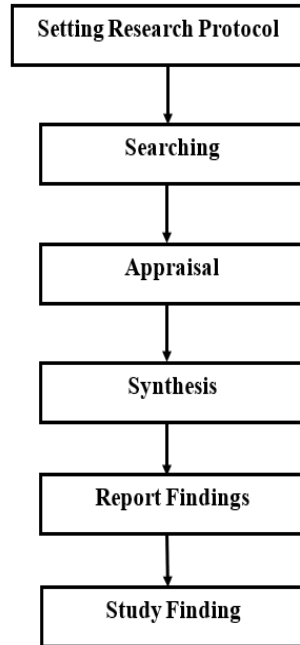


Figure 3-3: Flowsheet for systematic literature review

Appropriate search strings were used to identify relevant published scientific reports in the subjects under investigation in renowned databases, especially Elsevier Science Direct (Mengist & Soromessa, 2020) and Google Scholar (Hoseth, 2011). The search strings included the following; "geology of Kishushe," "iron ore geology," "iron ore mining," "mining in Kishushe," "iron ore mining methods," "iron ore mining waste," "mining and processing waste," and "environmental effects of iron ore mining." Inclusion and exclusion criteria were developed and applied during the search (Table 3-1).

Table 3-1: Search criteria

| Criteria | Decision |
|---|----------|
| 1. Predefined keywords exist as whole or in title, keyword, or abstract | Include |
| 2. Did the paper publish in a peer-reviewed journal? | Include |
| 3. Is the paper written in English? | Include |
| 4. The article addressed the mining of iron ore? | Include |
| 5. Duplicate papers? | Exclude |
| 6. Do the papers address at least one set objective? | Include |
| 7. Papers, not original research | Exclude |
| 8. Papers not downloadable | Exclude |
| 9. Research not carried out in Kenya | Include |
| 10. Research not carried in Taita Taveta County | Include |
| 11. Papers that got published before 2000 | Exclude |

The extracted published scientific reports were appraised based on the research protocol and search criteria set to determine the quality of relevant information needed.

a. Data Organization and Analysis

The data on the geology, mining methods, the type of solid mining waste, mining waste pollution potential, and their effects on the environment in Kishushe region was extracted from the appraised papers. All the data collated was organized in a tabular format (In MS Excel spreadsheet), exported, and statistically analyzed using SPSS Statistics Software. The findings

were presented in graphical and tabular form. The criteria used for the selection of articles were as shown in Table 3-2.

The general screening process and the systematic flow of selecting literature relevant to the study objective were presented in Figure 4-1. In the initial stage, scientific publication records were found; (2,526 from Google scholar, i.e., using the general search technique, and 1,253 from science directly applying various filters). After filtering further by applying various approaches and exclusions, only 17 articles remained for main body skim-reading; 14 papers were downloaded for further reading and analysis. Information was then summarized to develop the three main environmental pollutants (solid mine waste) resulting from iron ore mining and processing at SRKL Mine.

Table 3-2: article selection criteria

| Criteria | Categories Considered | Justification |
|--------------------------------------|--|---|
| 1. Publication Year | Between 2000 and 2020 | Before 2000 were discarded |
| 2. Study Site | County: Taita Taveta | Outside Taita Taveta Count was discarded |
| 3. Data Sources | <ol style="list-style-type: none"> 1. Primary 2. Secondary | <ol style="list-style-type: none"> 1. Field data from the field 2. Data obtained from other sources |
| 4. Method | <ol style="list-style-type: none"> 1. Expert knowledge 2. Investigations 3. Lab analysis | Studies involving geologists, mining engineers, environmental studies, etc. were relied on |
| 5. Assessment | <ol style="list-style-type: none"> 1. Quantification 2. Qualification 3. Mapping 4. Combined Studies | Studied involving iron ore in Kishushe for these categories |
| 6. No of the set objectives assessed | In number | At least one |

b. Environmental Survey in the Iron Ore Mining Site

A reconnaissance visit was carried out at the Kishushe area to establish the iron ore mining activities and management of solid mining waste in the study area. Because of the rugged terrain and the lack of a study site map to identify the access routes, the study area was traversed on foot and using a motorcycle. The information collected during the survey included geological features, iron ore mining pits and processing methods, and solid mining waste dumps, and iron ore stockpiles. Several dumps and stockpiles around the mine were investigated and marked as areas of interest for subsequent sampling using a geographic information system (GPS) mapping method. A GPS gadget (Garmin Oregon 750) was used to collect coordinate points of the solid mining wastes dumps and stockpiles. A geological hammer was used to assist in splitting and breaking rocky samples to distinguish features for structural geology, including rock types, rock formation, lineation, dip, and ore strikes.

Every waypoint was recorded using a unique label to denote the type and location of the solid mining waste dump or stockpile. The wastes dump, stockpiles, and overburden solid wastes were denoted as WD_n , SP_n , and OB_n , respectively, where n is the number of locations from 1, 2, 3, n where solid mining waste was disposed of around the SRKL Mine. The GPS coordinates of the four corners of the study area were collected and recorded to compute the study area in cubic meters. The coordinates were used to develop a map of the study area showing the locations where solid mining wastes were dumped using ArcGIS Software, Version 10.8 on Dell Inspiron 3693 laptop.

3.3. Quantification of the Extent and Volume of Solid Mine Wastes from Samruddha Resources Kenya Limited Mine

In this study, the data on the extent and volume of solid mine waste dumps were estimated using GIS and Remote sensing Methods. All workflows for extent and volume quantification at SRKL were performed using ArcGIS Software, Version 10.8 on Dell Inspiron 3693 laptop.

3.3.1. Data Extraction

The data used to quantify the extent and volume of solid mine wastes were extracted from open-access satellite remotely sensed images and global positioning system (GPS) coordinates. One Sentinel 2 Level 2A satellite image without cloud cover was obtained in January 2019 from the USGS (<http://glovis.usgs.gov>). The image path and row were 167 and 062, respectively, with a 10-meter spatial resolution for Sentinel 2 image (*S2B_MSIL1C_20190928T072659_N0208_R049_T37MDS_20190928T101523*). The global positioning system (GPS) coordinates were picked for reference as control points using Google Earth Pro software version 7.3.2.5776.

The Keyhole Markup Language (KML) data were created, which contained the planar information for (X,Y)- coordinates and displayed the elevation profile shown in Figure 3-4 to determine the highest and lowest points. The KML data was exported to a GPS Visualizer Software (GPSV 2019 version), where the (Z)- coordinate, a component for altitude, was added and finally converted to Global Exchange Format (GPX) and stored in a file geodatabase in ArcGIS ArcCatalog.



Figure 3-4: Elevation profile of iron ore stockpile in google earth

3.3.2. Data Processing

A data processing workflow for areal extents quantification, as shown in Figure 3-5, was developed and used. The Sentinel-2 Data was processed to the Bottom of Atmosphere Reflectance data, corrected from variances caused by the sun angle, and georeferenced. The information was deduced in detail using only the 10 m spatial resolution bands of Blue, Red, Green (RGB), and Near Infrared (NIR). The data were stacked, and different RGB combinations were used to display relevant information with clarity.

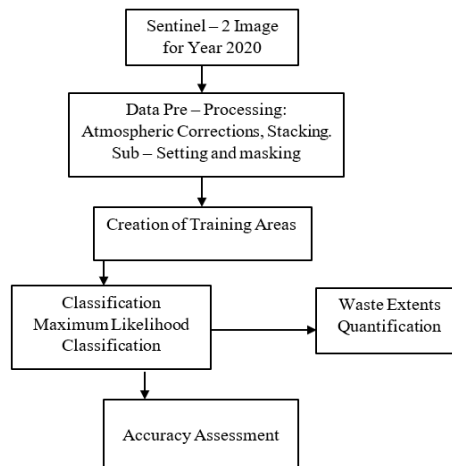


Figure 3-5: Data processing workflow

a. Creation of Training Areas

Training sites were collected from the study site using a global positioning system (GPS). Additional training sites were generated remotely from Google Earth. A classification scheme was developed based on the knowledge of the area and the classes of interest. Solid mine wastes were a priority; in this case, therefore, four classes were created, namely: iron ore stockpile, waste dumps, overburden dumps, cleared ground, and opencast pits

b. Classification and Accuracy Assessment

One hundred (100) random data points were created using the ‘create random points’ tools in the resampling toolbox. These data were used in the supervised classification of the four classes of solid mine waste created in Section 3.2.2.1. The Maximum Likelihood Classifier tool was used to classify the raster images into iron ore stockpiles, waste dumps, and overburden dumps. The accuracy of the classification was assessed using Kappa statistics. A confusion matrix was developed to determine the commission and omission errors resulting from the classification. Cohen's Kappa was statistically computed as per Equation 3-1 (Verma et al., 2020).

$$K = \frac{N \sum_{i=1}^r X_{ii} - \sum_{i=1}^r (X_{i+} * X_{X+1})}{N^2 - \sum_{i=1}^r (x_{ii} X_{X+1})} \quad \text{Equation 3-1}$$

Where; K = Cohen's Kappa, r = number of rows and columns in the error matrix, N = total number of pixels overserved, X_{ii} = observations in row i and column i, X_{i+} = marginal total of row i, $X + i$ = marginal sum of column i

The classification was categorized (Landis & Koch, (1977) based on Kappa values with a moderate to almost perfect strength of agreement following reported ratings as shown in Table 3-3 (Rwanga & Ndambuki, 2017).

. Table 3-3: Rating criteria of kappa statistics

| S/No | Kappa Statistics | Strength of Agreement |
|-------------|-------------------------|------------------------------|
| 1 | < 0.00 | Poor |
| 2 | 0.00 – 0.20 | Slight |
| 3 | 0.21 - 0.40 | Fair |
| 4 | 0.41 – 0.60 | Moderate |
| 5 | 0.61 – 0.80 | Substantial |
| 6 | 0.81 – 1.00 | Almost perfect |

3.3.3. Solid Mine Waste Extents Mapping

The extent of solid mine waste in each class was delineated and mapped. A statistic of each class's coverage per pixel was extracted and data compiled in a Microsoft Excel (MS Excel) spreadsheet. Similar class areas were combined using the statistical computation method in Microsoft Excel 2019.

3.3.4. Waste Volume Quantification

Figure 3-6 shows that the volume computation process was automated in the ArcGIS model builder and py script. The data inputs (solid mine waste gpx point clouds), represented by a blue-filled object (Figure 3.5), were exported to ArcGIS Software. The automation was run stepwise through geoprocessing tools, namely the Feature creation, TIN Creation,

Rasterization, and Volume Computation, represented by Yellow-filled objects as shown in Figure 3-5.

First, the GPX data (refer to Section 3.2.1) were converted to feature classes. Second, a triangulated irregular network (TIN) was created from the feature class. Finally, the TIN was rasterized and georeferenced to estimate the volume in (m^3) after running the surface volume tool in the 3D analyst toolbox. The maximum and the minimum height of the solid mine waste piles and dumps were derived from Google Earth and set during volume computation to give a 3-D volume estimation and enhance the estimate's accuracy.

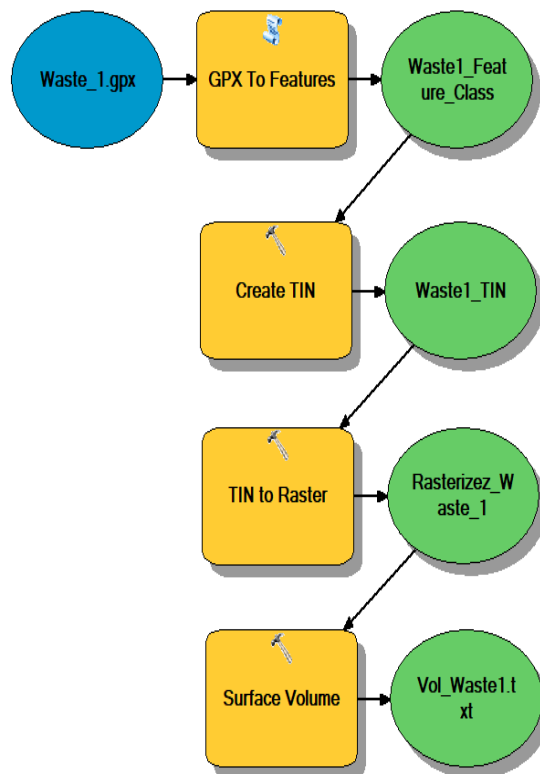


Figure 3-6: Model for volume computation

3.4. Determination of the Geochemistry and Mineralogy of Solid Mine Wastes from the Study Mine

3.4.1. Collection of Samples

Representative samples of solid mine wastes were collected from the following;

1. Overburden materials near the open pit,
2. Waste dumps from blasting operations and waste rocks
3. Stockpiles of iron ore fines/dust resulting from size reduction processes, especially grinding and crushing the extracted iron ore.

A stratified sampling method was used, with twelve sampling locations identified at the study site. In each location, three samples were collected to allow replication and representation with the number of increments determined according to International Standard Organization (ISO) 3082 (ISO, 2017), as illustrated in Figure 3-7.

Sampling pits were dug using a hand mattock to depths of 50 cm. The sample materials were collected, placed in Khaki bags, and weighed using a PCE-BS 3000 digital balance. All samples were uniquely labelled based on their origin to distinguish them. For instance, samples from the iron ore stockpile, waste dump, and overburden were labelled as SP_x, WD_x, and OB_x, where x is the number of samples collected. Table 3-4 summarises the details of the samples collected. Figure 3-8 shows the map developed to show where the samples were collected at the study mining site.

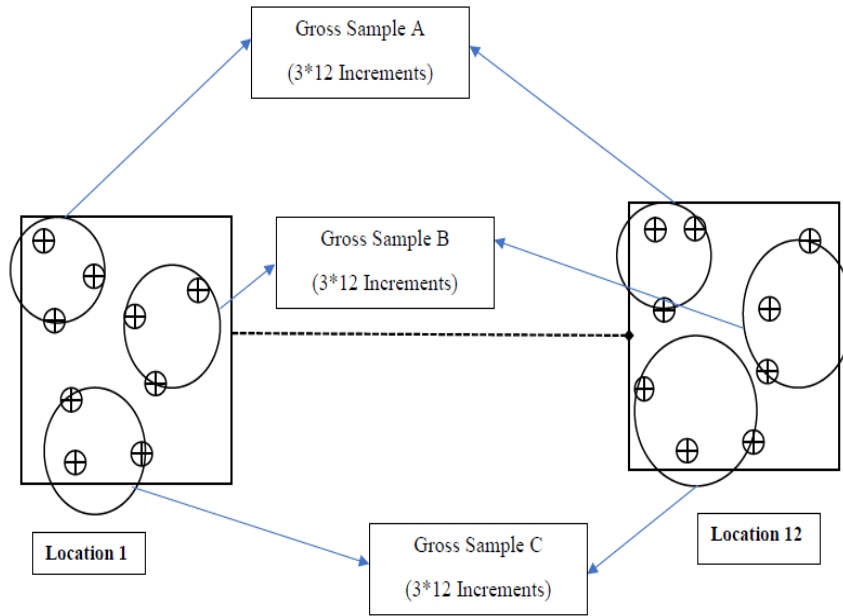


Figure 3-7: Stratified sampling design

The samples were temporarily stored under shade for less than 12 hours before transportation to the laboratory for analysis. All the geochemical and mineralogy properties of the solid mining wastes were characterized in the laboratories based at the Ministry of Mining and Petroleum, Madini House, Nairobi, Kenya.

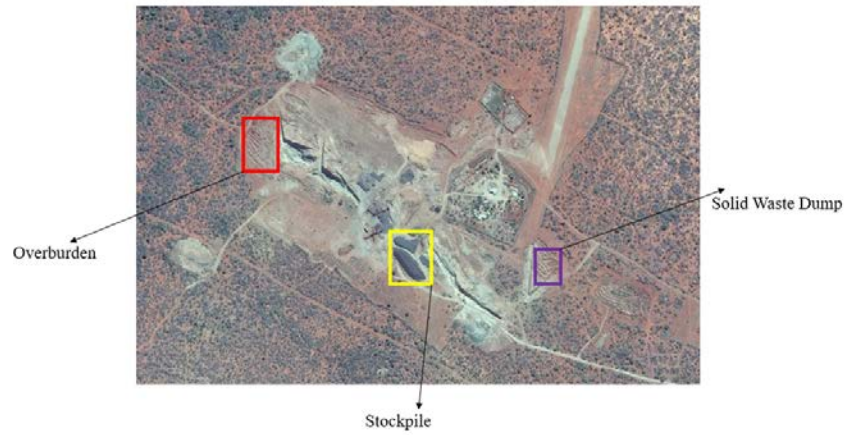


Figure 3-8: Location where samples were collected. Source: image; (google earth)

Table 3-4: Summary of samples collected

| Solid Samples | Mine Waste | Sample Identity | Mass (g) | Coordinates | |
|---------------|------------|-----------------|----------|--------------|---------------|
| Stockpile | | SP1 | 600 | 3°15'5.46"S | 38°10'34.44"E |
| | | SP2 | | 3°15'3.93"S | 38°10'36.69"E |
| | | SP3 | | 3°15'8.57"S | 38°10'36.20"E |
| | | SP4 | | 3°14'58.51"S | 38°10'35.61"E |
| Waste Dump | | WD1 | 600 | 3°14'47.10"S | 38°10'24.59"E |
| | | WD2 | | 3°15'5.66"S | 38°10'15.17"E |
| | | WD3 | | 3°15'8.45"S | 38°10'49.53"E |
| | | WD4 | | 3°14'53.88"S | 38°10'19.35"E |
| Overburden | | OB1 | 600 | 3°14'54.91"S | 38°10'18.83"E |
| | | OB2 | | 3°15'0.07"S | 38°10'24.96"E |
| | | OB3 | | 3°14'55.27"S | 38°10'29.49"E |
| | | OB4 | | 3°14'57.80"S | 38°10'20.36"E |

3.4.2. Preparation Of Samples

a. Samples for XRF Analysis

The samples were prepared following the International Standards Organization (ISO) procedure (ISO 3082) for preparing iron ore samples (ISO, 2017). Figure 3-9 illustrates the steps to prepare the solid mining waste samples for subsequent geochemical analysis.

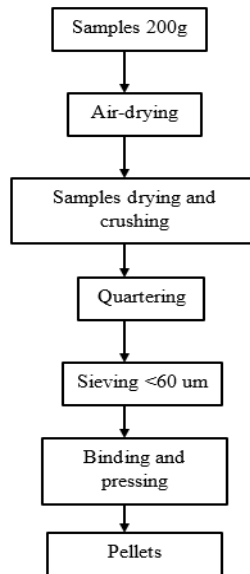


Figure 3-9: Solid waste samples preparation

The samples were initially air-dried in a clean open place to prevent oxidation and contamination (Byers, McHenry, & Grundl, 2019). Two hundred grams (200 g) of the samples were weighed using a PCE-BS 3000 digital balance with a precision of 0.00001g. The weighed samples were crushed using a Laboratory Jaw Crusher (Model 11MPEJC100-M/T, Drill Core)

and ground using a grinder (Model AB 3600411, Nyberg and Westerberg). The ground samples were subdivided by a quartering method (ISO, 2017) to obtain portions of heterogeneous materials for replicating analytical experiments. The ground samples were sieved using a 60-um sieve and the retained particles reground to achieve a homogeneous particle size for the binding process. Binding was then done by pressing the samples with the two holding cups to produce pellets measuring 20 mm in diameter for XRF analysis.

The elemental composition of the solid mining wastes was determined using the X-ray fluorescence (XRF) spectroscopy technique. The 20 mm diameter pellets prepared in Section 3.3.2 were placed in an XRF analyzer (S1 Titan 600N, Bruker AXS) for real-time analysis, Figure 3-10. The results for each assay were recorded for subsequent analysis and interpretation.



Figure 3-10: XRF equipment

b. Samples for Mineralogy Analysis

Rock mass samples measuring 20 mm by 10 mm were cut from the whole samples with a diamond blade saw cutter (Motacutta IFG.IIE NO. 822, Drill Core), as shown in Figure 3-11. The samples were then ground using carborundum sanding stone, starting with the coarse grind (80 grade) to fine grind (200 grade) to remove sore lines and rough edges from the samples, respectively. The samples were then mounted on a glass slide using Canada balsam and left to dry for two hours before lapping.



Figure 3-11: Diamond saw cutter

The samples were labeled on one side to differentiate different samples. The other side lapped flat on an iron lap of about 400 grit, then finished on a plate with 600 grit carborundum sanding stone using water to avoid damaging the grains (Figure 3-11). The lapped samples were dried and a glass slide glued to the sample face using Canada Balsam. The mounted samples were reduced further to thinner sections using a sectioning plate as shown in Figure 3-12 and repeatedly ground until a thin specimen of 30 microns was obtained to allow light to pass through in subsequent analysis using a microscope.



Figure 3-12: Sectioning plate (30 microns)

The Canada Balsam was applied and let sit for 5 minutes before the samples were polished using a dry cloth and covered using a slide for the final inspection to avoid contamination, as shown in Figure 3-13.



Figure 3-13: Polished sample ready for analysis

3.4.3. Properties of Solid Mining Wastes

a. Geochemistry of Solid Mining Wastes

The geochemistry of the mining wastes was determined using the X-ray diffractometry technique. Fifty grams (50 g) of the samples were pulverized to fine sizes of 60 microns

following Knorr and Bornefeld's (2005) procedures. The fine samples were homogenized and placed on the sample holder of a benchtop XRD diffractometer (Bruker AXS D2 PHASER SSD16, Bruker Corporation), as shown in Figure 3-14.



Figure 3-14: XRD equipment

The data for each assay were acquired using the Diffrac Eva software platform, Bruker. The XRD machine was calibrated as per the manufacturer's standards before the experiments were carried out.

b. Mineralogy of Solid Mining Iron Wastes

The mineralogy of the solid mining wastes was determined using optical and petrographic procedures. The petrographic analysis was undertaken to determine the wastes' transparent composition and mineral crystallization. Both cross-polarized light (XPL) and plane-polarized light (PPL) optical techniques were used to identify the minerals in the wastes.

The 30 microns thin sections of polished samples described in Section 3.3.2.2 were placed on 75 mm by 25 mm S8400 plain glass slides and inspected using the cross-polarized light (XPL), and plane-polarized light (PPL) mounted on a Fein Optic Polarizing Light Microscope

(R40POL-RT) 400X magnification (Figure 3-15). Individual mineral grains for each sample were observed, and their images were analyzed using Optica Software.



Figure 3-15: Photograph of the fein optic polarized light microscope r40pol-rt

CHAPTER FOUR

4. RESULTS AND DISCUSSION

This chapter presents the results of the environmental pollutants resulting from iron ore mining and operations at the study mine, the extent and the volume of the solid mine wastes, and the geochemical and mineralogical properties of the solid mine waste resulting from mining and processing of iron. A discussion of these results is also presented in this chapter.

4.1. Environmental Pollutants Resulting from Iron Ore Mining and Processing Operations at the Study Mine

4.1.1. Secondary Data on Environmental Pollutants from Iron Ore Mining Activities in Kishushe Area

From a record of 3,779 published reports extracted from the scientific literature, 13 reports presented information concerning iron ore mining in Kishushe area (Figure 4.1). A summary of the information obtained is presented in Table 4.1 and Figure 4.2. The findings show that there is limited information in the published literature concerning iron ore mining and processing activities in Kishushe area, and disposal, pollution, and potential environmental effects of solid mining wastes generated from the mining activities.

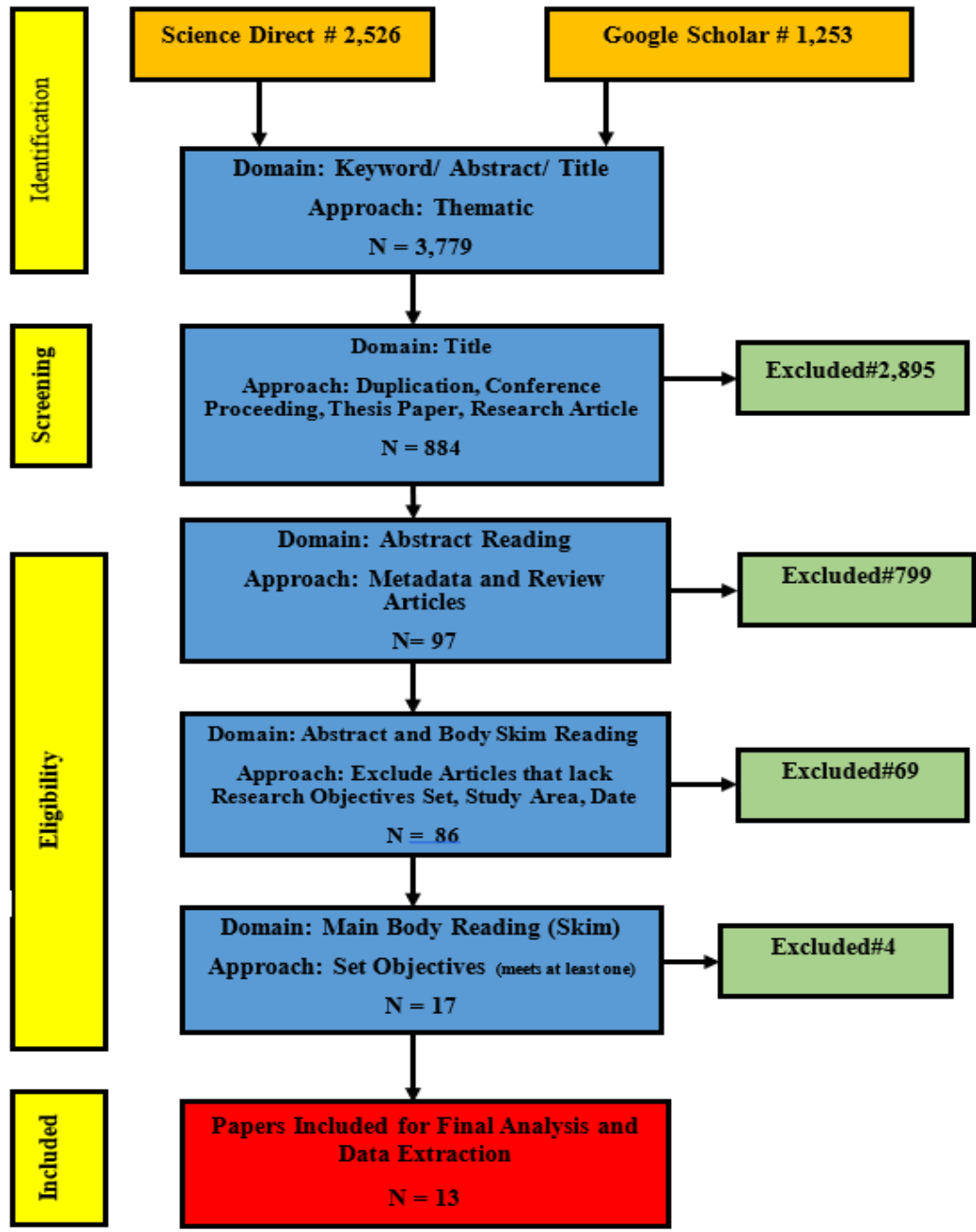


Figure 4-1: Systematic literature review procedures

Table 4-1: Summary of information on iron ore mining activities

| Research question | Finding | Reference |
|--|--|--|
| Geology of Kishushe area | The geology and mineralogy at the mine site are complex, affecting iron ore mining. Iron ore in alluvial and lode iron ore. The geographical distribution of iron ore and the intensity of their anomalies dictate a biased mode of extraction for alluvial and a different method to exploit the reef iron ore. | (G. Bett, Baru, Kabugu, & Rop, 2014; Peter, Gilbert, & Bernard, 2015; Rop, 2014) |
| Iron Ore Mining Methods at SRKL Mine | The primary mining method is open cast mining; however, iron “floats” reef on the surface is shoveled and loaded to trucks to the crushing unit. Blasting operations are also carried out at the mines to access the iron ore. | (G. Bett et al., 2014; Cheneket, 2018; Maranga, Bett, Ndeto, & Bett, 2013) |
| Types of solid mining wastes | The solid mine waste present at the mine site is determined by the geology, the type of the iron ore, and the mining and processing methods or ore. They include; stockpiles results, solid waste dumps, and overburden. | (A. K. Bett, 2018; G. Bett et al., 2014; Cheneket, 2018) |
| Potential pollution from the disposal of solid mining wastes | Iron ore mining has left severe environmental impacts such as physical, chemical, and organic pollution of water sources and damage to the landscape. | (Apollo, Ndinya, Ogada, & Rop, 2017; KNCHR, 2016) |

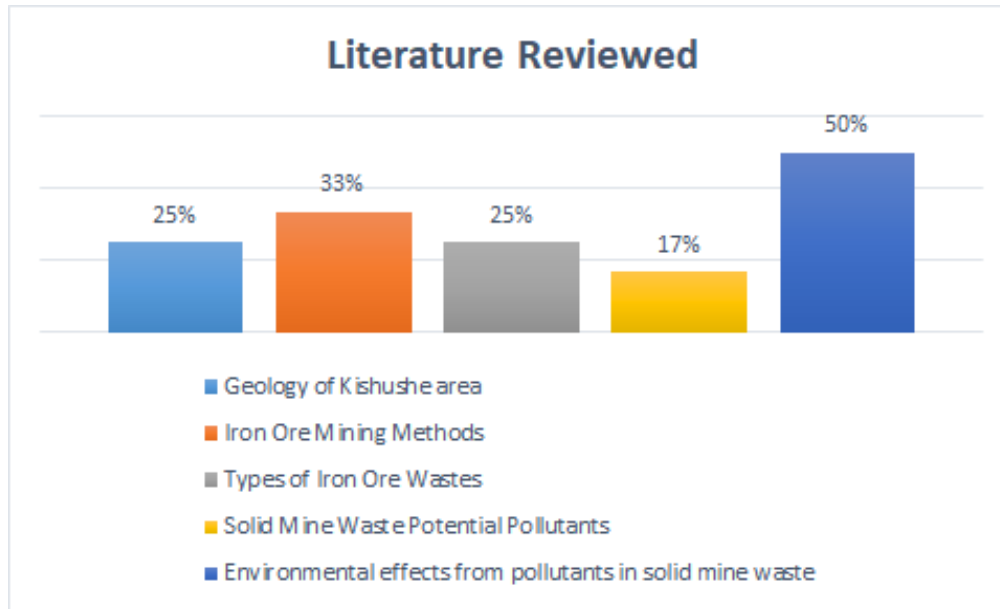


Figure 4-2: Literature reviewed

From the analysis, 25% of the papers that were reviewed for literature revealed information about the Geology of Kishushe area, 33% revealed iron ore mining methods at SRKL Mine, 25% gave insight into the type of solid mining waste at SRKL Mine, 17% of the papers revealed more on the potential pollution from disposal of solid mine wastes and the largest percentage of articles talking about the environmental effects from the pollutants in solid mining wastes as shown in Figure 4-2.

4.1.2. Mining Activities At Samruddha Resources Kenya Limited Mine

Active iron ore mining is currently taking place at SRKL, presently done in mining blocks at Kishushe Area.

The mine sits on the slopes of Wanjala and Taita Hills to the west. There is also a seasonal river, Mkuru River, that drains to Mkuru swamp on the western side of the mine area, as seen in the relief map in Figure 4-3.

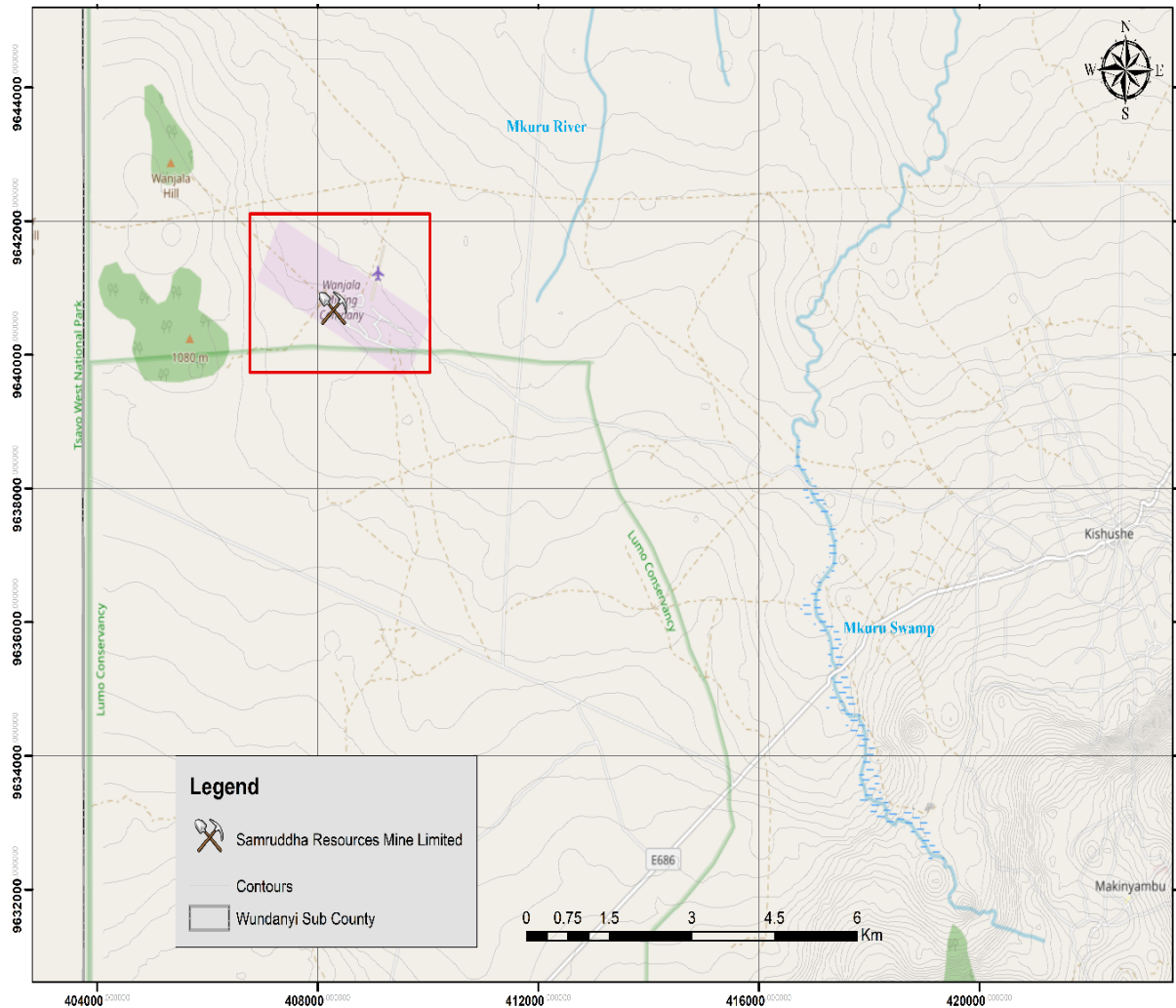


Figure 4-3: Relief map of the area surrounding the study area

The mining of magnetite and hematite iron ore at SRKL has been influenced by various factors, including the geological structure, geology, topography, soil type, and ground stability. This has resulted in the mining method's implications, choice of equipment, production rate, and

stripping ratio. The rock structure and the dip and strike have also determined the pit geometry in SRKL Mines, thereby influencing the amount of solid mine waste produced. The quantity and quality of iron ore mined are determined by the gangue materials, which results in the production of wastes (Stumbea et al., 2019). The iron ore deposits are brecciated, fractured, and jointed due to brittle deformation caused by both extension and compression of tectonics. The dip of the iron ore is approximately minimum 45° NW – maximum 60° NE, and the reefs strike at a minimum 5° NW and maximum 30° NE. The reefs containing the iron ore at any location within the mining site assume the dip and the strike of rocks surrounding them.

The reef ore and the alluvial deposits are not compact, hard, and resistant to weathering; therefore, they require blasting, producing solid mine waste that ends up in the waste dumps. The deposits have host rocks that formed sedimentary iron pyrite deposits on top of basaltic rocks metamorphosed under various oxidizing conditions, forming iron ore (magnetite and hematite) and other minerals such as amphibolite. The pyrite ore results in the formation of sulphide minerals responsible for acid mine drainage, as per research done by (Torres et al., 2018).

The iron ore deposit in the Kishushe area resulted from thermo - tectonic phases of the Neoproterozoic Mozambique belt evolution (Peter et al., 2015). During mining, magnetite and hematite are selectively extracted. This causes other minerals to be the gangue materials that end up being solid mine waste produced at the mine. Hematite at SRKL Iron Ore Mine also occurs in an alluvial form commonly referred to as float iron. The strip ratio for the iron reef, which is thin and structurally and geologically set between rock masses of hanging and

footwall, is higher than that experienced in the excavation of the ore and screening of the alluvial deposits (float iron) therefore forming waste rocks that end up in the waste dumps.

The alluvial deposit, whose gangue mineral is quartz, is easier to mine due to its surface occurrence (Anyona & Rop, 2015). It is mechanically excavated by dozers and loaded into trucks for screening without blasting. In contrast, iron reef mining is challenging due to the hanging wall that needs to be blasted to access the 1 – 1.5-meter-thick ore reef. Drilling and blasting utilize rectangle cuts where the drilling holes are drilled to depths of 10 meters, spaced 3 meters by 5 meters. Before blasting, the overburden material is dozed off from the surface and is often deposited on the mine's edges. This overburden (Figures 4-4 and 4-5) forms one of the solid mine wastes found at SRKL mines.



Figure 4-4: Overburden material from blasting operation piled near the open pit



Figure 4-5: Overburden material as a result of the extraction of alluvial iron ore

The blasted material containing a mixture of ore and gangue materials is loaded into trucks and deposited in piles away from the mine to pave the way for ore extraction. These blasted materials also form the solid mine wastes produced in SRKL Mines and end up in the waste dumps or the overburden materials dumped at the mine shoulders. The alluvial ore is passed through screens to remove soil, weathered schist, and quartzite materials mixed with the blasted material in the waste dumps to recover iron ore (hematite) maximally; the materials passing through the screen are dumped in waste dumps, as shown in Figure 4-6.



Figure 4-6: Screened non-magnetic material both from the alluvial and reef

The clean boulders of alluvial and reef ore are crushed and screened. The high-grade iron ore is piled for shipping (Figure 4-7).



Figure 4-7: Screened iron ore ready for shipping

Iron ore fines and low-grade hematite iron ore is stockpiled near the plant as waste, Figure 4-8; this is commonly referred to as iron ore dust and does not have any economic value, which needs to be beneficiated (Pattanaik & Venugopal, 2018). Currently, the company can't recover and concentrate the low-grade iron and the iron ore fines; therefore, it is treated as solid mine waste.



Figure 4-8: Iron ore fines (circled in red) stockpiled near the plant

Manual sorting of the iron ore by color happens at SRKL Mine. The light color rocks, weathered schist, quartz, and mica, are piled on one side, and the darker and brown rocks,

basically the hematite and Magnetite, are piled on the other side. The ore is screened, and the waste (schist, hornblende, quartz, and mica) is loaded into trucks and dumped in waste dumps.

From the research analyzed and the site visit, it was discovered that the two companies' mining and processing of iron ore were similar. However, the latter (SRKL) preferred drilling and blasting to impact crushing as the former (Wanjala Mining Company) did.

It was also pointed out that various processes of iron ore mining and processing have also resulted in the production of various solid waste such as:

1. Overburden – This is the material produced during the opening of mines and the advancing of open pits.
2. Waste dumps – This waste is produced during drilling and blasting operations, processing operations such as iron ore screening, and separating iron ore and gangue materials by handpicking.
3. Stockpiles – These are produced as a result of processing operations. The material in these stockpiles is disregarded ores of low grade and iron ore dust (fines).

Finally, the solid mine waste samples collection locations were mapped, as shown in Figure 4-9.

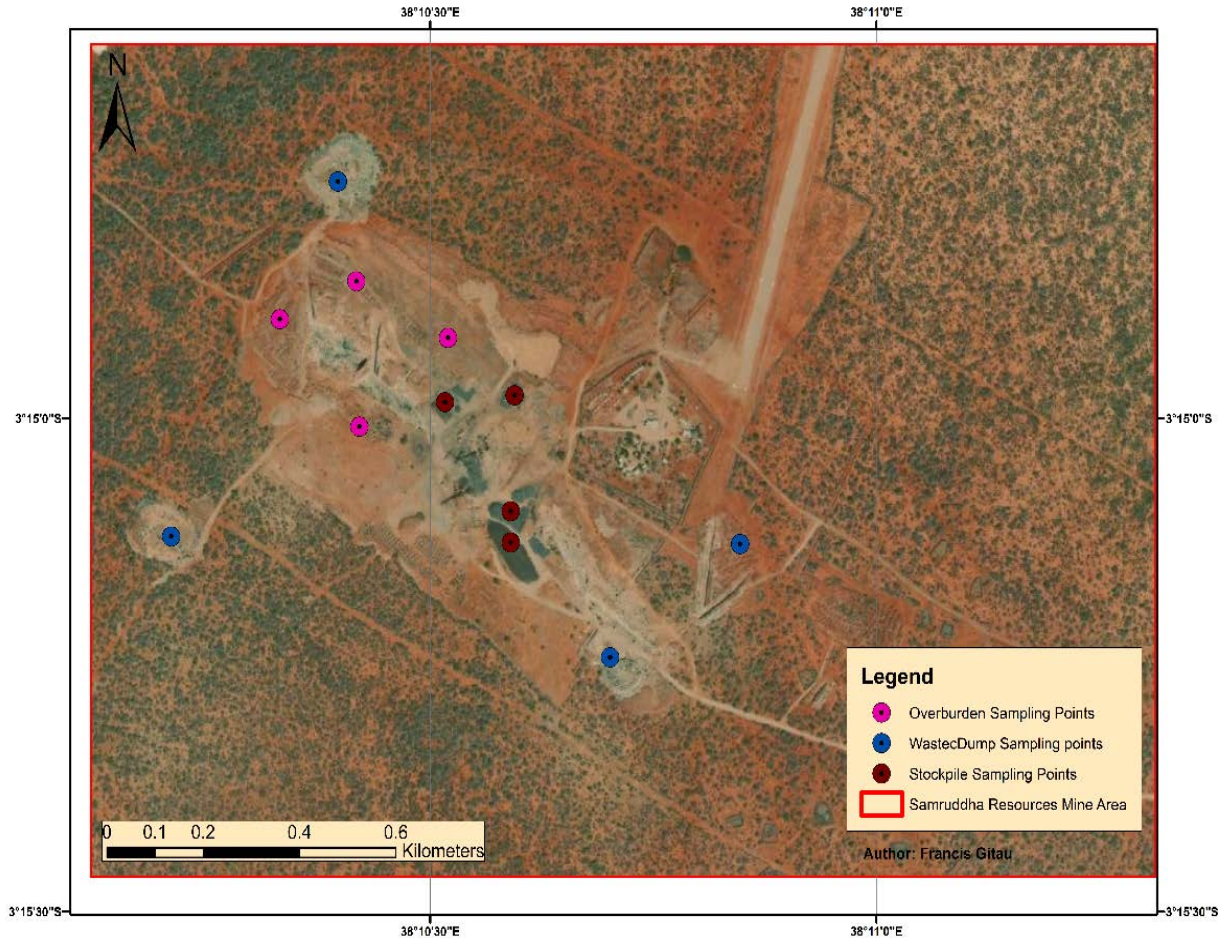


Figure 4-9: Map of the sample location in the study area

It was observed that the primary pollutants resulted from iron ore mining and processing activities at SRKL Mine. The waste resulting from iron ore exploration, the initial stage of mining where a search of the promising reserve is done, ends up being dumped as an overburden.

There is the clearing of vegetation and removal of topsoil and rocks during mine development to prepare the pit for mineral exploitation. The resulting materials, the overburden, add up as solid mine waste in the area. Given the geology of Kishushe and the ore structure in the area,

some of the iron ore starts dipping from the surface, and some iron ore occurs as alluvial deposits (Bett, 2018). This material, despite having a small ore percentage, is disregarded because the dilution is very high. The materials then become overburden, which are piled near the open pit or deposited in waste dumps.

Ore extraction produces the biggest percentage of solid mine wastes. These unwanted materials from blasting operations end up in waste dumps.

Beneficiation of iron ore is done physically at SRKL Mine. During the magnetite and hematite screening, the screened materials that consist of quartz end up as waste and are dumped in the waste dump located away from the mine site. The iron ore fines, which are disregarded by the mine, are stored in the stockpile. These solid mine wastes, waste dumps, stockpiles, and overburden are the main environmental pollutants in the study mine, whose volumes and extents were determined and geochemical and mineralogical properties determined. These solid mine wastes contain materials that undergo various geochemical processes such as oxidation to produce unwanted pollutants that may end up causing environmental hazards and are discussed in the following sections.

4.2. The Extent and Volume of Dumps and Stockpiles of Solid Mining Wastes at the Study Mine

4.2.1. Solid Mine Waste Extents

The areal extent maps generated from the MLC classification based on the classes identified for the various land use classes to delineate the areas where solid mine waste is dumped at SRKL Mine was generated.

In the map, the waste dumps, iron ore stockpiles, overburden, and opencast pits are represented by brown, black, yellow, and grey colors, respectively.

The par pixel statistical computation revealed that the largest area was covered by waste dumps which occupied an area of 136,100 m² translating to a percentage of 54.58 %. The iron ore stockpile and the overburden occupied areas of 28,800 m² and 84,500 m² respectively. The par pixel area for the stockpile and the computed areas for the solid mine wastes are shown in Tables 4-2 and 4-3, respectively.

Table 4-2: Attribute table for par pixel areal coverage

| Study Area | | | | | | | | | | | |
|------------|---------|----------|-----|----------|------|------|--------------------|-------|------------|------------|--|
| FID | Shape * | OBJECTID | Id | gridcode | Area | ha | Classname | Class | Shape_Leng | Shape_Area | |
| 4 | Polygon | 14 | 464 | 1 | 100 | 0.01 | Iron Ore Stockpile | 1 | 40 | 100 | |
| 5 | Polygon | 15 | 465 | 1 | 100 | 0.01 | Iron Ore Stockpile | 1 | 40 | 100 | |
| 6 | Polygon | 18 | 477 | 1 | 100 | 0.01 | Iron Ore Stockpile | 1 | 40 | 100 | |
| 7 | Polygon | 19 | 478 | 1 | 200 | 0.02 | Iron Ore Stockpile | 1 | 60 | 200 | |
| 8 | Polygon | 24 | 501 | 1 | 200 | 0.02 | Iron Ore Stockpile | 1 | 60 | 200 | |
| 11 | Polygon | 36 | 533 | 1 | 100 | 0.01 | Iron Ore Stockpile | 1 | 40 | 100 | |
| 16 | Polygon | 44 | 555 | 1 | 200 | 0.02 | Iron Ore Stockpile | 1 | 60 | 200 | |
| 33 | Polygon | 87 | 671 | 1 | 100 | 0.01 | Iron Ore Stockpile | 1 | 40 | 100 | |
| 124 | Polygon | 244 | 939 | 1 | 1700 | 0.17 | Iron Ore Stockpile | 1 | 180 | 1700 | |
| 160 | Polygon | 306 | 102 | 1 | 100 | 0.01 | Iron Ore Stockpile | 1 | 40 | 100 | |
| 164 | Polygon | 312 | 102 | 1 | 100 | 0.01 | Iron Ore Stockpile | 1 | 40 | 100 | |
| 175 | Polygon | 327 | 104 | 1 | 200 | 0.02 | Iron Ore Stockpile | 1 | 60 | 200 | |
| 186 | Polygon | 342 | 106 | 1 | 100 | 0.01 | Iron Ore Stockpile | 1 | 40 | 100 | |
| 229 | Polygon | 409 | 115 | 1 | 100 | 0.01 | Iron Ore Stockpile | 1 | 40 | 100 | |

Table 4-3: Areas of solid mine waste extents

| Areal classes | Iron Ore Stockpile | Waste | | Overburden | Estimated Total Area Covered |
|------------------------|--------------------|---------|--|------------|------------------------------|
| | | Dump | | | |
| Area m ² | 28,800 | 136,100 | | 84,500 | 249,400 |
| Percent land cover (%) | 11.55 | 54.58 | | 33.87 | 100.00 |

The hematite stockpile, which is disregarded as mine waste, occupied the smallest percentage of 11.55%, while waste dump and overburden occupied 54.58% and 33.87%, respectively. Research done by (Guan, & Cheng, 2015b; Matthew et al., 2019; Mi et al., 2019; Basommi et al., 2020; Orimoloye & Ololade, 2020) on different mine sites revealed that GIS and remote sensing techniques could be used successfully in delineation and mapping of solid mine waste extents, this compares to the results in this research.

During open-pit mining operations, solid mine wastes are emitted (Kakaie et al., 2019). The developing SRKL Iron Ore Mine in Taita Taveta, Kenya, was chosen as the study area to examine these problematic solid mine wastes as little information on the volumes and areal extent are known. The criterion for determining waste and ore at SRKL is a cut-off grade (Kakaie et al., 2019). Ore less than 70% of the iron ore concentration at SRKL is termed subeconomic and therefore disregarded as waste. Various types of wastes exist at SRKL Iron Ore Mine, such as waste dump, stockpile, and overburden, as shown in Figure 4-10.



Figure 4-10: Mine wastes at samruddha resources kenya limited iron ore mine; a. Overburden material, b. Waste dump, c. Stockpiled iron ore fines, and d. Waste rock dump. Waste rock is generally excavated and mined rocks during access from ore and includes rocks resulting from blasting operations (Kakaie et al., 2019). These waste rocks are usually dumped in non-designated waste dumps around the SRKL Iron Ore Mine mining area. The overburden material at SRKL Iron Ore Mine is mainly topsoil, and rocks dozed off during the opening up of new open pits, as shown in Figure 4-11. The overburden material is piled on the sides of the mine and constitutes solid mine waste produced during mining operations under consideration in this research.



Figure 4-11: Overburden material at the sides of the active open pit

The stockpiled material at SRKL Mine is generally iron ore fines and iron ore of low grade, not of economic value to the company. The iron ore fines and low-grade iron ore are mainly stockpiled near the processing plant.

4.2.2. Accuracy Assessment

The extent of solid mine waste was mapped at an overall accuracy of 74%, which depicts reliable performance regarding the classification done to estimate the areal extents. A Cohen's Kappa of 0.65 was achieved, which is above the recommended Kappa of 0.5 (Rwanga & Ndambuki, 2017). The kappa coefficient is rated as substantial, and hence the calculated areas based on classification are found to fit for this research. This is as shown in the confusion matrix in Table 4-4. The accuracy was influenced by global positioning exchange (GPX) points coverage, which creates an unclear definition of the footprint and the outline at different areas of interest, such as the stockpile. Figure 4-12 shows the parts circled not covered by the GPX points, which influenced the accuracy of the areal and volumetric calculations.

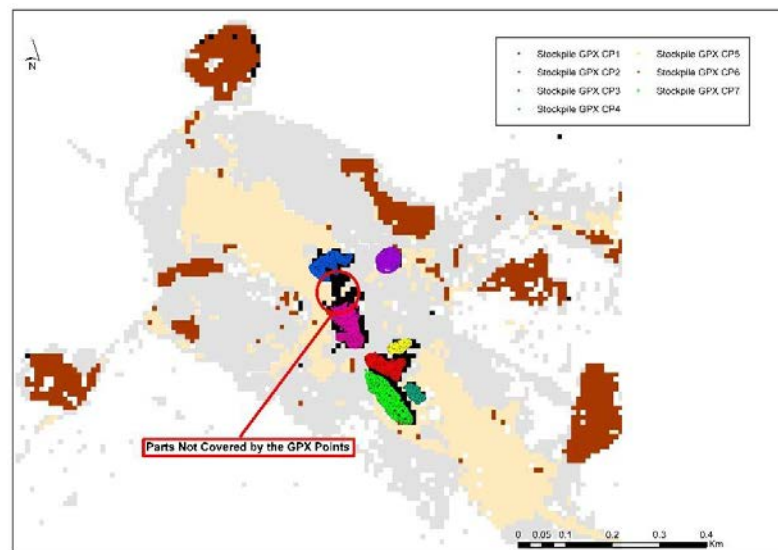


Figure 4-12: GPX point features overlaying stockpiles

Table 4-4: confusion matrix

| | | Reference data | | | | | |
|------------------------|---------------------------|-----------------------|---------------------------|----------------|---------------|------------------------|-----------------------|
| Classified Data | Classes | Iron Ore Stockpile | Waste Dump and Overburden | Cleared Ground | Open Cast Pit | Total Reference Points | Users Accuracy |
| | Iron Ore Stockpile | 23 | 0 | 0 | 0 | 23 | 100% |
| | Waste Dump and overburden | 1 | 5 | 1 | 0 | 7 | 72% |
| | Cleared Ground | 0 | 10 | 26 | 1 | 37 | 71% |
| | Open Cast Pit | 0 | 13 | 0 | 19 | 32 | 60% |
| | Total Reference Points | 24 | 28 | 27 | 20 | | |
| | Producers Accuracy | 96% | 58% | 96% | 95% | | |
| | Overall Accuracy | 74% | | | | | |
| Kappa Coefficient | 0.65 | | | | | | |

4.2.3. Volumes of Solid Mine Waste Dumped

The estimated volume of waste dump and overburden occupied the largest volume of approximately 185,734.42 m³ and 303,477.52 m³, respectively, while iron ore stockpiles occupied a volume of approximately 34,025.17 m³, as shown in Table 4-5. Waste rock dumped occupied 34.92 %, iron ore stockpile (hematite) at 6.55% compared to overburden which occupied the highest percentage of 58.58 %.

Table 4-5: Volumes of solid mining wastes

| Estimated variable | Iron Ore Stockpile | Waste Dump | Overburden | Estimated Total Volume |
|-----------------------------------|---------------------------|-------------------|-------------------|-------------------------------|
| Volume in m ³ | 34,025.17 | 185,734.42 | 303,477.52 | 523,237.11 |
| Percent volume of solid waste (%) | 6.50 | 34.92 | 58.58 | 100.00 |

An estimated total volume of solid mine waste produced at SRKL Iron Ore Mine is 523, 237.11 M³ and covered an approximated area of about 249,400 M³ as shown in Table 4-6.

Table 4-6: Area and volume of solid mine waste

| | |
|--|-------------|
| Estimated area of solid mine waste M^2 | 249, 400.00 |
| Estimated Volume of Mine Waste M^3 | 523, 237.11 |

Generally, these volumes are translated from the stripping ratio that the mine utilizes, which is 2:1. For every part of ore mined, the company produces two parts of waste (Kuranchie, 2015).

The waste dump covers a volume and area of 185,734.42 M^3 , and 136,100 M^2 respectively. The waste dump covers over half of the solid mine wastes produced at the study mine, 54.8 % of the area, and 58.58 % of total volumes of solid mine waste. This translates to the highest amount of solid mine waste generated during iron ore stripping and mining operations. This waste is from blasting operations, stripping of gangue materials heterogeneous to the geology of the ore. The waste dumps are dumped in locations away from the open pit, as shown in the solid mine waste map in Figure 4-13.

The stockpiled materials at the mine cover an approximate volume and area of 34, 025.17 M^3 and 28, 800 M^2 respectively. This translates to the least amount of solid waste produced during iron ore mining at the mine. The stockpiled material is generally mineral processing waste produced due to grinding, crushing, and screening of hematite and magnetite ore. Due to the selective mining taking place at SRKL mine, the materials that end up in the processing plant are of high grade, often identified traditionally by their color. Therefore, minimal amounts of stockpiled waste are produced. These stockpiles also appear to be clustered at one central location near the processing plant, as shown in Figure 4-13.

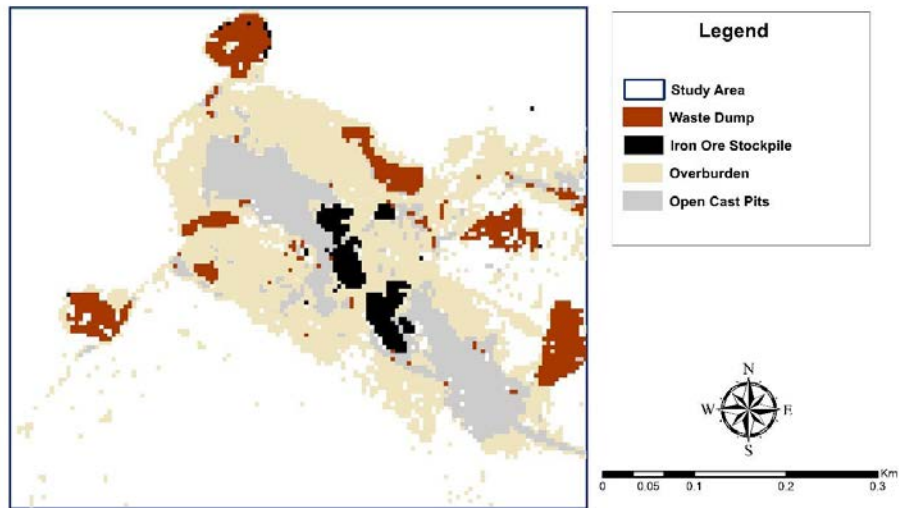


Figure 4-13: Solid mine waste map

The overburden materials cover a volume and area of 303, 477.52 M^3 , and 84,500 M^2 respectively. The overburden materials are dumped near the open-pit mine to reduce the operational costs for materials transport (Suleman & Baffoe, 2017). This waste generally results from topsoil and mechanically excavated rocks to open up new open pits and expand existing pits.

The exposure of these solid wastes to the atmosphere and the environment may cause various impacts, such as acid drainage due to sulphide minerals (Almeida et al., 2018). Trace metal concentrations in these mine wastes pose an environmental concern (Cheneket, 2018a). This is why there's a need to map out their extent and the volumes to plan for various post-mining operations such as mine rehabilitation and plan monitoring activities. The volume quantifications are also essential to avert the anticipated environmental impacts. As they

progressively carry out mining and processing operations, a mining company needs to know the approximate volumes and extent of mine waste they produce. At times, this may prove to be a costly affair that results in these wastes' uncontrolled disposal. Studies done by Cheneket (2018) reveal that the disposal of mine wastes by SRKL poses a grave danger to the community living around the mine as the soils are laced with potentially toxic elements such as lead, zinc, iron, manganese, and titanium resulting from the mine waste. This information on volumes and areal coverage of these problematic solid mine wastes, which was missing, can help the company refocus on planning for waste disposal, treatment techniques, and some situations consider value addition and reusing. Iron had the highest average mass in the stockpile samples because they were unutilized and disregarded as waste. The iron ore mass dump for the waste dump was moderate at an average of 40%. Some moderate amounts of iron were discovered in the waste samples because of the high dilution of the ore and the gangue material owing to the geology and the parent rock at the mining site. The waste dump had materials from blasting operations that didn't pass through screening and therefore contained iron ore. The overburden, however, had high amounts of silica and calcium carbonate compared to the waste dump and stockpile samples. The overburden material is generally the gangue minerals consisting of quartz, the predominant caprock in the study area. Sulphur, chromium, zinc, nickel, lead, copper, bismuth, vanadium, thorium, rubidium, zirconium, potassium, and strontium were in traces. Among these elements are potentially toxic elements contaminants such as titanium, vanadium, chromium, manganese, nickel, copper, lead, and zinc that were also identified in similar research done by Cheneket (2018).

4.3. Properties Of Solid Mine Wastes From The Study Mine

4.3.1. Chemical Elements And Compounds

a. Solid Mine Waste Dumps

Table 4-7 summarises the elements and compounds determined in four representative samples of waste dumps from mining and mineral processing operations and their estimated mass and volume. The major elements and compounds present in the samples are presented in Figure 4-15. The minor elements are shown in Figure 4-16 with the error bars for their standard error (S.E) of the mean.

Table 4-7: Elements and compounds in the solid waste dumps samples

| Element / Compound | Mean Mass % | Estimated Mass in the Waste Dumps (g) | Estimated Volume in the Waste Dumps(m^3) |
|--------------------|--------------|---------------------------------------|--|
| Iron | 39.92 ± 4.02 | 2.00 | 1,853,536.64 |
| Silica | 35.88 ± 5.23 | 1.79 | 1,665,712.71 |
| Calcium Carbonate | 16.77 ± 6.63 | 0.84 | 778,598.69 |
| Manganese | 2.19 ± 1.27 | 0.11 | 101,689.59 |
| Barium | 1.29 ± 1.11 | 0.06 | 59,899.35 |
| Aluminum | 1.29 ± 0.31 | 0.06 | 59,806.48 |
| Phosphorous | 1.13 ± 0.09 | 0.06 | 52,237.81 |
| Titanium | 0.95 ± 0.65 | 0.05 | 44,111.92 |
| Sulphur | 0.440 ± 0.36 | 0.02 | 20,430.79 |
| Chromium | 0.04 ± 0.02 | 0.00 | 1,764.48 |
| Zinc | 0.03 ± 0.01 | 0.00 | 1,160.84 |
| Nickel | 0.02 ± 0.01 | 0.00 | 1,067.97 |
| Lead | 0.02 ± 0.01 | 0.00 | 696.50 |
| Copper | 0.01 ± 0.01 | 0.00 | 603.64 |
| Bismuth | 0.01 ± 0.01 | 0.00 | 464.34 |
| Vanadium | 0.01 ± 0.01 | 0.00 | 464.34 |
| Thorium | 0.01 ± 0.01 | 0.00 | 371.47 |

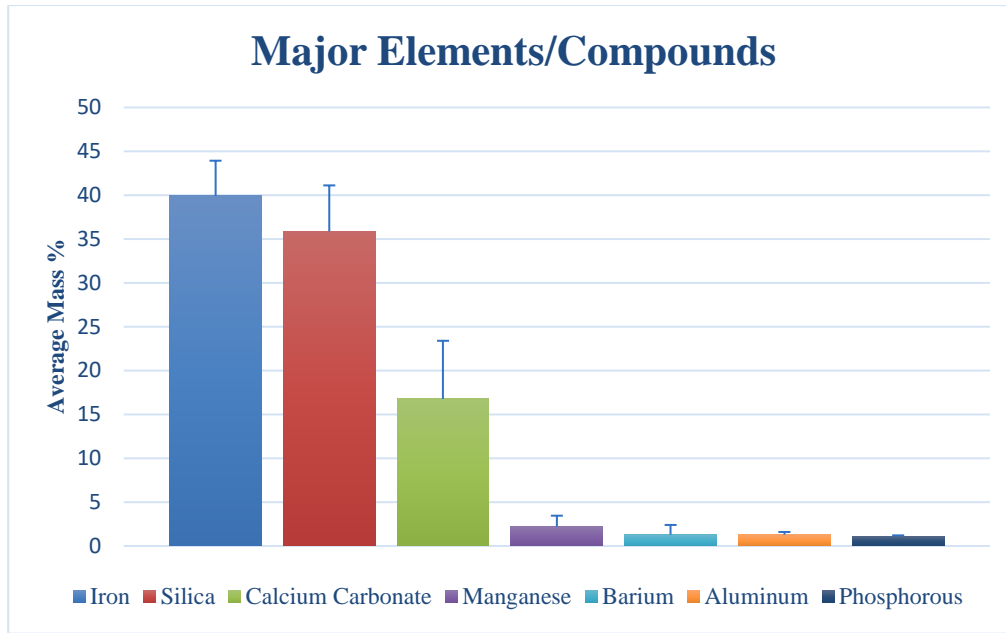


Figure 4-14: Graph of major elements and error bars of the s.e for waste dump samples

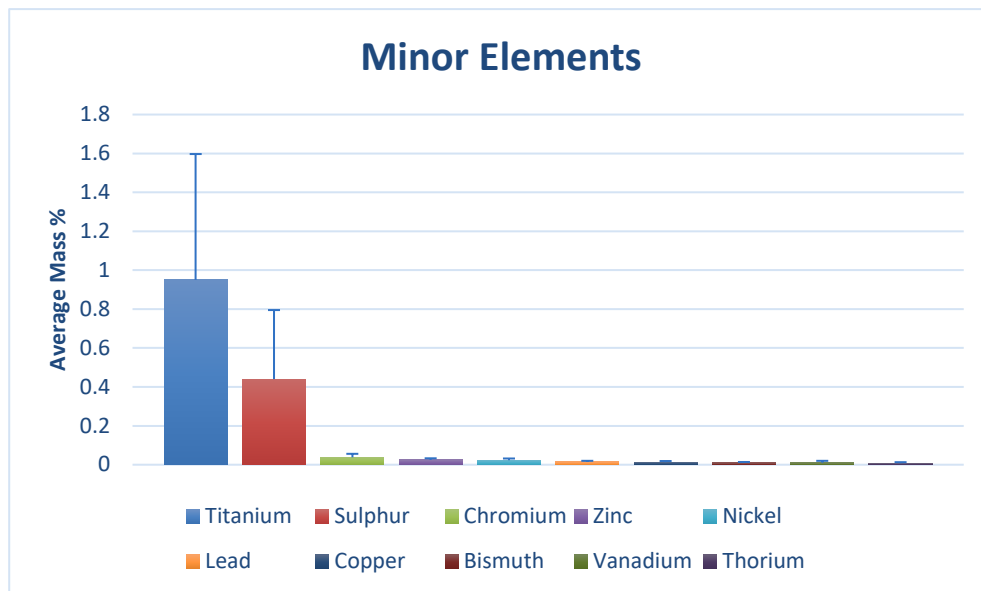


Figure 4-15: Graph of minor elements and error bars of the s.e for waste dump samples

Potentially toxic elements were present in the waste dump samples. High amounts of iron ore identified in waste dump samples inferred high dilution during mining. Only high-grade iron

ore is mined at SRKL Mine; therefore, highly diluted ore with gangue minerals (Silica) is disregarded as waste. The waste dumps, generally containing blasted material, contain chemical elements such as sulphur, a potential agent for environmental pollution.

b. Stockpiles

The XRF analysis result and the estimated mass and volumes for each element/ compound from the stockpile samples are presented in Table 4-8. The graphs of the major and minor elements/ compounds in the stockpile samples are presented in Figures 4-17 and 4-18, respectively, and the error bars of the standard error (S.E) of the mean are shown.

Table 4-8: Elements and compounds in the stockpiles samples

| Element/ Compound | Mean Mass % | Estimated Mass in the Stockpile (g) | Estimated Volume in the Stockpile (m ³) |
|-------------------|--------------|---|--|
| Iron | 81.44 ± 3.58 | 4.07 | 27,710.10 |
| Silica | 13.35 ± 2.94 | 0.67 | 4,541.68 |
| Aluminium | 1.67 ± 0.34 | 0.08 | 568.22 |
| Calcium Carbonate | 1.01 ± 0.26 | 0.05 | 344.67 |
| Phosphorous | 0.87 ± 0.23 | 0.04 | 295.34 |
| Barium | 0.73 ± 0.15 | 0.04 | 246.68 |
| Manganese | 0.69 ± 0.12 | 0.03 | 234.09 |
| Titanium | 0.623 ± 0.11 | 0.03 | 211.98 |
| Sulphur | 0.22 ± 0.10 | 0.01 | 75.88 |
| Nickel | 0.10 ± 0.04 | 0.01 | 35.05 |
| Bismuth | 0.08 ± 0.02 | 0.01 | 26.54 |
| Lead | 0.04 ± 0.01 | 0.01 | 14.63 |
| Rubidium | 0.04 ± 0.01 | 0.01 | 11.91 |
| Copper | 0.03 ± 0.01 | 0.01 | 8.51 |
| Zinc | 0.02 ± 0.01 | 0.01 | 6.81 |
| Vanadium | 0.01 ± 0.01 | 0.01 | 1.70 |
| Zirconium | 0.01 ± 0.01 | 0.01 | 1.02 |

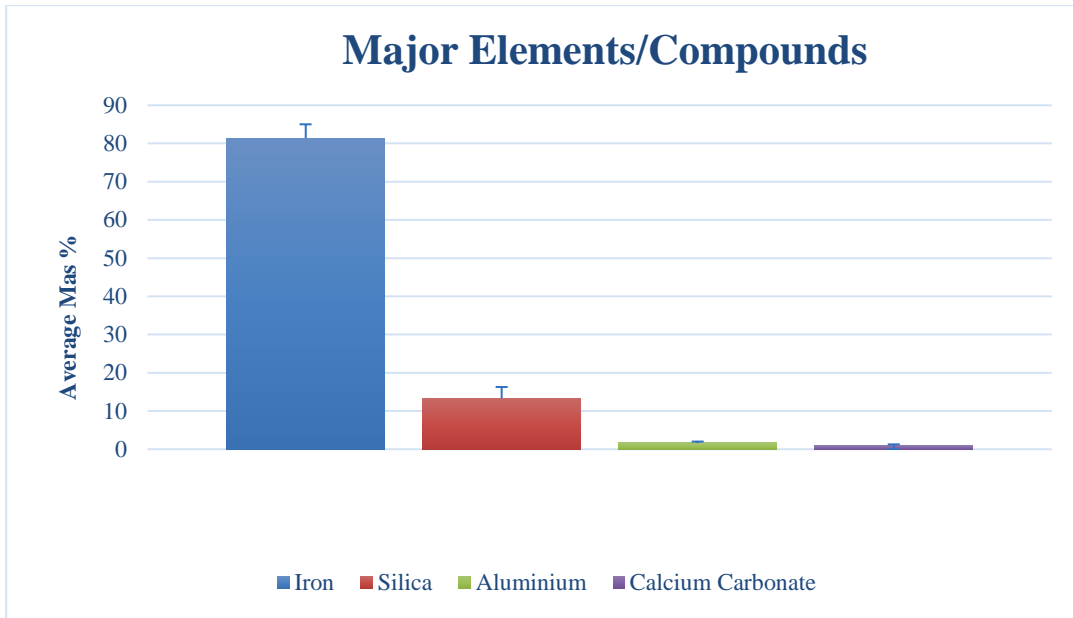


Figure 4-16: Graph of major elements and error bars of the s.e for stockpile samples

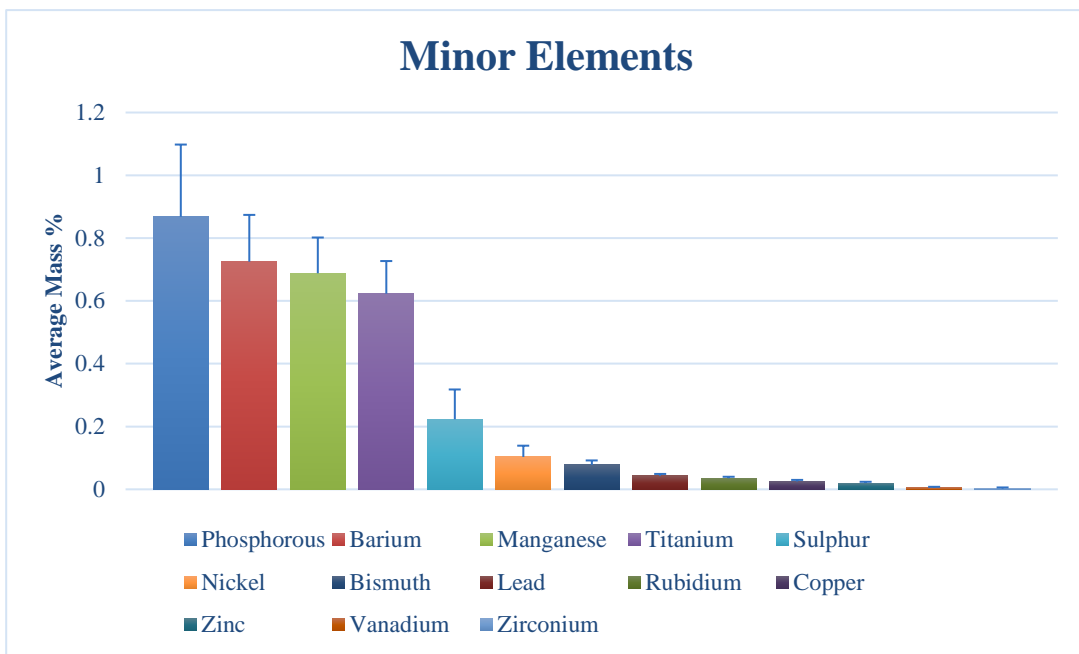


Figure 4-17: Graph of minor elements and error bars of the s.e for stockpile samples

The stockpile samples contained very high amounts of Fe_2O_3 and low amounts of other elements. SP1 and SP4 samples were iron ore fines; despite high iron ore concentrations, the material is unwanted and is therefore waste. These fines are stockpiled near the processing plant for disposal. The other stockpiled materials (SP2, SP3) are low-grade iron ore, with small (50mm) float iron occurring alluvially in the area. Currently, the mining company does not utilize these materials and contains potential environmental pollutants, as revealed in the XRF analysis in Table 4-8.

a. Overburden

Table 4-8 summarises the XRF results The major and minor elements and compounds present in the samples are presented in Figure 4-19. and Figure 4-20 .

Table 4-9: Elements and compounds in the overburden samples

| Element/ Compound | Mean Mass % | Estimated Mass in the overburden(g) | Estimated Volume in the overburden (m^3) |
|-------------------|---------------|-------------------------------------|--|
| Silica | 41.02 ± 10.59 | 20.51 | 1,244,864.79 |
| Calcium Carbonate | 31.15 ± 15.52 | 15.57 | 945,180.74 |
| Iron | 12.42 ± 3.13 | 6.21 | 376,767.34 |
| Aluminium | 6.82 ± 1.49 | 3.41 | 207,062.71 |
| Phosphorous | 5.51 ± 0.08 | 2.76 | 167,216.11 |
| Titanium | 1.70 ± 0.05 | 0.85 | 51,591.18 |
| Potassium | 0.66 ± 3.84 | 0.33 | 19,968.82 |
| Chromium | 0.25 ± 0.01 | 0.13 | 7,586.94 |
| Barium | 0.25 ± 0.05 | 0.12 | 7,435.20 |
| Manganese | 0.18 ± 0.11 | 0.09 | 5,553.64 |
| Copper | 0.04 ± 0.01 | 0.02 | 1,213.91 |
| Sulphur | 0.03 ± 0.08 | 0.01 | 849.74 |
| Zirconium | 0.03 ± 0.01 | 0.01 | 849.74 |
| Strontium | 0.02 ± 0.01 | 0.01 | 546.26 |
| Rubidium | 0.02 ± 0.01 | 0.01 | 455.22 |
| Zinc | 0.01 ± 0.01 | 0.00 | 242.78 |

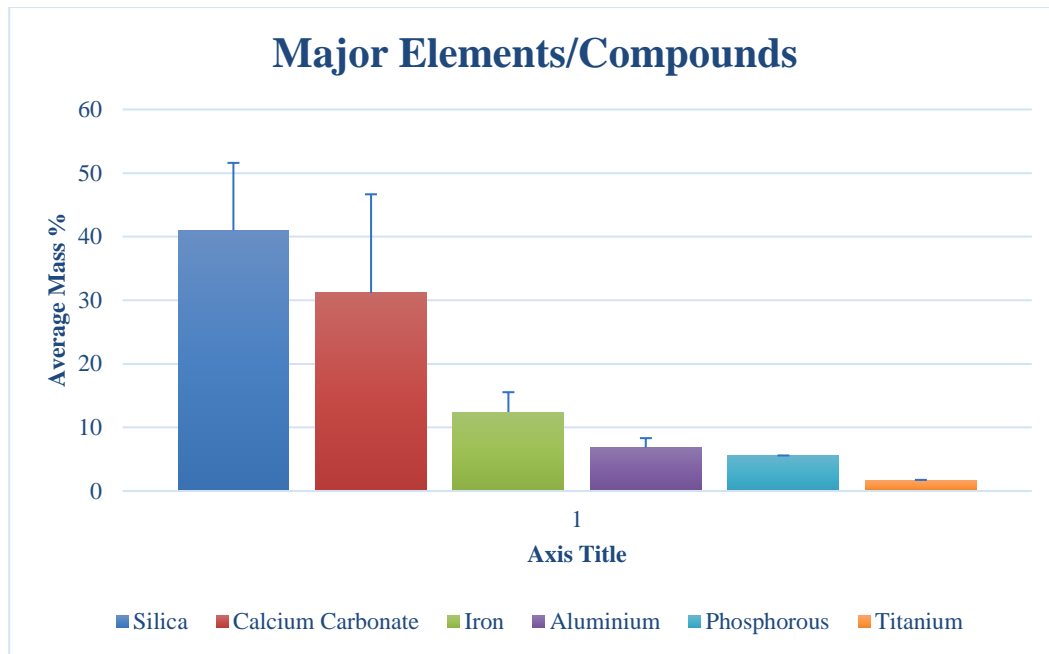


Figure 4-18: Graph of major elements and error bars of the s.e for overburden samples

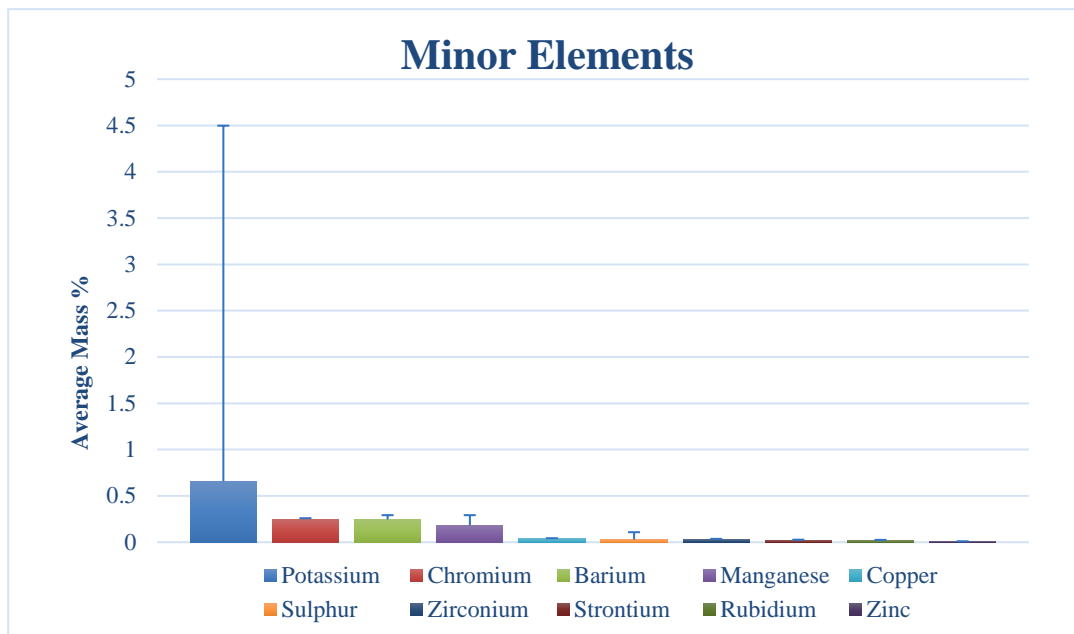


Figure 4-19: Graph of minor elements and error bars of the s.e for overburden samples

The chemical elements and compounds in the solid mine waste due to mining activities compare to results from Cheneket (2018) studies in the same mine determining potentially toxic elements concentrations in the soil. He et al., (2019) research on waste gangue from coarse iron ore using XRF analysis revealed elements such as *Fe*, *Si*, *S*, *Mg*, *Al*, and *Ca*, and oxides compounds, this also compares to the results in this research.

4.3.2. Mineral Composition

XRD technique was used successfully to determine the mineral composition of the solid mine waste samples as presented below;

a. Waste Dump Samples

The XRD results for the waste dump, as shown in the spectra in Figures (4-21, 4-22, and 4-23) and Tables (4-10, 4-11, and 4-12), show Quartz and Berlinite minerals in high amounts. Helvine mineral, a silicate, was in high amounts in the third waste dump (WD3), and Magnetite and Braunite minerals were in low quantities.

i. Waste Dump Sample 1 (WD1)

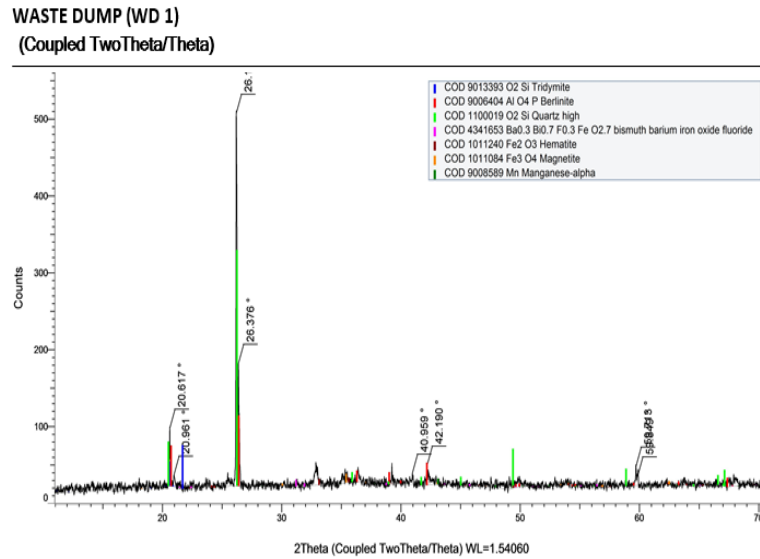


Figure 4-20: Phase graph of waste dump sample 1

Table 4-10: Mineralogical composition of wd 1

| Mineral | Chemical Formula | Weight % |
|-----------------|------------------|----------|
| Quartz | SiO_2 | 50.5 |
| Tridymite | SiO_2 | 32.2 |
| Berlinite | $Al (PO_4)$ | 12.3 |
| Hematite | Fe_2O_3 | 1.9 |
| Magnetite | Fe_3O_4 | 1.6 |
| Manganese-alpha | Mn | 0.8 |

ii. Waste Dump Sample 2 (WD 2)

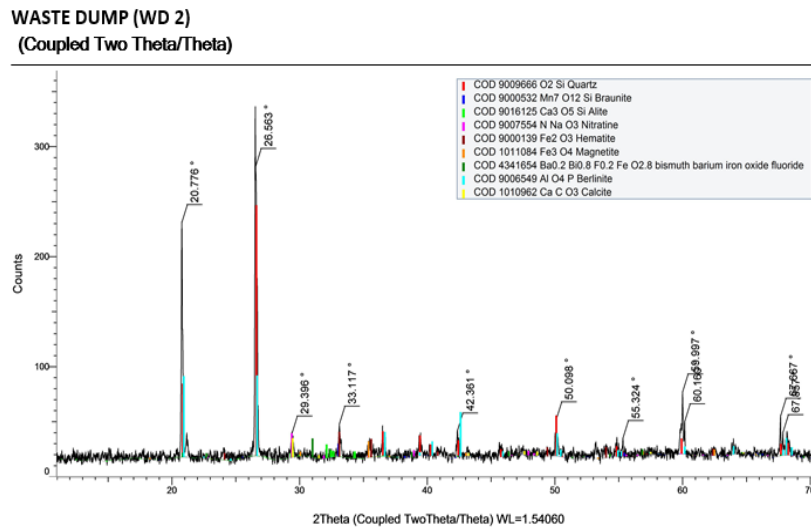


Figure 4-21: Phase graph of waste dump sample 2

Table 4-11: Mineralogical composition of wd 2

| Mineral | Chemical Formula | Weight % |
|-----------|-----------------------------------|----------|
| Quartz | SiO_2 | 42.7 % |
| Berlinite | $Al(PO_4)$ | 23.0 % |
| Alite | Ca_3O_5Si | 13.4 % |
| Nitratine | $Na(NO_3)$ | 6.9 % |
| Hematite | Fe_2O_3 | 5.1 % |
| Calcite | $CaCO_3$ | 3.9 % |
| Magnetite | Fe_3O_4 | 2.1 % |
| Braunitz | $Mn^{2+}Mn^{3+}(O_8 \cdot SiO_2)$ | 1.8 % |

iii. Waste Dump Sample 3 (WD 3)

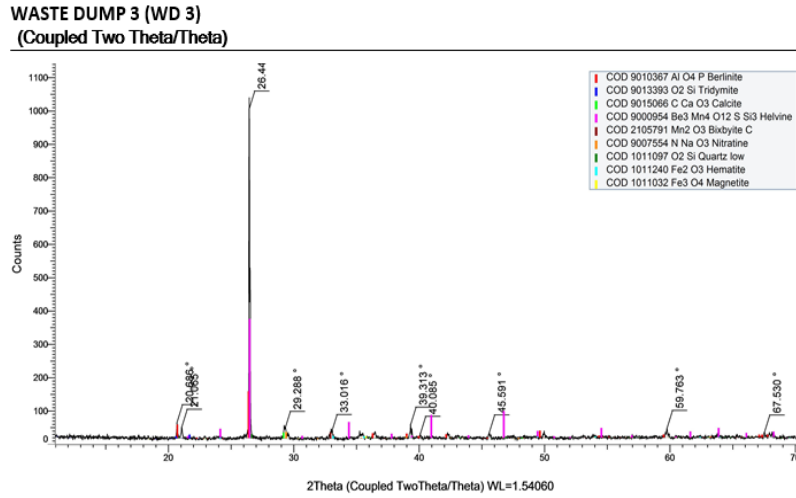


Figure 4-22: Phase graph of waste dump sample 3

Table 4-12: Mineralogical composition of wd 3

| Mineral | Chemical Formula | Weight % |
|------------|---------------------------|----------|
| Helvine | $Be_3Mn_4^{2+}(SiO_4)_3S$ | 54.7 % |
| Berlinite | $Al(PO_4)$ | 23.0 % |
| Tridymite | SiO_2 | 5.7 % |
| Nitratine | $NaNO_3$ | 5.4 % |
| Calcite | $CaCO_3$ | 4.2 % |
| Bixbyite C | $(Mn,Fe)_2O_3$ | 2.4 % |
| Quartz | SiO_2 | 2.2 % |
| Hematite | Fe_2O_3 | 1.7 % |
| Magnetite | Fe_3O_4 | 0.8 % |

a. Stockpile Samples

The predominant crystalline element in the stockpile samples is hematite and magnetite. Quartz and bismuth Barium Iron Oxide Fluoride minerals were in low amounts, as shown in spectra graphs for XRD analysis shown in Figures (4-24, 4-25, and 4-26), and the weight percentages for each mineral as shown in Tables (4-13, 4-14 and 4-15).

i. Stockpile Sample 1 (SP 1)

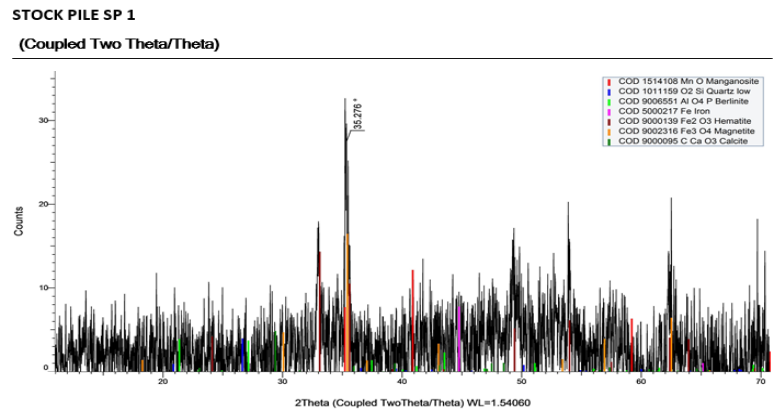


Figure 4-23: Phase graph of stockpile (sp 1) sample 1

Table 4-13: Mineralogical composition of sp 1

| Compound Name | Chemical Formula | Weight % |
|---------------|------------------|----------|
| Hematite | Fe_2O_3 | 29.0 % |
| Magnetite | Fe_3O_4 | 21.1 % |
| Manganosite | MnO | 16.6 % |
| Berlinite | $Al(PO_4)$ | 11.6 % |
| Calcite | $CaCO_3$ | 10.8 % |
| Quartz low | SiO_2 | 6.3 % |

ii. Stockpile Sample 2 (SP 2)

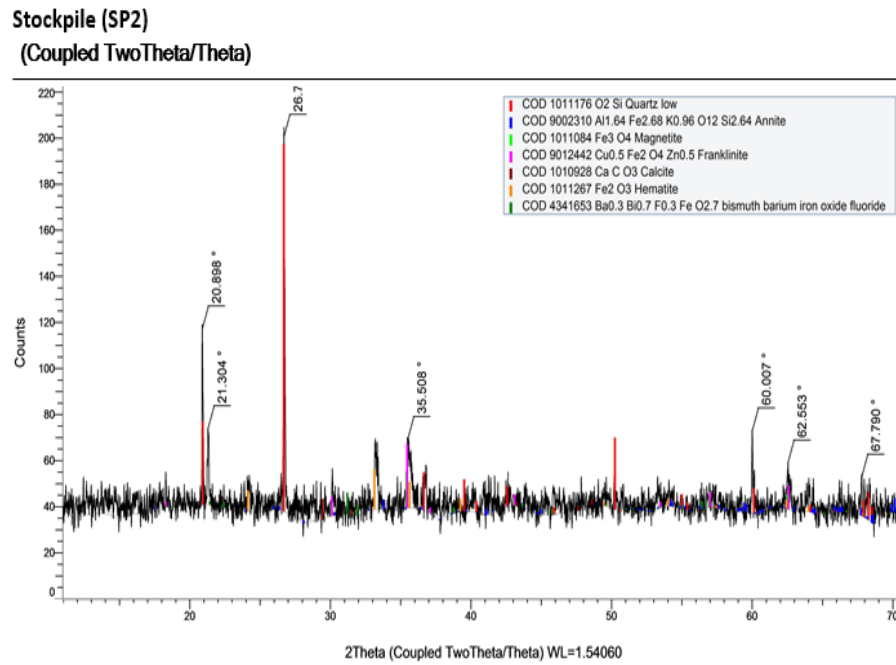


Figure 4-24: Phase graph of stockpile (sp 2) sample 2

Table 4-14: Mineralogical composition of sp 2

| Compound Name | Chemical Formula | Weight % |
|------------------------------------|---|----------|
| Quartz low | SiO_2 | 53.0 % |
| Annite | $KFe_2Al(Al_2Si_2O_{10})(OH)_2$ | 24.8 % |
| Franklinite | $ZnFe^{3+} \cdot 2 O_4$ | 6.7 % |
| Hematite | Fe_2O_3 | 5.7 % |
| Calcite | $Ca CO_3$ | 4.4 % |
| Magnetite | Fe_3O_4 | 4.2 % |
| Bismuth Barium Iron Oxide Fluoride | $BaO_2 \cdot BiO_8 \cdot FeO_{.8}^{2+}$ | 1.2 % |

iii. Stockpile Sample 3 (SP 3)

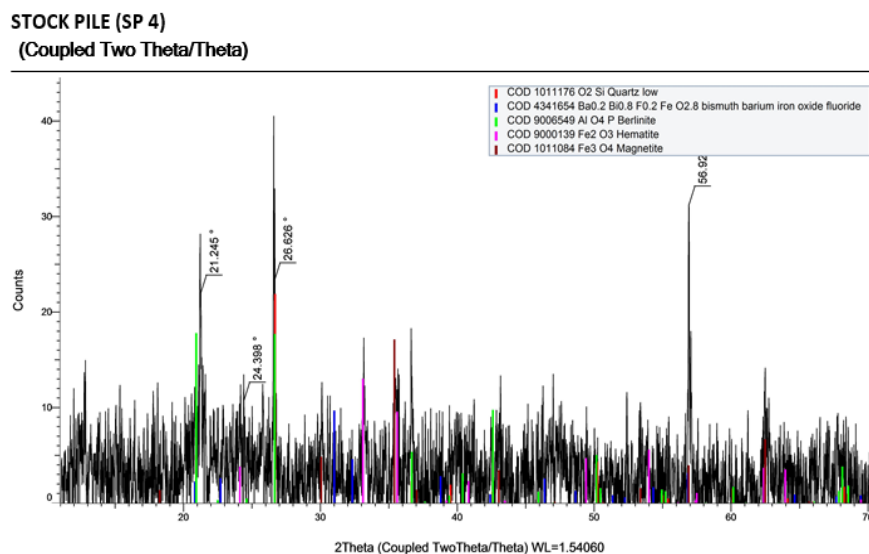


Figure 4-25: Phase graph of stockpile (sp 4) sample 4

Table 4-15: Mineralogical composition of sp 4

| Compound Name | Chemical Formula | Weight % |
|------------------------------------|--|----------|
| Berlinite | $Al(PO_4)$ | 36.2 % |
| Quartz low | SiO_2 | 25.2 % |
| Hematite | Fe_2O_3 | 18.9 % |
| Magnetite | Fe_3O_4 | 15.7 % |
| Bismuth Barium Iron Oxide Fluoride | $BaO_2 \cdot BiO_8 \cdot FeO_{0.8}^{2+}$ | 4.1 % |

a. Overburden Samples

Berlinite and Quartz revealed high phases in the overburden samples, as shown in Figures (4-27, 4-28, and 4-29). Hematite and Calcite minerals were in low amounts in the overburden

samples. The weight percentage for the individual minerals is shown in Tables 4-16, 4-17, and 4-18, respectively.

i. Overburden Sample 2 (OB 2)

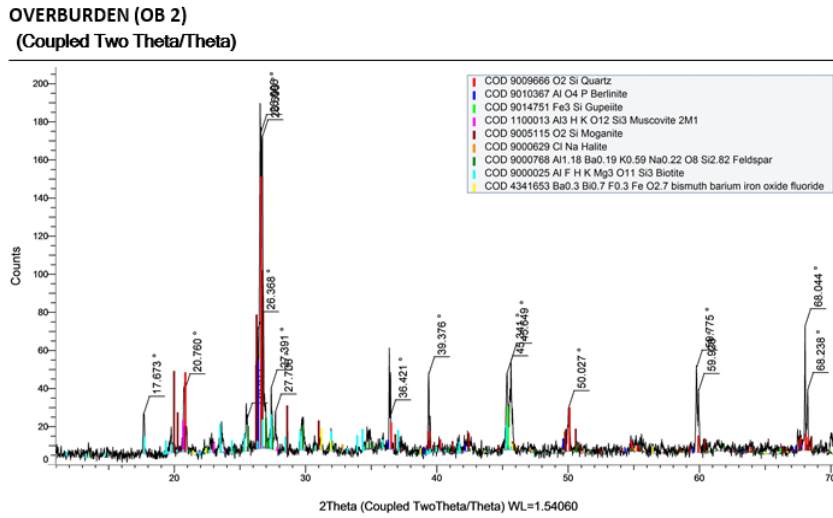


Figure 4-26: Phase graph of overburden material (ob2) sample 2

Table 4-16: Mineralogical composition of ob

| Compound Name | Chemical Formula | Weight % |
|------------------------------------|--------------------------------------|----------|
| Biotite | $K(Mg, Fe)_3(AlSi_3O_{10})(F, OH)_2$ | 34.5 % |
| Moganite | SiO_2 | 32.5 % |
| Quartz | SiO_2 | 15.3 % |
| Feldspar | $CaAlSi_3O_8$ | 8.3 % |
| Berlinite | $Al(PO_4)$ | 5.0 % |
| Muscovite | $KAl_2(AlSi_3O_{10})(F, OH)_2$ | 2.5 % |
| Gupeite | $Fe_3 Si$ | 1.0 % |
| Bismuth Barium Iron Oxide Fluoride | $BaO_2. BiO_8. FeO_{.8}^{2+}$ | 0.5 % |

ii. Overburden Sample 3 (OB 3)

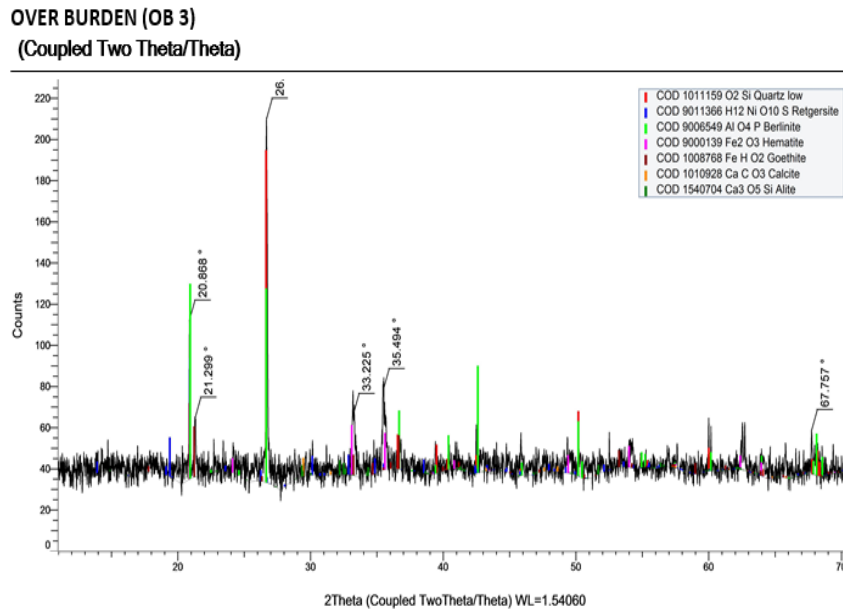


Figure 4-27: Phase graph of overburden material (ob3) sample 3

Table 4-17: Mineralogical composition of ob 3

| Compound Name | Chemical Formula | Weight % |
|---------------|-----------------------|----------|
| Berlinite | $Al (PO_4)$ | 32.5 % |
| Quartz low | SiO_2 | 31.2 % |
| Retgersite | $NiSO_4 \cdot 6 H_2O$ | 14.7 % |
| Goethite | $FeO(OH)$ | 6.7 % |
| Alite | Ca_3O_5Si | 6.5 % |
| Hematite | Fe_2O_3 | 5.9 % |
| Calcite | $Ca CO_3$ | 2.5 % |

iii. Overburden Sample 4 (OB 4)

Table 4-18: Mineralogical composition of ob 4

| Compound Name | Chemical Formula | Weight % |
|--|--|----------|
| Qingheite | $NaMn^{3+}Mg(Al, Fe^{3+})(PO_4)_3$ | 31.5 % |
| Quartz | SiO_2 | 28.9 % |
| Retgersite | $NiSO_4 \cdot 6 H_2O$ | 13.9 % |
| Hematite | Fe_2O_3 | 8.3 % |
| Lanarkite | $Pb_2(SO_4)O$ | 7.9 % |
| Magnetite | Fe_3O_4 | 5.2 % |
| Calcite | $Ca CO_3$ | 3.3 % |
| Bismuth Barium Iron Oxide Fluoride | $BaO_2 \cdot BiO_8 \cdot FeO \cdot 8^{2+}$ | 0.9 % |

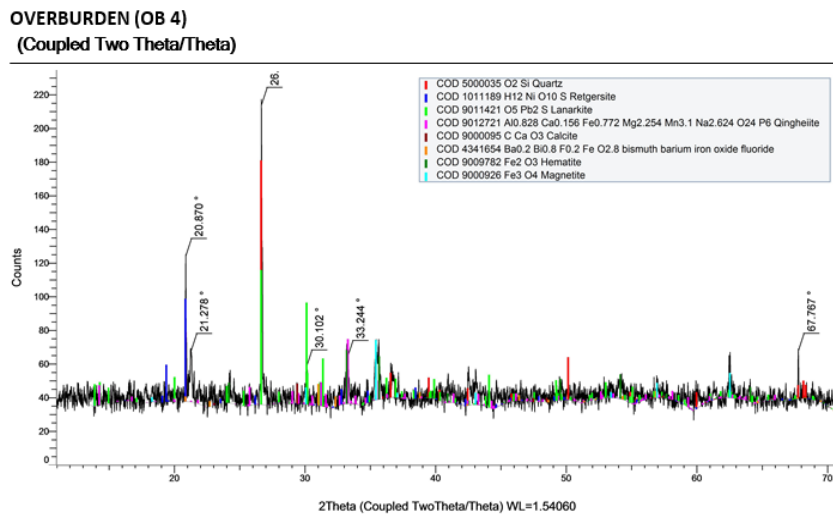


Figure 4-28: Phase graph of overburden material (ob4) sample 4

From the XRD results analysis, it is evident that the predominant minerals in the waste dump samples are silicate minerals such as quartz, helvine, and tridymite. In contrast, minerals such

as hematite and magnetite exist in traces. There is also a considerable amount of calcites and berlinite in the waste dumps.

The dominant crystalline element in the stockpile samples is hematite and magnetite minerals which showed very high phase. Silicate minerals and bismuth barium iron oxide have low phases. In contrast, minerals such as franklinite and annite were in considerable amounts. Berlinite, biotite, and qingheiite minerals were dominant, whereas feldspar, berlinite, and retgersite minerals were in significant quantities. Bismuth barium iron oxides in low amounts. These results compare to research done by Kiptarus et al. (2015) on iron ores from Kitui County and findings by Cheneket (2018a) at Kishushe area to evaluate the impacts of iron ore on potentially toxic elements concentration in soils in areas surrounding the mine site.

4.3.3. Mineral Crystallization

The petrographic analysis was applied successfully to study and determine solid mine waste samples' mineral crystallization and transparent constituents. The results are as follows;

a. Waste dump Samples

A thin section of the waste dump sample (Figure 4-30) shows minerals with dominant opaque dark grey color, indicating traces of magnetite and the rust-like colors of brown-red iron hydroxide (hematite). The white, pink color indicates the quartz. Feldspar is structured in a network with intrusions of quartz. There are olivine, biotite, and zircon minerals appearing in between mineral grains of magnetite.

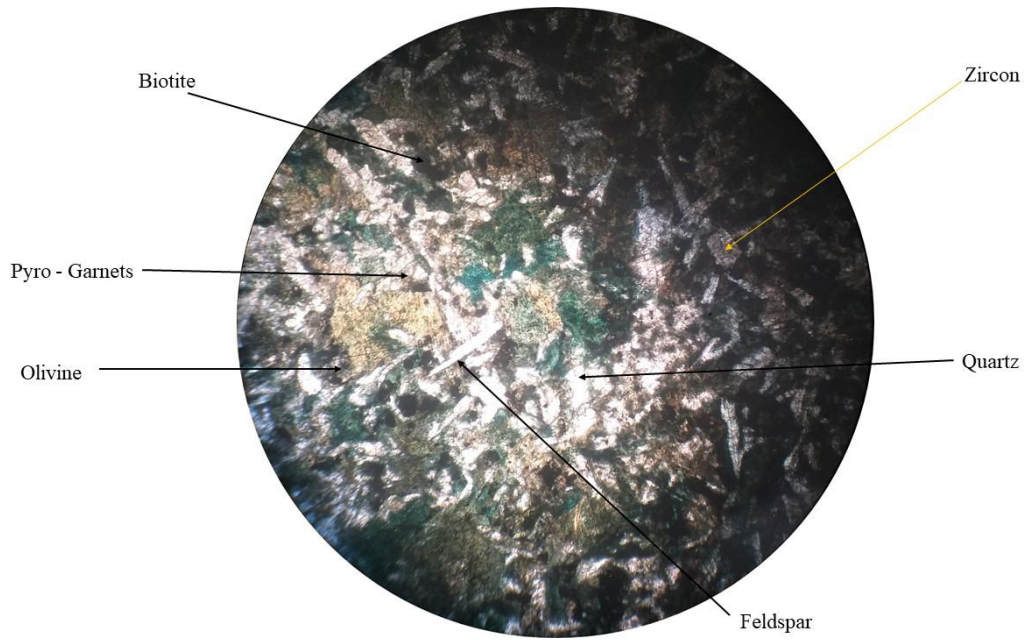


Figure 4-29: Thin section of waste dump sample in ppl

b. Stockpile Sample

The thin section of stockpile sample 1 (SP1) consists of magnetite, pyro - garnets, quartz, biotite, and hematite minerals. The dark opaque visible color in the thin sections is the magnetite, as shown in Figure 4-31. The whitish color indicates the biotite iron ore and bands of quartz assuming different shades. The brownish-grey color indicates martitized magnetite in the sample hence occurring as Hematite.

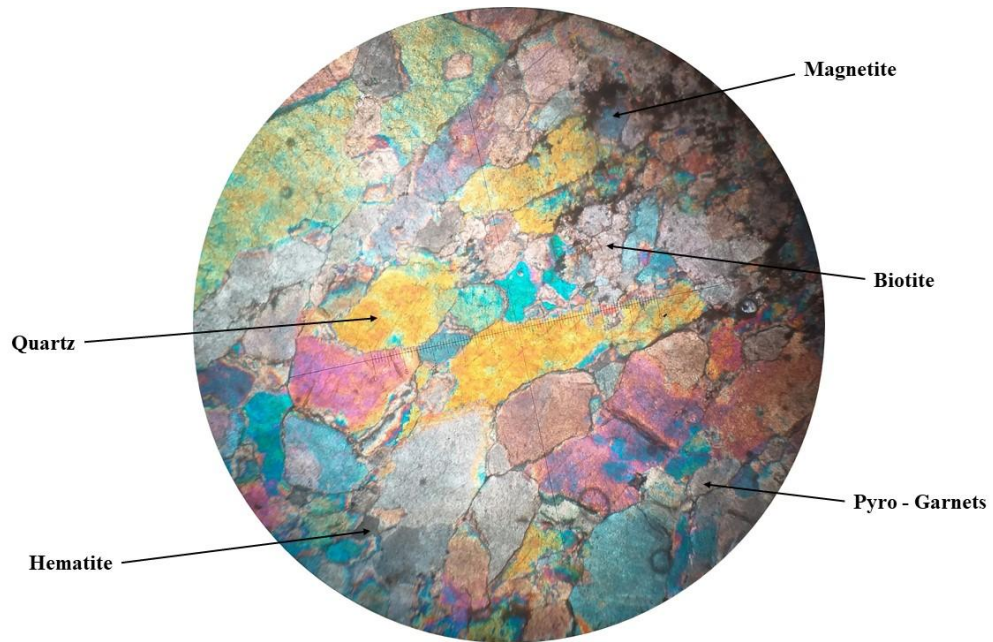


Figure 4-30: Thin section of stockpile sample 2 in x.p.l

Figure 4-32 shows that magnetite is the dominant mineral in stockpile sample 2 (SP2). It occurs as opaque; however, hematite occurs as a brownish color. The solid waste is characterized by specula and simple lamellae texture with mutual grain boundaries between various mineral intrusions suggesting that the minerals break along the grain boundaries.

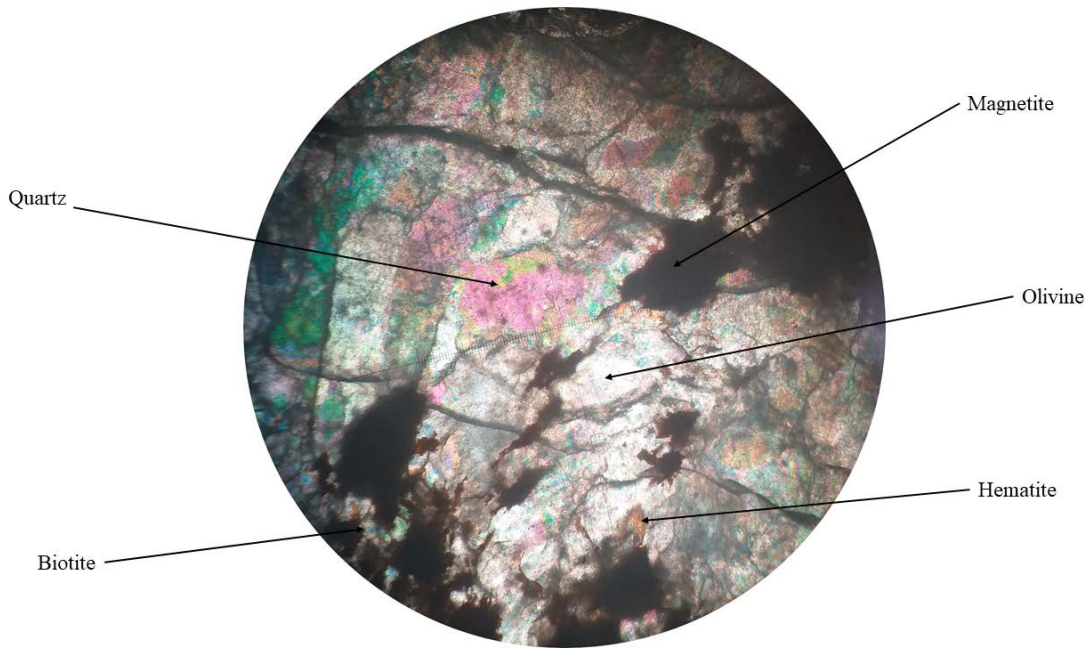


Figure 4-31: Thin section of stockpile sample 3 in x.p.l

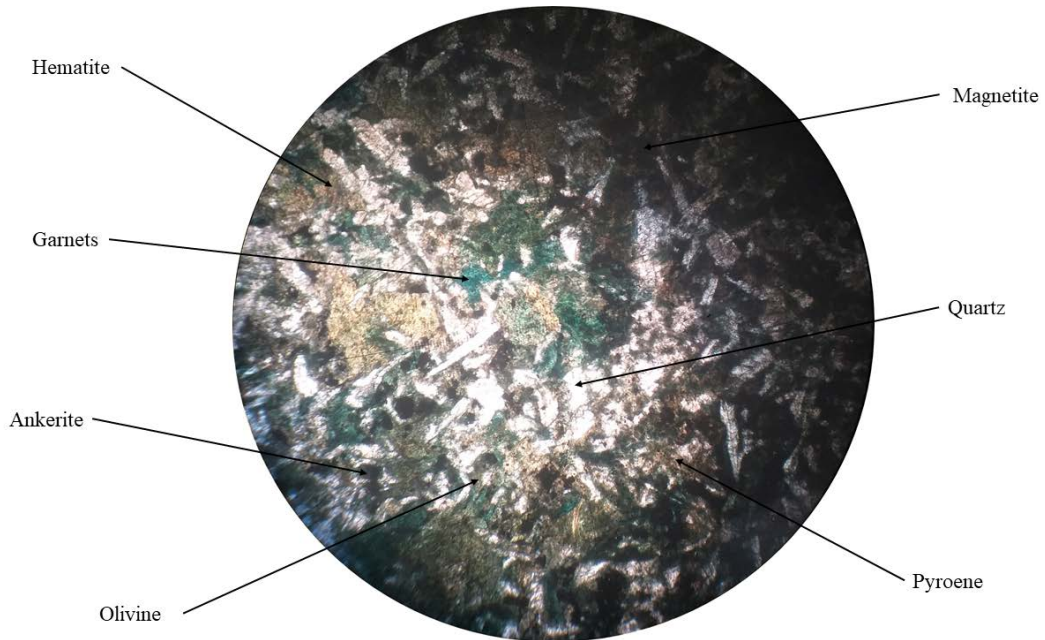


Figure 4-32: Thin section of stockpile 1 (s.p. 1) in ppl

Sample of stockpile (SP3) (Figure 4-33) contains high amounts of magnetite and hematite minerals occurring in opaque and brown shades. There are traces of gangue minerals such as quartz, pyroxene, garnet, and olivine minerals in the sample. The occurrence of the individual grains, which are well-formed, exhibit resistance to weathering. Grain boundaries also separate different minerals with varying sizes without individual grains interlocking.

c. Overburden samples

The overburden material sample generally occurs, and needlelike crystals of feldspar with inclusions of quartz, mica, and shades of pyroxene as viewed in Figure 4-34.

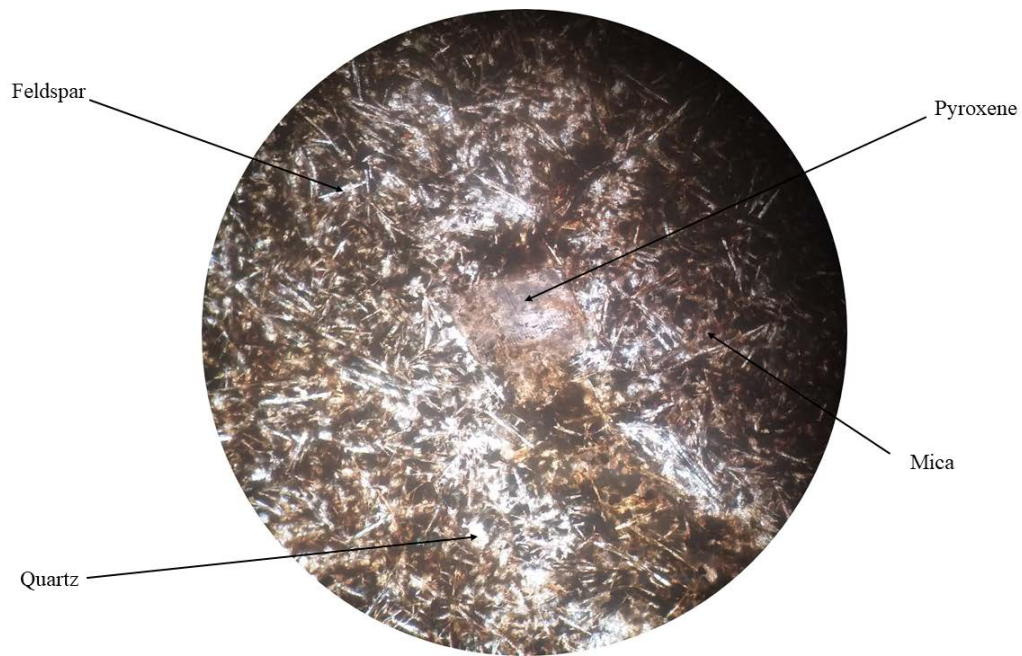
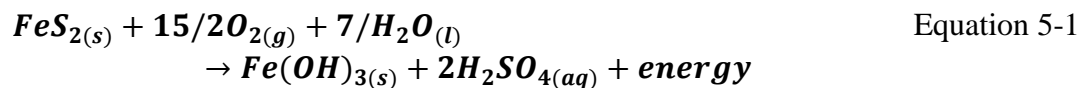


Figure 4-33: Thin section of overburden material (o.b. 4) in x.p.l

Most of the environmental impacts of iron ore mining and processing are associated with releasing various toxic elements from the mine wastes produced (Gabre et al., 2015). These mine wastes pose severe problems because of the volumes produced and the areal extent and

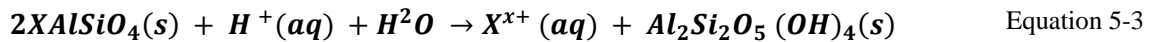
coverage (St-Arnault et al., 2020). They also impact the ecosystems negatively (Kakaie et al., 2019). Due to the continuous pollution and contamination, solid mine wastes from iron ore mining must be isolated and treated to reduce oxidation, erosion, toxicity or dumped in well-designed waste dumps to be used for other purposes after mining operations (Pagona et al., 2020). These contaminants in these solid mine wastes may travel through the soil, water, biosphere, and atmosphere to cause environmental impacts (Frascoli & Hudson-Edwards, 2018). Most of the adverse environmental effects caused by solid mine wastes are their tendencies to chemically react with available water or air hence producing contaminants (Assawincharoenkij et al., 2017a). Airborne dust and winds may also cause the transportation of these chemical elements in solid mine waste to soils and surface water (Jamieson et al., 2015).

There is a presence of considerable amounts of Sulphide minerals such as pyrite (FeS_2), helvine ($Be_3Mn^{2+}_4(SiO_4)_3S$), and sphalerite (ZnS) in the stockpile and waste dump samples. Exposure of these sulfide elements to an oxygenated environment, surface runoff, and groundwater will cause the sulfides to be oxidized, rendering it chemically unstable, producing acid that can produce acid mine drainage (AMD). Direct oxidation for pyrite mineral likely to occur is presented in equation 5-1, whereby the atmospheric oxygen may oxidize the sulphide minerals to produce dissolved ferrous hydroxide and sulphuric acid that has adverse effects on the environment (Akoto & Anning, 2021)



These mine wastes also contain phosphates, silicates, oxides, hydroxides, carbonates, and halides.

The chemical weathering of silicate minerals consumes hydrogen (Mungai, 2014). This occurs as an incongruent or congruent weathering process. The mineral's complete dissolution and soluble components are produced during congruent weathering, but the silicate mineral is altered to another phase (Bernd G. Lottermoser, 2011). The solid mine waste at SRKL Iron Ore Mine contains silicates such as pyroxenes, olivines, garnets, amphibole, feldspar, and micas. Therefore, a reaction is shown in Equations 5-2 and 5-3 may likely occur in the location where they are dumped.



Where *X* may be *Ca*, *Na*, *K*, *Mg*, or *Fe*

Weathering of silicates produces silicic acid and dissolved cations, and secondary minerals formation (He et al., 2019). These products may be the sources of environmental pollution in the mine.

The presence of carbonate minerals in some of these solid mine wastes has played a crucial part in neutralizing the acids generated from sulfide oxidations. During acidity neutralization, the pH and alkalinity in water increase (Jamieson et al., 2015). Different minerals have

different lifetimes of reactivity and weathering. Olivines tend to react more as compared to quartz (Almeida et al., 2018).

Mineral crystallization also plays a major role in chemical reactions. The minerals are likely to weather along the grain boundaries and increase their potential exposure to oxidation. Petrography analysis also revealed poorly crystalline samples with structural defects that contained distorted crystal lattice. This eventually leads to building up stresses in the rock structure, making the mineral susceptible to chemical attack.

CHAPTER FIVE

5. CONCLUSION AND RECOMMENDATIONS

5.1. Conclusion

In this study, characterization of solid waste generated from iron ore mining and processing at SRKL iron mine, Taita Taveta County, Kenya, was carried out. Firstly, the environmental pollutants from iron ore mining and processing operations were determined. Secondly, the extents and volumes of solid mine wastes from the SRKL mine were quantified. Finally, the geochemistry and the mineralogy of the solid mine wastes were effectively determined using XRF, XRD, and petrographic analysis.

5.1.1. Environmental Pollutants Resulting From Iron Ore Mining and Processing Operations at the Study Mine

The environmental pollutants that resulted from the iron ore mining and processing operations at SRKL mine were as follows:

1. Waste dumps – Drilling & blasting operations, screening & separation of iron ore and gangue
2. Stockpiles – Iron ore fines and low-grade iron ore
3. Overburden – produced during opening & mine advancing of open pit

5.1.2. The Extent and Volume of Dumps and Stockpiles of Solid Mining Wastes at the Study Mine

Findings from this research revealed solid mine waste such as waste dumps, stockpiles, and overburden that result from iron ore mining and processing at SRKL mine. This study also showed that by effectively applying GIS and Remote Sensing techniques, solid mine dynamic wastes could be quantified and easily monitored progressively during stages of mining. This can, in turn, assist in curbing environmental effects that may be likely to be felt by their deposition in the environment. This method, as proved, can be a relatively cost-friendly yet fast and reliable way to quantify the extents and the volumes dumped. The information on the areal extent and the volume of these wastes can assist the mining company in effectively planning for the rehabilitation and restoration of the areas affected by these wastes.

The following inferences from the quantification of the area and the volume of solid mine waste were noted:

1. Waste dumps – Occupied the most significant area, 136,100 m^2 at 54.58%
2. Iron ore stockpiles – Occupied the least area, 28,800 m^2 at 11.55 %
3. Overburden – Had the largest volume 303,477.52 m^3 at 58.58 %
4. Iron ore stockpile – Had the least volume 34,025.17 m^3 at 5.6 %

5.1.3. Properties of Solid Mining Wastes

Iron ore mining produces solid mine wastes that may be toxic and harmful to humans and the resulting environment. potentially toxic elements such as Chromium, Cadmium, Zinc, Manganese, and Copper were present. These elements present in the wastes are candidates for

environmental pollution and adverse effects due to their exposure to oxygen and water sources. The presence of sulphide minerals such as pyrite in the waste dumps may lead to the formation of acid mine drainage in the presence of water.

High amounts of iron in waste dumps inferred the level of dilution and selective mining done at SRKL mine. The waste dumps mainly consisted of blasted materials containing Sulphur, an agent of environmental pollution.

Poor crystalline in the samples analyzed and revealed from the petrographic analysis proved the possibility of weathering along mineral grains, increasing the surface area for chemical attacks.

The precise mineralogy and geochemistry of the solid mine waste may play a crucial role in predicting the environmental effects likely to be experienced if they are disposed of to the environment. This may require interdisciplinary efforts to determine these solid mine wastes and quantify their volume and areal extents as achieved in this research. Due to the adverse effects of the solid mine wastes, reducing their environmental and health impacts would require proper management and expertise. As seen in this research, understanding the interactions of solid mine waste to the various conditions can benefit the mining company.

5.2. Recommendations

In the future, a tool that integrates the dynamic volumes and areas of these solid wastes with real-time information for geochemistry and geochemical properties of the mine wastes needs to be created to address the issue of environmental pollution from solid mine waste at any mine as mining takes place in real-time.

Low-grade iron ore disregarded as waste could also be beneficiated further to avoid dumping on the environment, causing environmental impacts. The iron ore fines that are unutilized may also be alternatively used to reduce dumping into the environment. Studies by Chen (2016) proved that iron ore fines can be utilized as an alternative for alumina-silicate used in cement manufacturing and also provide raw material for brick making.

Dumping of the solid mine waste at SRKL mine remains a menace as their dispersion and leaching may potentially contaminate the environment. Historically, mine waste disposal techniques involved dumping the material in receiving ponds or returning the material to the mining site (Plumlee and Morman, 2011). Modern practices such as containing the mine wastes in embankments remain a common waste management technique and are highly recommended. Alternatively, waste materials may be returned to the mine and used for backfilling.

5.3. Recommendations for Further Study

1. This study can be expanded to cover a large area, mostly the regions neighboring the mining area towards Tausa and Oza Ranches.
2. Considering this study as a baseline study, other follow-up studies need to be undertaken to assess the mining operations impact in the area.
3. Further studies need to be conducted on the water sources neighboring the mine. Besides, the impact of the mining process on air quality needs to be assessed.

REFERENCES

- Abaidoo, C. A., Matthew, E., Jnr, O., & Arko-adjai, A. (2019). Monitoring the Extent of Reclamation of Small Scale Mining Areas Using Artificial Neural Networks. *Heliyon*, (March 2018), e01445.
- Akoto, R., & Anning, A. K. (2021). Heavy metal enrichment and potential ecological risks from different solid mine wastes at a mine site in Ghana. *Environmental Advances*, 3, 100028.
- Almeida, C. A., Oliveira, A. F. de, Pacheco, A. A., Lopes, R. P., Neves, A. A., & Lopes Ribeiro de Queiroz, M. E. (2018). Characterization and evaluation of sorption potential of the iron mine waste after Samarco dam disaster in Doce River basin – Brazil. *Chemosphere*, 209, 411–420.
- Alrashidi, M. (2016). *Surface Volume Calculation using ArcGIS*.
- Amos, R. T., Blowes, D. W., Bailey, B. L., Segó, D. C., Smith, L., & Ritchie, A. I. M. (2015). Waste-rock hydrogeology and geochemistry. *Applied Geochemistry*, 57, 140–156.
- Anyona, S., & Rop, B. K. (2015). Environmental Impacts of Artisanal and Small-scale Mining in Taita Taveta County. *Sustainable Research and Innovation*, 228–241.
- Apollo, F., Ndinya, A., Ogada, M., & Rop, B. (2017). Feasibility and acceptability of environmental management strategies among artisan miners in Taita Taveta County, Kenya. *Journal of Sustainable Mining*, 16(4), 189–195.
- Ashton, P., Love, D., Mahachi, H., & Dirks, P. (2001). An Overview of the Impact of Mining and Mineral Processing Operations on Water Resources and Water Quality in the Zambezi, Limpopo, and Olifants Catchments in Southern Africa.
- Assawincharoenkij, T., Hauzenberger, C., Ettinger, K., & Sutthirat, C. (2018). Mineralogical and geochemical characterization of waste rocks from a gold mine in northeastern Thailand: application for environmental impact protection.
- Assawincharoenkij, T., Hauzenberger, C., & Sutthirat, C. (2017a). Mineralogy and geochemistry of tailings from a gold mine in northeastern Thailand. *Human and Ecological Risk Assessment*, 23(2), 364–387.
- Assawincharoenkij, T., Hauzenberger, C., & Sutthirat, C. (2017b). Mineralogy and geochemistry of tailings from a gold mine in northeastern Thailand. *Human and Ecological Risk Assessment*, 23(2), 364–387.
- Aznar-Sánchez, J. A., García-Gómez, J. J., Velasco-Muñoz, J. F., & Carretero-Gómez, A. (2018). Mining waste and its sustainable management: Advances in worldwide research. *Minerals*, 8(7).
- Basommi, P. L., Guan, Q., & Cheng, D. (2015a). Exploring Land use and Land cover change in the mining areas of Wa East District, Ghana using Satellite Imagery. *Open Geosciences*, (1).
- Basommi, P. L., Guan, Q., & Cheng, D. (2015b). Exploring Land use and Land cover change in the mining areas of Wa East District, Ghana using Satellite Imagery. *Open Geosciences*, 7(1), 618–626.

- Bassi, S. (2015). What will it take for CSS to have a Future in the European Union? *Cornerstone - The Official Journal of World Coal Industry*, 3(4), 1–66.
- Bastos, L. A. de C., Silva, G. C., Mendes, J. C., & Peixoto, R. A. F. (2016). Using Iron Ore Tailings from Tailing Dams as Road Material. *Journal of Materials in Civil Engineering*, 28(10), 04016102.
- Bernd G. Lottermoser. (2011). Mine Wastes. In *Waste*.
- Bett, A. K. (2018). *Investigation on the beneficiation methods for local iron ore for making steel*.
- Bett, A. K., Onyango, J. A., Maranga, S. M., & Rop, B. K. (2016). *Quality of Iron ores in Kenya ; TharakaNithi and Samia*. (May), 4–6.
- Bett, G., Baru, K. J., Kabugu, M., & Rop, B. K. (2014). *Beneficiation of Iron Ore in Kishushe for the Steel Manufacturing Plant*. 5(May), 7–11.
- Blachowski, J. (2015). Gis-Based spatial assessment of rock minerals mining - A case study of the lower silesia region (sw Poland). *Mining Science*, 22, 7–22.
- Brouwer, P. (2010). Theory of XRF. In *Almelo: PANalytical BV*.
- Byers, H. L., McHenry, L. J., & Grundl, T. J. (2019). XRF techniques to quantify heavy metals in vegetables at low detection limits. *Food Chemistry: X*, 1(November 2018), 100001.
- Carrillo-Chávez, A., Salas-Megchún, E., Levresse, G., Muñoz-Torres, C., Pérez-Arvizu, O., & Gerke, T. (2014). Geochemistry and mineralogy of mine-waste material from a “skarn-type” deposit in central Mexico: Modeling geochemical controls of metals in the surface environment. *Journal of Geochemical Exploration*, 144, 28–36.
- Chen, J., Li, K., Chang, K.-J., Sofia, G., & Tarolli, P. (2015). Open-pit mining geomorphic feature characterisation. *International Journal of Applied Earth Observation and Geoinformation*, 42, 76–86.
- Cheneket, B. K. (2018a). *Impact Of Iron Ore Mining On Heavy Metal Concentration In Soils Of Kishushe Area In Wundanyi, Taita Taveta County*. University of Nairobi.
- Cheneket, B. K. (2018b). *Impact Of Iron Ore Mining On Heavy Metal Concentration In Soils Of Kishushe Area In Wundanyi, Taita Taveta County*.
- Choi, Y., Baek, J., & Park, S. (2020). Review of GIS-Based Applications for Mining: Planning, Operation, and Environmental Management. *Applied Sciences* , Vol. 10.
- Colburn, P., & Thorntorn, I. (2014). Lead pollution in agricultural soils. *Journal of Soil Science*, 29(4), 513–526.
- Dauce, P. D., Castro, G. B. de, Lima, M. M. F., & Lima, R. M. F. (2019). Characterisation and magnetic concentration of an iron ore tailings. *Journal of Materials Research and Technology*, 8(1), 1052–1059.

- David Meehan. (2012). *Life Cycle of a Mine*.
- Dias, B. M., Velázquez, V. F., Lucena, R. F., & Azevedo Sobrinho, J. M. (2020). Petrographic Microscope Digital Image Processing Technique for Texture and Microstructure Interpretation of Earth Materials. *Earth Science Research*, 9(1), 58.
- Dutta, S. K. (2020). *An Overview : Utilization of Iron Ore Fines and Steel Plant Wastes*. (August 2019).
- Ericsson, M., Löf, A., & Löf, O. (2021). Iron ore market report 2019-2020. *Gornaya Promyshlennost*, 2021(1), 74–82.
- Ferreira, H., & Leite, M. G. P. (2015a). A Life Cycle Assessment study of iron ore mining. *Journal of Cleaner Production*, 108, 1081–1091.
- Ferreira, H., & Leite, M. G. P. (2015b). A Life Cycle Assessment study of iron ore mining. *Journal of Cleaner Production*, 108, 1081–1091.
- Festin, E. S., Tigabu, M., Chileshe, M. N., Syampungani, S., & Odén, P. C. (2019). Progresses in restoration of post-mining landscape in Africa. *Journal of Forestry Research*, 30(2), 381–396.
- Frascoli, F., & Hudson-Edwards, K. A. (2018). Geochemistry, mineralogy and microbiology of molybdenum in mining-affected environments. *Minerals*, 8(2), 1–18.
- Gabr, S. S., Hassan, S. M., & Sadek, M. F. (2015). Prospecting for new gold-bearing alteration zones at El-Hoteib area, South Eastern Desert, Egypt, using remote sensing data analysis. *Ore Geology Reviews*, 71, 1–13.
- Geelani, M., Geelani, S. H., Haq, S. S., Mir, N. A., Qazi, G., & Wani, S. (2016). Mining and Its Impacts on Environment With Special Reference To Review Article Mining and Its Impacts on Environment With Special Reference To India. *International Journal of Current Research*, 5(12), 3586–3590.
- Gleeki, A. M. G. D., & Sah, H. B. (2012). *Assessment of Environmental Impacts of Iron Ore Mining and Its Mitigation Measures*. 200, 2012.
- Government of Kenya - GoK, S. (2019). *The Hansard*. Kenya: GOK.
- Harraz, H. Z. (2009). *The mining cycle*. (March), 5–6.
- He, J., Liu, C., Hong, P., Yao, Y., Luo, Z., & Zhao, L. (2019). Mineralogical characterization of the typical coarse iron ore particles and the potential to discharge waste gangue using a dry density-based gravity separation. *Powder Technology*, 342, 348–355.
- Hoseth, A. (2011). Google Scholar. *The Charleston Advisor*, 12.
- Hosseini, S. A. R., Gholami, H., & Esmailpoor, Y. (2019). Assessment of land use and land cover change detection by using remote sensing and gis techniques in the coastal deserts, South of Iran. *International Archives of the Photogrammetry, Remote Sensing and Spatial Information Sciences - ISPRS Archives*, 42(4/W18), 489–492.

- IHRB. (2019). Overview of Kenya's Extractive Sector. *Institute for Human Rights and Business* |, 3–11.
- ISO. (2017). *International Standard ISO: Iron ores — Experimental methods for checking the precision of sampling, sample preparation and measurement* *Minerais*.
- Jamali, A. (2019). A fit-for-purpose algorithm for environmental monitoring based on maximum likelihood, support vector machine and random forest. *International Archives of the Photogrammetry, Remote Sensing and Spatial Information Sciences - ISPRS Archives*, 42(3/W7), 25–32.
- Jamieson, H. E. (2011a). Geochemistry and mineralogy of solid mine waste: Essential knowledge for predicting environmental impact. *Elements*, 7(6), 381–386.
- Jamieson, H. E. (2011b). Geochemistry and Mineralogy of Solid Mine Waste: Essential Knowledge for Predicting Environmental Impact. *Elements*, 7(6), 381–386.
- Jamieson, H. E., Walker, S. R., & Parsons, M. B. (2015). Mineralogical characterization of mine waste. *Applied Geochemistry*, 57, 85–105.
- Jelenová, H., Majzlan, J., Amoako, F. Y., & Drahota, P. (2018). Geochemical and mineralogical characterization of the arsenic-, iron-, and sulfur-rich mining waste dumps near Kaňk, Czech Republic. *Applied Geochemistry*, 97, 247–255.
- John Obiri. (2014). *Extractive industries for sustainable development in kenya final assessment report*. (September).
- Joseph, K., Junior, K., & Matsui, K. (2018). *The Impact of Environmental Degradation by Surface Mining on Sustainable Agriculture in Ghana*. 2018(02), 1–5.
- Kakaie, R., Ataei, M., & Tavakoli Mohammadi, M. R. (2019). A review of studies on sustainable development in mining life cycle. *Journal of Cleaner Production*, 229, 213–231.
- Khan, I. (2016). *Land Use / Land Cover Change Due To Mining Activities in Singrauli Land Use / Land Cover Change Due To Mining Activities in Singrauli Industrial Belt , Madhya Pradesh Using Remote*. (December).
- Kiptarus, J. J., Muumbo, A. M., Makokha, A. B., & Kimutai, S. K. (2015). Characterization of Selected Mineral Ores in the Eastern Zone of Kenya: Case Study of Mwingi North Constituency in Kitui County. *International Journal of Mining Engineering and Mineral Processing*, 2015(1), 8–17.
- KNCHR. (2016). Public inquiry report on mining and impact on human rights. In *Taita Taveta County, 2016*.
- Knorr, K., & Bornefeld, M. (2005). Analysis of Iron Ore – A combined XRD, XRF and MLA study Iron. *Process Mineralogy 2012*, (May), 2–3.
- Krumbein, W. (2016). E. M. WINKLER, Stone: Properties, Durability in Man's Environment (2nd revised Edition). 230 S., 150 Abb., 38 Tab. Wien-New York 1975. Springer-Verlag. DM 91,00. *Zeitschrift Für Allgemeine Mikrobiologie*, 18(3), 230.

- Kuranchie, F. A. (2015). *Characterisation and Applications of Iron Ore Tailings in Buildings and Construction Projects*. 397. Retrieved from
- Landis, J. R., & Koch, G. G. (1977). A One-Way Components of Variance Model for Categorical Data
Published by : International Biometric Society Stable
- Lascalles, D. (2011). *Bedded martite/microplaty hematite- ore genesis: environmental evolution in the Palaeoproterozoic era*.
- Levett, A., Vasconcelos, P. M., Jones, M. M. W., Paz, A., Gagen, E. J., & Southam, G. (2020). Jo ur l
P re. *Chemical Geology*, 119955.
- Lin, Z. (2016). Leachate chemistry and precipitates mineralogy of rudolfsgruvan mine waste rock dump
in central Sweden. *Water Science and Technology*, 33(6), 163–171.
- Lindsay, M. B. J., Moncur, M. C., Bain, J. G., Jambor, J. L., Ptacek, C. J., & Blowes, D. W. (2015).
Geochemical and mineralogical aspects of sulfide mine tailings. *Applied Geochemistry*, 57, 157–
177.
- Lottermoser, B., & Lottermoser, B. (2003). Introduction to Mine Wastes. *Mine Wastes*, 1–30.
https://doi.org/10.1007/978-3-662-05133-7_1
- Luo, L., Zhang, Y., Bao, S., & Chen, T. (2016). Utilization of Iron Ore Tailings as Raw Material for
Portland Cement Clinker Production. *Advances in Materials Science and Engineering*, 2016,
1596047.
- Maranga, M., Bett, A. K., Ndeto, K., & Bett, G. (2013). *Kenyan Iron Ore: Mining and prospects of
processing*.
- Meli, R., Gadinga, W., Meli, V., & Nyuyki, B. (2020). The Egyptian Journal of Remote Sensing and
Space Sciences Multi-temporal forest cover change detection in the Metchie-Ngom Protection
Forest Reserve , West Region of Cameroon. *The Egyptian Journal of Remote Sensing and Space
Sciences*, 23(1), 113–124.
- Mengist, W., & Soromessa, T. (2020). MethodsX Method for conducting systematic literature review
and meta-analysis for environmental science research. *MethodsX*, 7, 100777.
- Mensah, A. K., Mahiri, I. O., Owusu, O., Mireku, O. D., Wireko, I., & Kissi, E. A. (2015).
Environmental impacts of mining: a study of mining communities in Ghana. *Applied Ecology and
Environmental Science*, 3(3), 81–94.
- Mi, J., Yang, Y., Zhang, S., An, S., Hou, H., & Hua, Y. (2019). *remote sensing Tracking the Land Use
/ Land Cover Change in an Area with Underground Mining and Reforestation via Continuous
Landsat Classification*. 1–22.
- Mineral Resources Department. (2008). *An Overview of South Africa's Iron, Manganese and Steel
inudstry for the Period 1986 to 2006*.
- Modabberi, S. (2018). Mineralogical and geochemical characterization of mining wastes: remining
potential and environmental implications, Muteh Gold Deposit, Iran. *Environmental Monitoring*

and Assessment, 190(12), 734.

- Mohr, S., Giurco, D., Yellishetty, M., Ward, J., & Mudd, G. (2015). Projection of Iron Ore Production. *Natural Resources Research, 24(3), 317–327.*
- Mungai, G. (2014). *AN INVESTIGATION OF MINERALS IN THE WATER AND SOURCE ROCKS OF RURII BY.*
- Munyao Mulwa, B., Muchori Maina, D., & Pushotami Patel, J. (2012). Multielemental Analysis of Limestone and Soil Samples of Kitui South (Kenya) Limestone Deposits. *International Journal of Fundamental Physical Sciences, 2(4), 48–51.*
- Muwanguzi, A. J. B., Karasev, A. V., Byaruhanga, J. K., & Jönsson, P. G. (2012). Characterization of Chemical Composition and Microstructure of Natural Iron Ore from Muko Deposits. *ISRN Materials Science, 2012, 1–9.*
- Mwakumanya, M. A., Maghenda, M., & Juma, H. (2016). Socio-economic and environmental impact of mining on women in Kasigau mining zone in Taita Taveta County. *Journal of Sustainable Mining, 15(4), 197–204.*
- Mwandawiro, M. (2011). Heinrich Böll Stiftung, East and Horn of Africa All. In *Mining in Taita Taveta County: Prospects & Problems.*
- National Minerals Information Center, U. G. S. (2017). Global Iron Ore Production. *US Geological Survey, (February), 20–23.*
- Nordstrom, D. K. (2011). Mine waters: Acidic to circumneutral. *Elements, 7(6), 393–398.*
<https://doi.org/10.2113/gselements.7.6.393>
- Ochieng, G. M., Seanego, E. S., & Nkwonta, O. I. (2010). Impacts of mining on water resources in South Africa: A review. *Scientific Research and Essays, 5(22), 3351–3357.*
- Odoh, B., Kenneth, C., Kalu, A. U., & Francis, A. (2017). Environmental Impacts of Mineral Exploration in Nigeria and their Phytoremediation Strategies for Sustainable Ecosystem. *Journal of Environmental Management, (January), 19–27.*
- Orimoloye, I. R., & Ololade, O. O. (2020). Spatial evaluation of land-use dynamics in gold mining area using remote sensing and GIS technology. *International Journal of Environmental Science and Technology, 17(11), 4465–4480.*
- Overman, F., & Overman, F. (2011). Iron Ore. In *The Manufacture of Iron.*
- Pagona, Tzamos, E., Grieco, G., Zouboulis, A., & Mitrakas, M. (2020). Characterization and evaluation of magnesite ore mining by-products of Gerakini mines (Chalkidiki, N. Greece). *Science of the Total Environment, 732, 139279.*
- Pattanaik, A., & Venugopal, R. (2018). Investigation of Adsorption Mechanism of Reagents (Surfactants) System and its Applicability in Iron Ore Flotation – An Overview. *Colloids and Interface Science Communications, 25(December 2017), 41–65.*

- Peter, K. K., Gilbert, B. K., & Bernard, R. K. (2015). The Implications of Geology and Structure on Iron Ore Mining at Wanjala Mine , Taita-Taveta County , Kenya. *Proceedings of the Sustainable Research and Innovation (SRI) Conference 6 - 8 May, 2015*, 70–73.
- Pilon-Smits, E. (2005). Phytoremediation. *Annu. Rev. Plant Biol.*, 56, 15–39.
- Plumlee, G. S., & Morman, S. A. (2011). *and Human Health*. (March 2016).
- Pranab Das, Beulah Matcha, Nabil Hossiney, Mothi Krishna Mohan, A. R. and A. K. (2018). *Utilization of Iron Ore Mines Waste as Civil Construction Material through Geopolymer Reactions*. 18.
- Prospecting, A. M. E. &. (2011). *Enironmental Effect Assessment for Mineral Exploration & Prospecting*. (July).
- Raeva, P. L., Filipova, S. L., & Filipov, D. G. (2016). Volume computation of a stockpile - A study case comparing GPS and uav measurements in an open pit quarry. *International Archives of the Photogrammetry, Remote Sensing and Spatial Information Sciences - ISPRS Archives, 2016-Janua*(June), 999–1004.
- Rahman, A. A. A., Maulud, K. N. A., Mohd, F. A., Jaafar, O., & Tahar, K. N. (2017). Volumetric calculation using low cost unmanned aerial vehicle (UAV) approach. *IOP Conference Series: Materials Science and Engineering*, 270(1). <https://doi.org/10.1088/1757-899X/270/1/012032>
- Raju, A. (2020). *COMPARATIVE STUDY ON METHODS OF CREATING GEODATABASE USING*. 11(8), 13–21.
- Rea, S. M., McSweeney, N. J., Dwyer, R. B., & Bruckard, W. J. (2015). 13 - Application of biotechnology in iron ore beneficiation. In L. Lu (Ed.), *Iron Ore* (pp. 373–391).
- Rhodes, R. K. (2017). *UAS as an Inventory Tool: A Photogrammetric Approach to Volume Estimation*. 115.
- Robertson, L. D., & King, D. J. (2011). Comparison of pixel-and object-based classification in land cover change mapping. *International Journal of Remote Sensing*, 32(6), 1505–1529.
- Roller, J. (2011). X-ray diffraction. *PEM Fuel Cell Diagnostic Tools*, 289–313.
- Rop. K.B. (2014). Economic and Job Creation Potential of Artisanal and Small-Scale Mining In Taita Taveta County. *Undp Report*, 1–137.
- Roy, S. K., Nayak, D., & Rath, S. S. (2020). A review on the enrichment of iron values of low-grade Iron ore resources using reduction roasting-magnetic separation. *Powder Technology*, 367, 796–808.
- Rs, F., & Limited, M. (2012). *Geochemical Characterisation of Mine Waste and Tailings Implications for Mine Waste Management*.
- Rwanga, S. S., & Ndambuki, J. M. (2017). Accuracy Assessment of Land Use/Land Cover Classification Using Remote Sensing and GIS. *International Journal of Geosciences*, 08(04), 611–622.

- Sadeghi, B., & Khalajmasoumi, M. (2014). A futuristic review for evaluation of geothermal potentials using fuzzy logic and binary index overlay in GIS environment. *Renewable and Sustainable Energy Reviews*, 43, 818–831.
- Sang, K. K. (2020). *Designing Material Handling System Based On Volumes Extracted Using UAV-Based Photogrammetry*. 1(2), 88–100.
- Sarvamangala, H., A. Natarajan, K., & T. Girisha, S. (2012). Biobeneficiation of Iron Ores. *International Journal of Mining Engineering and Mineral Processing*, 1(2), 21–30.
- Shrimali, K., Jin, J., Hassas, B. V., Wang, X., & Miller, J. D. (2016). The surface state of hematite and its wetting characteristics. *Journal of Colloid and Interface Science*, 477, 16–24.
- Sikaundi, G. (2015). *Copper Mining Industry in Zambia*. 1, 1–14.
- Siljander, M., Adero, N., Francis, G., & Nyambu, E. (2019). *Land-use land-cover classification for the iron mining site of Kishushu, Kenya: A feasibility study of traditional and machine learning algorithms*. 1(September), 1–24.
- Singh, M., Kumar, S., Kumar, S., Nandan, G., & Gupta, M. (2018). Characterization of Iron-ore suspension at In-situ conditions. *Materials Today: Proceedings*, 5(9), 17845–17851.
- Ssenku, J., Ntale, M., Backeus, I., & Oryem-Origa, H. (2017). Phytoremediation Potential of *Leucaena leucocephala* (Lam.) de Wit. for Heavy Metal-Polluted and Heavy Metal-Degraded Environments.
- St-Arnault, M., Vriens, B., Blaskovich, R., Aranda, C., Klein, B., Ulrich Mayer, K., & Beckie, R. D. (2020). Geochemical and mineralogical assessment of reactivity in a full-scale heterogeneous waste-rock pile. *Minerals Engineering*, 145(October 2019), 106089.
- Stumbea, D., Chicoş, M. M., & Nica, V. (2019). Effects of waste deposit geometry on the mineralogical and geochemical composition of mine tailings. *Journal of Hazardous Materials*, 368(January), 496–505.
- Suleman, H. A., & Baffoe, P. E. (2017). Selecting Suitable Sites for Mine Waste Dumps Using GIS Techniques at Goldfields, Damang Mine. *Ghana Mining Journal*, 17(1), 9-17–17.
- Torres, E., Lozano, A., Macías, F., Gomez-Arias, A., Castillo, J., & Ayora, C. (2018). Passive elimination of sulfate and metals from acid mine drainage using combined limestone and barium carbonate systems. *Journal of Cleaner Production*, 182,
- Tucci, G., Gebbia, A., Conti, A., Fiorini, L., & Lubello, C. (2019). Monitoring and computation of the volumes of stockpiles of bulk material by means of UAV photogrammetric surveying. *Remote Sensing*, 11(12).
- Vajda, S., Dem'yanov, V. F., Malozemov, V. N., & Louvish, D. (2016). Introduction to Mining. *Journal of the Royal Statistical Society. Series A (General)*, 139(4), 276.
- Verity, E., & Kang, M. (2013). *Land Conflicts in Taita Taveta, 1963 - 2010*.

- Verma, P., Raghubanshi, A., Srivastava, P. K., & Raghubanshi, A. S. (2020). Appraisal of kappa-based metrics and disagreement indices of accuracy assessment for parametric and nonparametric techniques used in LULC classification and change detection.
- Wei, L., Zhang, Y., Zhao, Z., Zhong, X., Liu, S., Mao, Y., & Li, J. (2018). Analysis of mining waste dump site stability based on multiple remote sensing technologies.
- Wilson, S. A. (2019). Mining-induced displacement and resettlement: The case of rutile mining communities in Sierra Leone.
- Wu, S., Liu, Y., Southam, G., Robertson, L., Chiu, T. H., Cross, A. T., ... Huang, L. (2019). Geochemical and mineralogical constraints in iron ore tailings limit soil formation for direct phytostabilization.
- Yankson, P. W. K., & Gough, K. V. (2019). Gold in Ghana: The effects of changes in large-scale mining on artisanal and small-scale mining (ASM). *Extractive Industries and Society*, 6(1), 120–128.
- Yellishetty, M., Ranjith, P. G., & Tharumarajah, A. (2010). Resources, Conservation and Recycling Iron ore and steel production trends and material flows in the world :
- Yilmaz, H. M. (2010). Close range photogrammetry in volume computing. *Experimental Techniques*, 34(1), 48–54.

APPENDICES

Appendix A: Py Script Code on Volume Computation

```
# -*- coding: utf-8 -*-  
  
# -----  
  
# Vol_SP1.py  
  
# Created on: 2020-04-13 11:20:56.00000  
  
# (generated by ArcGIS/ModelBuilder)  
  
# Description:  
  
# -----  
  
# Import arcpy module  
  
import arcpy  
  
# Local variables:  
  
VolumeSP1 = "c2020041108395736243data_GPX"  
  
Tin_Stockpile = "D:\\Francis Data Analysis\  
\\SHP_LULC_Kishushe_mine\\Tin_Stockpile"  
  
Rasterize_Stockpile = "d:\\francis data analysis  
shp_lulc_kishushe_mine\\file_geodatabase.gdb\\Rasterize_Stockpile"  
  
Vol_SP7_txt = "C:\\Users\\User\\Desktop\\GPX Wastes\\Vol_SP7.txt"  
  
# Process: Create TIN  
  
arcpy.CreateTin_3d(Tin_Stockpile, "PROJCS['Arc_1960_UTM_Zone_37S',  
GEOGCS['GCS_Arc_1960',DATUM['D_Arc_1960',SPHEROID['Clarke_1880_RGS',  
6378249.145,293.465]],  
PRIMEM['Greenwich',0.0],UNIT['Degree',0.0174532925199433]],  
PROJECTION['Transverse_Mercator'],PARAMETER['False_Easting',  
500000.0],PARAMETER['False_Northing',10000000.0],  
PARAMETER['Central_Meridian',39.0],PARAMETER['Scale_Factor',
```

```

0.9996],PARAMETER['Latitude_Of_Origin',0.0],UNIT['Meter',1.0]]",
"c2020041108395736243data_GPX Elevation Mass_Points <None>", "DELAUNAY")

# Process: TIN to Raster

arcpy.TinRaster_3d(Tin_Stockpile, Rasterize_Stockpile, "FLOAT", "LINEAR",
"OBSERVATIONS 250", "1")

# Process: Surface Volume

arcpy.SurfaceVolume_3d(Rasterize_Stockpile, Vol_SP7_txt, "ABOVE", "", "1", "0")

import arcpy

# Local variables:

Waste_1_gpx = "C:\\Users\\User\\Desktop\\GPX Wastes\\Waste_1.gpx"

FeatureClassWaste = "D:\\Francis_Analysis
et.al\\SHP_LULC_Kishushe_mine\\File_Geodatabase.gdb\\FeatureClassWaste"

TINWaste = "D:\\Francis_Analysis et.al\\SHP_LULC_Kishushe_mine\\TINWaste"

RasterizedWaste = "d:\\Francis_Analysis
et.al\\shp_lulc_kishushe_mine\\file_geodatabase.gdb\\RasterizedWaste"

WasteVol1_txt = "C:\\Users\\User\\Desktop\\GPX Wastes\\WasteVol1.txt"

# Process: GPX To Features

arcpy.GPXtoFeatures_conversion(Waste_1_gpx, FeatureClassWaste)

# Process: Create TIN

arcpy.CreateTin_3d(TINWaste,
"PROJCS['Arc_1960_UTM_Zone_37S',GEOGCS['GCS_Arc_1960',DATUM['D_Arc_1960',
SPHEROID['Clarke_1880_RGS',
6378249.145,293.465]],PRIMEM['Greenwich',
0.0],UNIT['Degree',0.0174532925199433]],PROJECTION['Transverse_Mercator'],PARAMETER['False_Easti
ng',500000.0],PARAMETER['False_Northing',1000000.0]
,PARAMETER['Central_Meridian',39.0],PARAMETER['Scale_Factor',0.9996],
PARAMETER['Latitude_Of_Origin',0.0],UNIT['Meter',1.0]]", "D:\\Francis_Analysis
et.al\\SHP_LULC_Kishushe_mine\\File_Geodatabase.gdb\\FeatureClassWaste'

Elevation Mass_Points <None>", "DELAUNAY")

# Process: TIN to Raster

```

```
arcpy.TinRaster_3d(TINWaste, RasterizedWaste, "FLOAT", "LINEAR", "OBSERVATIONS 250", "1")
```

```
# Process: Surface Volume
```

```
arcpy.SurfaceVolume_3d(RasterizedWaste, WasteVol1_txt, "ABOVE", "", "1", "0")
```

Appendix B: XRF (X-ray fluorescence) Analysis Results

1. Waste dump samples

Table B-1: Waste dump samples XRF results

| Element/ Compound | WD1 | WD2 | WD3 | WD4 |
|--------------------------|---------------|---------------|---------------|---------------|
| | Mass % | Mass % | Mass % | Mass % |
| Iron | 51.35 | 33.96 | 39.66 | 34.70 |
| Silica | 29.10 | 49.50 | 38.56 | 26.33 |
| Manganese | 5.91 | 1.17 | 0.26 | 1.42 |
| Barium | 4.62 | 0.19 | 0.10 | 0.25 |
| Titanium | 2.88 | 0.17 | 0.24 | 0.51 |
| Aluminum | 1.73 | 0.49 | 1.10 | 1.83 |
| Calcium Carbonate | 1.60 | 12.97 | 19.07 | 33.43 |
| Sulphur | 1.50 | 0.16 | 0.00 | 0.10 |
| Phosphorous | 1.10 | 1.25 | 0.89 | 1.26 |
| Nickel | 0.05 | 0.02 | 0.02 | 0.01 |
| Zinc | 0.04 | 0.01 | 0.01 | 0.03 |
| Copper | 0.03 | 0.01 | 0.00 | 0.01 |
| Lead | 0.03 | 0.01 | 0.01 | 0.01 |
| Bismuth | 0.02 | 0.01 | 0.00 | 0.01 |
| Chromium | 0.00 | 0.08 | 0.05 | 0.02 |
| Thorium | 0.00 | 0.00 | 0.02 | 0.01 |
| Vanadium | 0.00 | 0.00 | 0.00 | 0.04 |

2. Stockpile samples

Table B-2: Stockpile

| Element/ Compound | SP1 Mass | SP2 Mass | SP3 Mass | SP4 Mass |
|--------------------------|-----------------|-----------------|-----------------|-----------------|
| | % | % | % | % |
| Iron | 88.75 | 71.94 | 76.92 | 84.53 |
| Silica | 5.85 | 19.37 | 16.31 | 11.86 |
| Aluminium | 1.73 | 1.90 | 1.65 | 1.40 |
| Calcium Carbonate | 0.83 | 1.29 | 0.82 | 1.11 |
| Phosphorous | 0.79 | 1.06 | 0.98 | 0.64 |
| Barium | 0.62 | 0.96 | 1.27 | 0.05 |
| Titanium | 0.56 | 0.90 | 1.03 | 0.00 |
| Sulphur | 0.26 | 0.63 | 0.00 | 0.00 |
| Manganese | 0.26 | 1.67 | 0.58 | 0.24 |
| Bismuth | 0.10 | 0.04 | 0.07 | 0.10 |
| Nickel | 0.05 | 0.07 | 0.21 | 0.08 |
| Rubidium | 0.05 | 0.02 | 0.04 | 0.03 |
| Lead | 0.04 | 0.04 | 0.05 | 0.04 |
| Copper | 0.04 | 0.02 | 0.02 | 0.02 |
| Zinc | 0.03 | 0.02 | 0.01 | 0.02 |
| Zirconium | 0.00 | 0.00 | 0.01 | 0.00 |
| Vanadium | 0.00 | 0.00 | 0.00 | 0.02 |

3. Overburden samples

Table B-3: Overburden samples XRF results

| Element/ Compound | OB1 % | OB2 % | OB3 % | OB4 % |
|--------------------------|--------------|--------------|--------------|--------------|
| Silica | 57.83 | 60.7 | 24.93 | 20.62 |
| Iron | 15.01 | 8.63 | 6.1 | 19.92 |
| Potassium | 10.36 | 15.98 | 0.37 | 0.58 |
| Calcium Carbonate | 7.42 | 1.76 | 62.86 | 52.54 |
| Aluminium | 6.13 | 9.48 | 3.11 | 3.32 |
| Phosphorous | 1.83 | 1.8 | 1.7 | 1.47 |
| Titanium | 0.51 | 0.69 | 0.67 | 0.76 |
| Barium | 0.38 | 0.24 | 0.17 | 0.19 |
| Sulphur | 0.25 | 0.37 | 0.1 | 0.01 |
| Manganese | 0.05 | 0.08 | 0.39 | 0.48 |
| Chromium | 0.05 | 0.06 | 0.03 | 0.02 |
| Zirconium | 0.04 | 0.04 | 0.01 | 0.02 |
| Strontium | 0.03 | 0 | 0.04 | 0.04 |
| Rubidium | 0.03 | 0.04 | 0 | 0 |
| Copper | 0.02 | 0.01 | 0.02 | 0.01 |
| Zinc | 0.01 | 0.01 | 0.01 | 0 |

Appendix C : Published article and anti plagiarism report

1. Published Article (Attached)

Gitau, F., Maghanga, J.K. & Ondiaka, M.N. Spatial mapping of the extents and volumes of solid mine waste at Samrudha Resources Mine, Kenya: a GIS and remote sensing approach. *Model. Earth Syst. Environ.* **8**, 1851–1862 (2022). <https://doi.org/10.1007/s40808-021-01192-7>

2. Anti plagiarism report (Attached)



Spatial mapping of the extents and volumes of solid mine waste at Samrudha Resources Mine, Kenya: a GIS and remote sensing approach

Francis Gitau¹ · Justin Kambale Maghanga² · Mary Nelima Ondiaka¹

Received: 22 March 2021 / Accepted: 18 May 2021

© The Author(s), under exclusive licence to Springer Nature Switzerland AG 2021

Abstract

Monitoring and estimating solid mine waste produced during mining operations at a spatial–temporal scale plays a fundamental role in waste management and mitigation of environmental impacts. Iron ore mining and processing results in waste production that may cause environmental degradation, therefore, the need to estimate their volumes and extents. This research aims at mapping and estimating the areal extents and the volumes of solid mine waste produced during iron ore mining and processing. Contours were generated from control points with X, Y, Z information and interpolated to create a Triangular Irregular Network (TIN), which was rasterized to create a 3D Digital Elevation Model (DEM) that was used in volume estimation. Maximum-Likelihood Classification method (MLC) was used for classification at an accuracy of 74% to estimate the areal extents of the solid mine wastes, with a Kappa Coefficient of 0.65. Solid mine waste approximately covered an area of 591,100 m² and a volume of 2694,670.55 Metric Tonnes. This research presents a fast and accurate method of mapping and estimating the areal extents and volume of solid waste dumped during mining and processing operations.

Keywords Mine wastes · Iron ore · Environmental monitoring · GIS · Remote sensing

Introduction

Mining has played a huge role in economic development in many parts of the world (Bansah et al. 2018). However, in Africa, mining consists of small-scale mines and many large-scale mines scattered throughout, mining different minerals (Hilson et al. 2017). The mining of various minerals in different parts of the world has had long-lasting negative impacts (Bansah et al. 2018). The most evident impacts of mining are the disposal of various harmful wastes and notable land use and land cover changes where vegetation is cleared (Elsaid and Abdelkareem 2018). There are various mine wastes such as overburden, slags, waste rock, and stockpiles of unwanted ore of low-grade in loose soil piled near open pits, tailings dam, and overburden surfaces

stripped areas (Sikaundi 2015; Akoto and Anning 2021). Apart from altering the landscape by changing the land use and land cover, these mine wastes, tailings, stockpiled overburden, and stockpiles pose a hazard to human health (Odoh et al. 2017). Ignoring these volumes and their extents may result in adverse impacts.

Mining, mineral exploration, and mineral extraction are spatial (Adero 2018). Both surface and underground mines cover large spans of land (Moraga and Gurkan 2020). During mining operations, various waste is produced and end up being dumped on the surface at different locations within the mine (Werner et al. 2019). Considering the time consumed, safety, accuracy, and frequency in monitoring and estimating these volumes of waste dumped, there is a need to employ GIS and remote sensing techniques for volume calculation (Tucci et al. 2019).

GIS and remote sensing technology plays a crucial part in mining and has vast applications, including mineral predictive mapping, area calculation using land use and land cover classification (LULC) methods, and volume measurements (Rahman et al. 2017). Various remote sensing and GIS software are used to stitch together and process geotagged photographs and remotely sensed images with high overlap

✉ Francis Gitau
fgitau26@gmail.com

¹ School of Mines and Engineering, Taita Taveta University, P.O. Box 635-80300, Voi, Kenya

² School of Science and Informatics, Taita Taveta University, P.O. Box 635-80300, Voi, Kenya

captured from multiple angles for various applications such as waste dump mapping (Tucci et al. 2019). This software generates very dense 3D point clouds, and the result is a 3D surface model for higher accuracy volume calculations safe and faster than before (Kevin and Nthenge 2020).

Maximum-Likelihood Classification (MLC) method utilizing machine learning has become popular in the recent past in identifying various land use and land cover classes at a higher accuracy (Verma et al. 2020). The statistics of these classes play a significant role in area calculation (Jamali 2019). Land use and land cover are spatial–temporal, and therefore, crucial in determining where various mine wastes are dumped. Land use and land cover (LULC) classes areas calculations have become a vital issue in the current sustainability and environmental monitoring tools (Hosseini et al. 2019). Remotely sensed data, GIS, and remote sensing techniques are used to detect land use and land cover classes whose classes are statistically computed to give the exact areas of specific classes (Hosseini et al. 2019). Accuracy is of great importance and needs a clear understating and due diligence in selecting and validating the classes and algorithms (Verma et al. 2020). According to Raeva et al. (2016), mining engineering legislation outlines that volume calculation should present an accuracy of $\pm 3\%$ of the whole amount. Therefore, there is a need to carry out a thorough accuracy assessment both for the LULC for areal calculations and volumetric computation to come up with desired results that can be used for sound environmental monitoring. Accurate land use and land cover analysis are critical in meeting this need as these areas will be used to inform evidence-based decisions on environmental management (Hale et al. 2016).

The study area, Samrudha Resources Mine, Taita Taveta County in Kenya, was suitably selected as it lies in the Mozambique belt along the coastal region rich with industrial minerals (Waweru 2020). Both remote sensing and GIS techniques utilizing photogrammetry and machine learning methods such as Maximum Likelihood Classification methods were used. The specific objectives of this research was to: (1) Mapping of the areal extents of solid mine waste dumped at Samrudha Resources Mine using Maximum Likelihood Classification by computation of per pixel statistics for land use and land cover classes based on Sentinel 2 Level 2A satellite image; (2) Estimation of the volumes of the solid mine waste dumped using ground control points and spatial analysts tools in ArcGIS.

The hypothesis of this research is that Geographical Information Systems (GIS) and remote sensing Method can be accurately used to spatially map and estimate solid mine wastes and stockpiled materials at a spatial–temporal scale in a dynamic area where active mining is taking place. The second part of this research presents the research scope, Samrudha Resources, Taita Taveta Kenya, and the research methodology

for volume and area estimations in depths, including the accuracy assessment of the various methods used. The third section of this research contains the findings that are discussed in the fourth section. The last part of this research, includes the key conclusions and recommendations for further research.

Data and methodology

Study area and datasets

This study was conducted within the Samrudha Resource Iron Ore Mine at Taita Taveta County, Kenya, where active mining occurs. This area lies approximately 450 km south-east of Nairobi and 250 km northwest of Mombasa, as between 3.1° S and 3.3° S, and 38.1° E and 38.3° E, as shown in Fig. 1. The area lies in the Mozambique belt, rich in industrial minerals (Cheneket 2018). Figure 2 shows a high-resolution true-colour image of the mining site with various solid waste dump locations. Samrudha Resources Mine Limited utilizes open cast mining and selectively mines iron ore of high grade, discriminating medium and low-grade iron ores < 65%, which are disregarded as mine waste. These materials are either stockpiled or dumped in locations near the open pit.

Satellite image datasets and ground control points

In this study, Sentinel 2 Level 2A satellite image was obtained in January 2020 from the USGS (<http://glovis.usgs.gov>) in the dry season with no cloud cover. The image path and row were 167 and 062, respectively, with a spatial resolution of 10-m spatial resolution (*S2B_MSILIC_20190928T072659_N0208_R049_T37MDS_20190928T101523*).

GPS coordinates control points were picked from the ground, and additional ground control points were established from google earth. Google earth was also used to create Keyhole Mark-up Language (KML) data, which contained the planer information for (X, Y), and display the elevation profile, as shown in Fig. 3, to determine the highest and lowest point for the locations of interest. The KML data were exported to GPS Visualizer Software, where the Z component for altitude was added and finally converted to GPS Exchange Format (GPX).

Image classification workflow and volume computation

Image classification

The workflow for image classification to delineate the areal extents for solid mine wastes dumped at Samrudha Resources Mine is shown in Fig. 4.

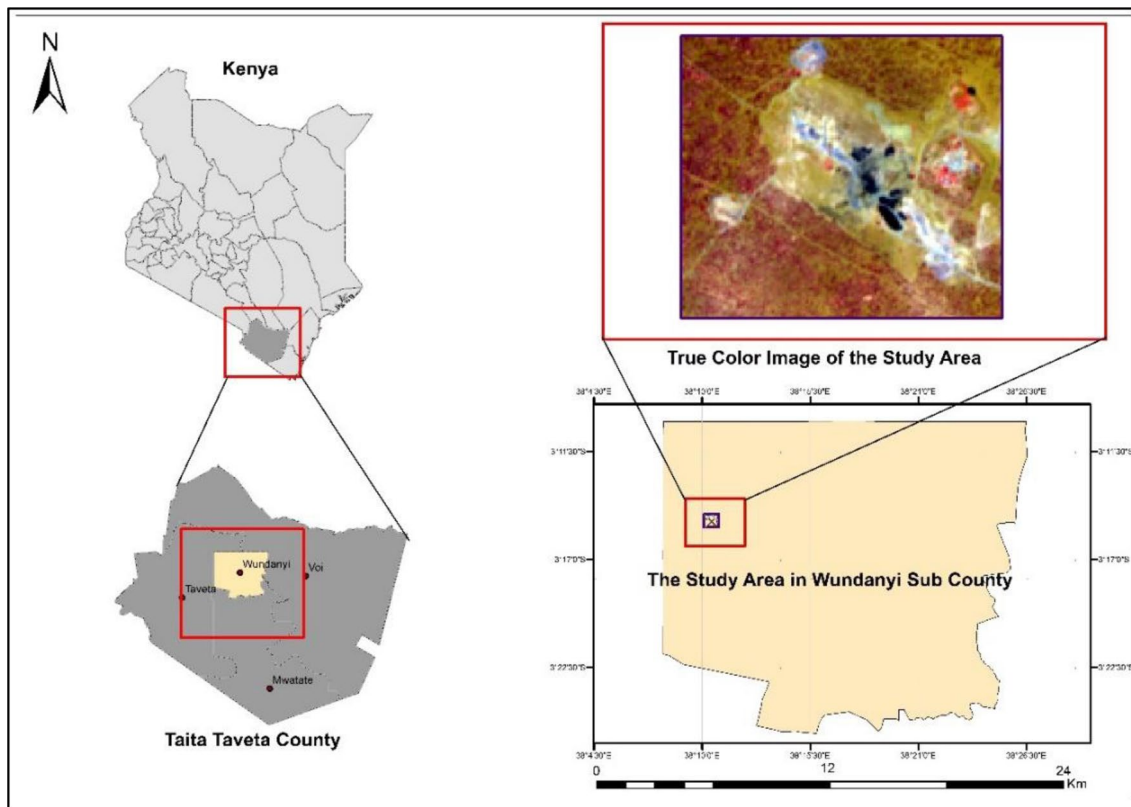


Fig. 1 Map of the study area, Samrudha Resources Mine, Taita Taveta County, Kenya

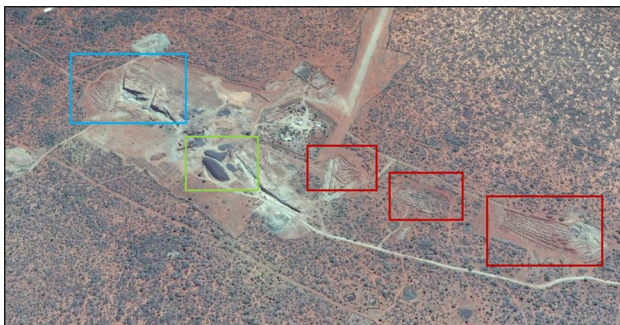


Fig. 2 True colour image highlighting various solid waste points in Samrudha Resources Mining Area Source: (Google Earth Pro, 2020)



Fig. 3 Elevation profile of one of the Iron ore Stockpile in Google Earth

The following key steps were adopted as part of the workflow and consisted of the following:

1. Data pre-processing
2. Creation of training areas
3. Classification and accuracy assessment
4. Wastes extents delineation
5. Waste volumes quantification

Data pre-processing The data downloaded were processed to the Bottom of the Atmosphere Reflectance and also cor-

rected from variances caused by the sun angle (Main-Knorn et al. 2017). The data were then exported to ArcGIS Software, where a subset of the mine outline at the study area was extracted; this process helped make the image pre-processing in R Studio by use of raster RS Toolbox Packages less time consuming (Leutner and Horning 2016). Only the 10 m spatial resolution bands of Blue, Red, Green, and Near Infrared (NIR) were used. To make the image pre-processing less time consuming, the data were then stacked, and

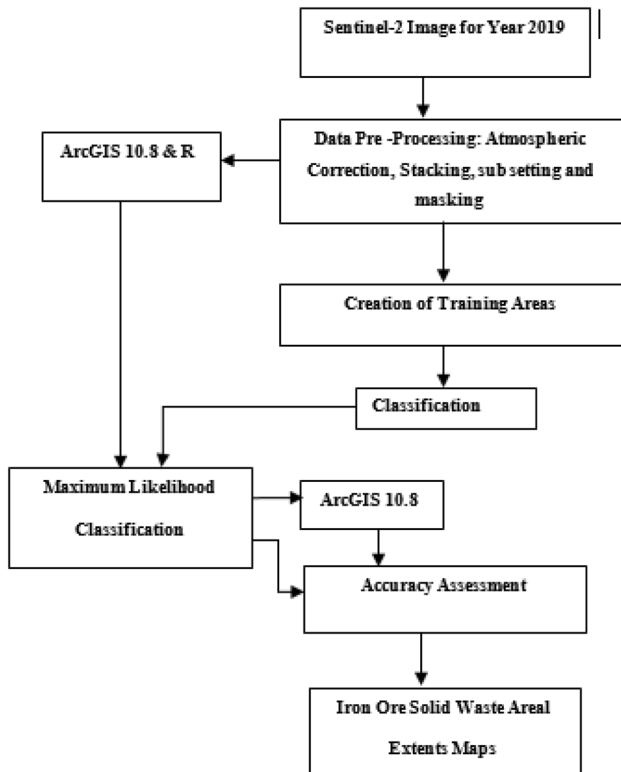


Fig. 4 Workflow for areal extents delineation

different RGB combinations were used to display relevant information in clarity.

Creation of training areas The training datasets for Maximum-Likelihood Classification (MLC) were produced by carefully selecting pure pixels from satellite imagery based on the ground knowledge experience and maps from Google Earth Pro (Qu et al. 2021). For training area selection, it is recommended that a maximum of 30 and not less than 10 points for each class be selected for training purposes (Ha et al. 2020). A total of 200 samples for training were collected for training the algorithm, and additional 50 sites were collected for validation.

Classification and accuracy assessment Maximum-Likelihood Classifier method utilizing supervised classification method was done in ArcGIS (Oyedotun 2020). The MLC method is based on the basic principle that the classes' data are distributed normally in a multidimensional space (Verma et al. 2020). During classification, both covariances and variances in the training datasets were considered. Each pixel is assigned to a specific class that has a maximum probability of being a member. A classification scheme was then developed basing on the knowledge of the area and the classes of interest. Solid mine wastes were a priority, in this case. Therefore, the classes identified from the MLC

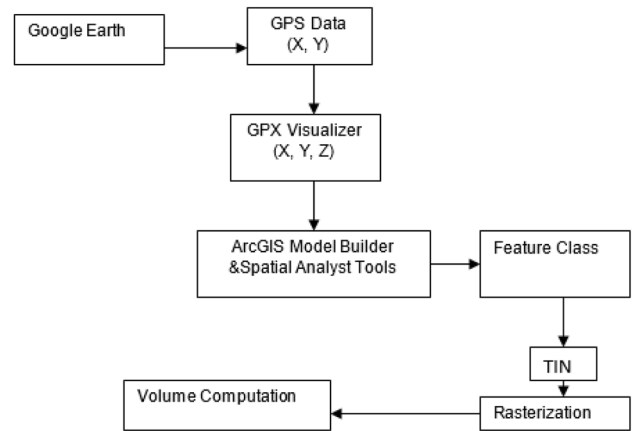


Fig. 5 Workflow for waste volume quantification

algorithm were reclassified to the following classes: iron ore stockpile, waste dumped and overburden, cleared ground, and open pits. This was done in ArcGIS Software.

In general, the accuracy assessment goal is to determine the quality of the extracted information and generated from the data (Hosseini et al. 2019). The classification accuracy, the rate of the correspondence between the referenced information and the data, is very vital (Ha et al. 2020). The overall accuracy, users' accuracy, producers' accuracy, and the overall kappa coefficient were done using the error matrix (Rwanga and Ndambuki 2017). Equation (1) was used for Kappa Coefficient Computation (Bhattacharjee and Jensen-Butler 2006). The K is the rows in the matrix; x_{ii} is the observations in column i and row i ; x_{i+} and x_{+i} are the marginal row totals of column i and row k , respectively, whereas, N are the observations made.

Equation 1 kappa coefficient formula:

$$K = \frac{N \sum_{i=1}^r x_{ii} - \sum_{i=1}^r (x_{i+} X x_{+i})}{N^2 - \sum_{i=1}^r (x_{ii} X x_{+i})} \quad (1)$$

Waste volumes quantification This was achieved with GPX data created from Google earth and GPS Visualizer using the workflow as illustrated in Fig. 5.

GCP taken from the field was exported to Google Earth and more GCP Extracted to create cloud points (Bhattacharjee and Jensen-Butler 2006). For each feature of interest, such as the waste dump identified, the elevation profile of each was displayed to identify the highest and the lowest points as these values were to be used for volume differencing. This data (X, Y) were then exported to GPX Visualiser Software, where the elevation (Z) was added for each point. The GPX points were exported to ArcGIS Software and converted to feature classes. Due to the many feature classes created for each of the solid mine waste classes and the need

for accuracy during the entire process, the ArcGIS model builder was used to automate the process, as shown in Fig. 6.

The data variables, the inputs (Blue), were GPX points shown in Fig. 7 exported to ArcGIS Software.

This was run through various tools (Yellow) in ArcGIS Toolbox. The first tool converted the GPX data to feature classes: the first data output (Green) was used to create a triangulated irregular network (TIN). The created TIN formed the input for the following process: rasterization of the TIN that included georeferencing of the raster output to convert the unit of measurement to Meters. The 3D raster was then used for volumetric calculation using the Surface Tool in the ArcGIS Spatial Analyst, whereby the maximum and minimum heights of each feature of interest were input. The surface tool was run, and the volumes were exported to a table for computation.

Results

Accuracy assessment

The extent of solid mine waste was mapped at an accuracy of 74% and a Cohen’s Kappa of 0.65 above the recommended Kappa of 0.5 (Rwanga and Ndambuki 2017). This is as shown in the confusion matrix in Table 1. The accuracy was influenced by GPX points coverage, which creates an unclear definition of the footprint and the outline at different areas of interest, such as the stockpile. Figure 8 shows the

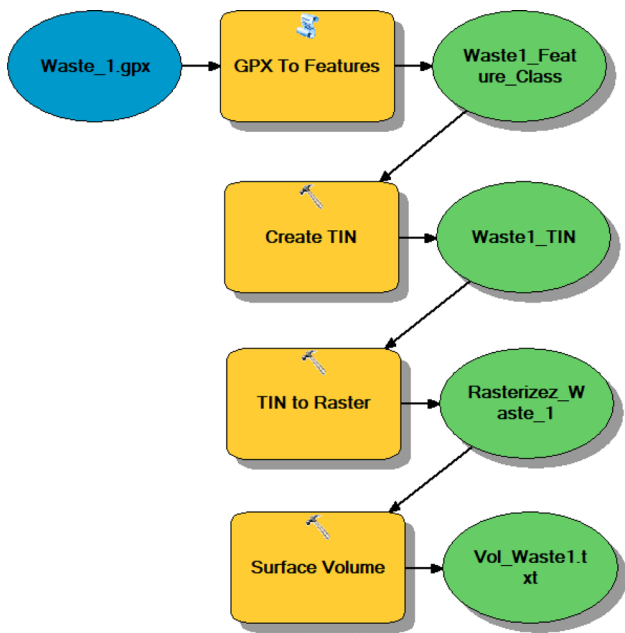


Fig. 6 Volume computation flow in the ArcGIS model builder

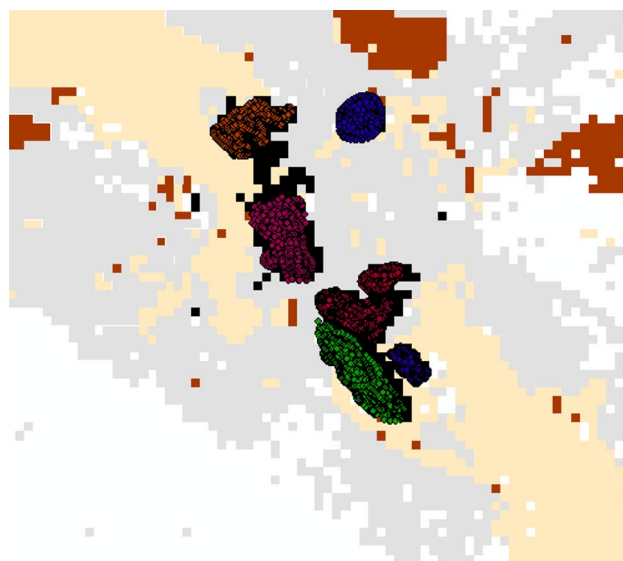


Fig. 7 GPX point features overlaying stockpile classes

parts circled not covered by the GPX points, which influenced the accuracy of the areal and volumetric calculations.

Areal extents mapping

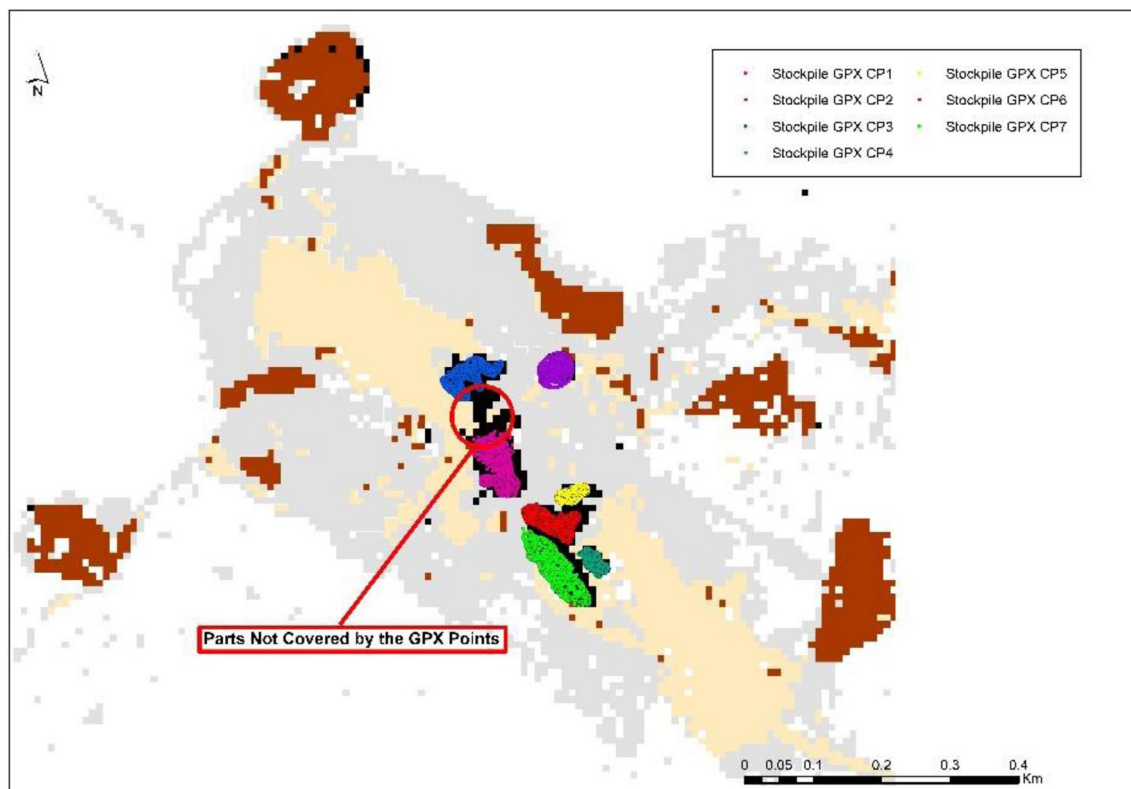
The areal extents were generated from the MLC classification based on the classes identified for the land uses. These classes were iron ore stockpiles, open cast pits where mining was taking place, cleared grounds, and waste dump and overburden dump. The iron stockpiles are represented in black color in the map, and the open cast pits are represented in purple; the cleared grounds are visualized in grey color. In contrast, the waste dump and the overburden are represented using brown color as shown in Fig. 9. A comparison is also drawn with a true color Sentinel 2A image that shows the extents of mine wastes for different classes to reinforce the results.

The area was calculated as per pixel, as shown in Fig. 10. This was then statistically computed and similar classes areas combined. The largest area was found out to be open ground and Open Cast Pits. Solid mine waste extent, waste rock, and overburden occupied the largest area of 0.0845 Km², and iron ore stockpile coming second with 0.00288 Km² as shown in Table 2.

Figure 11 shows a pie chart of different classes of the mine wastes found in the area. The significance of the open cast pits occupying a large area justifies why the overburden and the waste dump occupied the largest percentage than the stockpiles. This is because 80% of the mine’s materials waste from blasting operations, stripping, and removing overburdened material deposited on the mine edges. The iron ore stockpile, which is disregarded as mine waste, occupied the

Table 1 Confusion matrix

| Classes | Iron ore stockpile | Waste dump and overburden | Cleared ground | Open cast pit | Total reference points |
|---------------------------|--------------------|---------------------------|----------------|---------------|------------------------|
| Iron ore stockpile | 23 | 0 | 0 | 0 | 23 |
| Waste dump and overburden | 1 | 5 | 1 | 0 | 7 |
| Cleared ground | 0 | 10 | 26 | 1 | 37 |
| Open cast pit | 0 | 13 | 0 | 19 | 32 |
| Total reference points | 24 | 28 | 27 | 20 | |
| Accuracy | 74% | | | | |
| Kappa coefficient | 0.65 | | | | |

**Fig. 8** GPX point features overlaying stockpiles

smallest percentage of 11%, while waste dump and overburden occupied 345 of the total area under consideration.

Volumes of solid mine wastes dumped

The volumetric analysis revealed waste rock dumped and overburden occupied the largest volume of approximately 489,211.94 m³, and iron ore stockpiles occupied a volume of approximately 34,025.17 m³ shown in Table 3. Figure 12 shows a pie chart of solid mine waste volumes. Waste rock dumped, and overburden had the highest percentage (93%) compared to the stockpile (7%).

Volume computation model

A model that comprises workflows that string together the step-by-step sequences of the geoprocessing tool by feeding the various outputs of one tool to another as inputs was created. The model was created by ArcGIS ModelBuilder, which is a tool for visual programming and building important workflows (Raju 2020). The model, as shown in Fig. 13, was created.

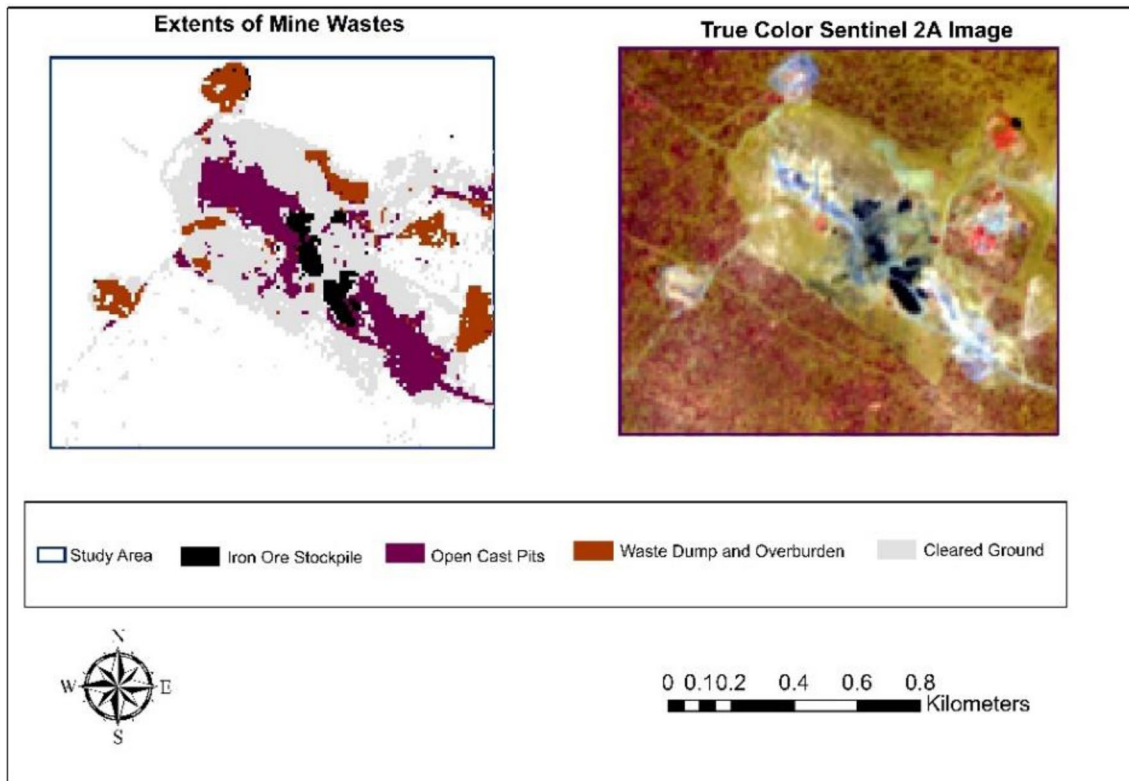


Fig. 9 Map of mine waste extents

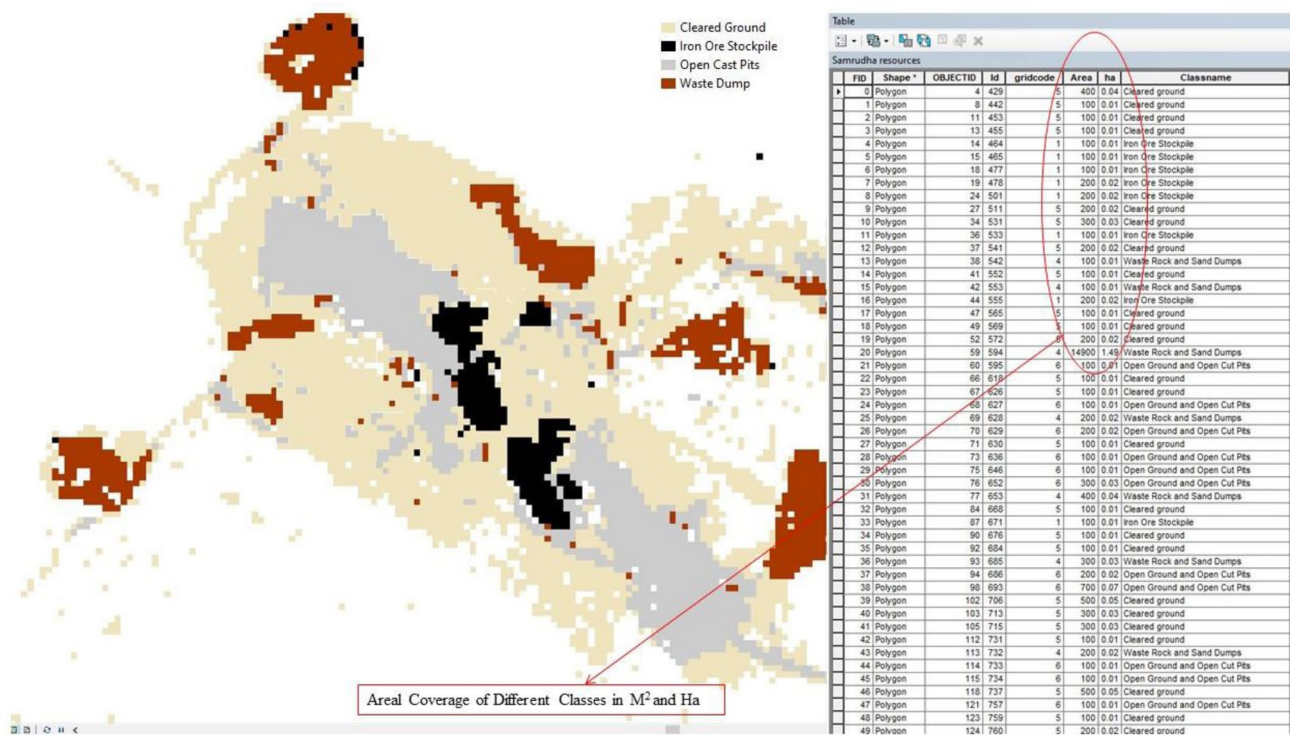
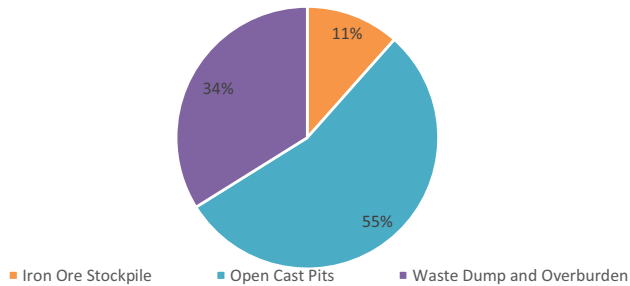


Fig. 10 Attribute table for pixel areal coverage

Table 2 Areas of extents

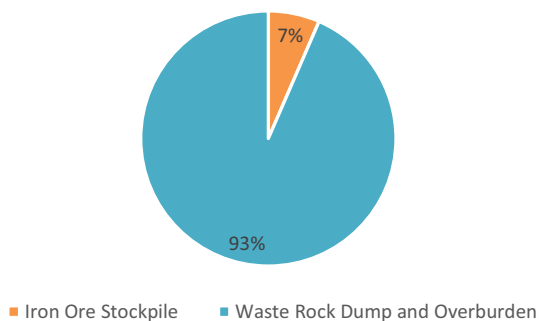
| | Iron ore stockpile area | Open cast pits area | Waste dump and overburden area | An estimate of total area covered |
|-----------------------------|-------------------------|---------------------|--------------------------------|-----------------------------------|
| Sum of area Km ² | 0.0288 | 0.1361 | 0.0845 | 0.2494 |

Coverage of Mine Wastes Areas

**Fig. 11** Pie chart of derived classes**Table 3** Volumes of mine wastes

| | Iron ore stockpile | Waste rock dump and overburden | An estimate of total volume |
|--------------------------|--------------------|--------------------------------|-----------------------------|
| Volume in m ³ | 34,025.17 | 489,211.94 | 523,237.11 |

Volumes of Mine Waste

**Fig. 12** Pie chart of the volumes of mine waste

Discussion

Mining and mineral processing produces gaseous, liquid, and solid waste (Lottermoser 2011). During open-pit mining operations, solid mine wastes such as; waste rocks, overburden, spoils, stockpiled materials, emissions and mine water may be emitted (Blight 2011). The developing

Samrudha Resources Mine in Taita Taveta, Kenya, was chosen as the study area to examine these problematic solid mine wastes as little information of the volumes and areal extents are known. The criterion for the determination of waste and ore at Samrudha resources is cut-off grade. Ore that is less than 70% of concentration of iron ore at Samrudha Resources is termed as subeconomic, and therefore, is disregarded as waste. At Samrudha Resources Mine, there exist various types of wastes such as Waste Rocks, Overburden and Stockpiled iron ore fine dust. This is shown in Fig. 14.

Waste rock is generally excavated and mined rocks during access from ore and includes rocks resulting from blasting operations (Lottermoser 2011). These waste rocks are generally dumped in non-designated places around the mining area at Samrudha Resources Mine. The overburden material at Samrudha Resources Mine is topsoil dozed-off during the opening up of new open pits, as shown in Fig. 15. The material is piled on the sides of the mine and constitutes solid mine waste produced during mining operations under consideration in this research.

The stockpiled material at Samrudha Resources Mine is generally iron ore fines and iron ore of low grade, not of economic value to the company. The iron ore fines and low-grade iron ore are stockpiled near the processing plant.

An estimated total volume of solid mine waste produced at Samrudha Resources Limited as of March 2020 stood at 523, 237.11 m³ as seen in (Table 4) and covered an approximated area of about 249,400 M². ArcGIS ModelBuilder was used to automate this process. This came in handy due to the many numbers of iteration for each class that was under consideration for the volume computation. Raju (2020) highlights that automating processes and workflows in ArcGIS ModelBuilder have proven effective in time management and improves user accuracy. This model can be used to compute for any volume of a selected pile of solid waste, where its inputs are the GPX point clouds.

Generally, the volumes are translated from the stripping ratio that the mine utilizes, which is 2:1. For every one part of ore mined, the company mines two parts of waste (Kuranichie 2015).

The stockpiled materials at the mine cover an approximate volume and area of 34,025.17 m³ and 28,800 m², respectively. This translates to the least amount of solid waste produced during the mining of iron ore at the mine. The stockpiled materials are generally mineral processing waste produced as a result of magnetic separation and screening of iron ore. Due to the selective mining taking place at Samrudha resources, the materials that end up in the processing plant are of high grade. Therefore, very small amounts of waste are produced. These wastes also appear to be clustered at one central location near the processing plant, as shown in Fig. 16.

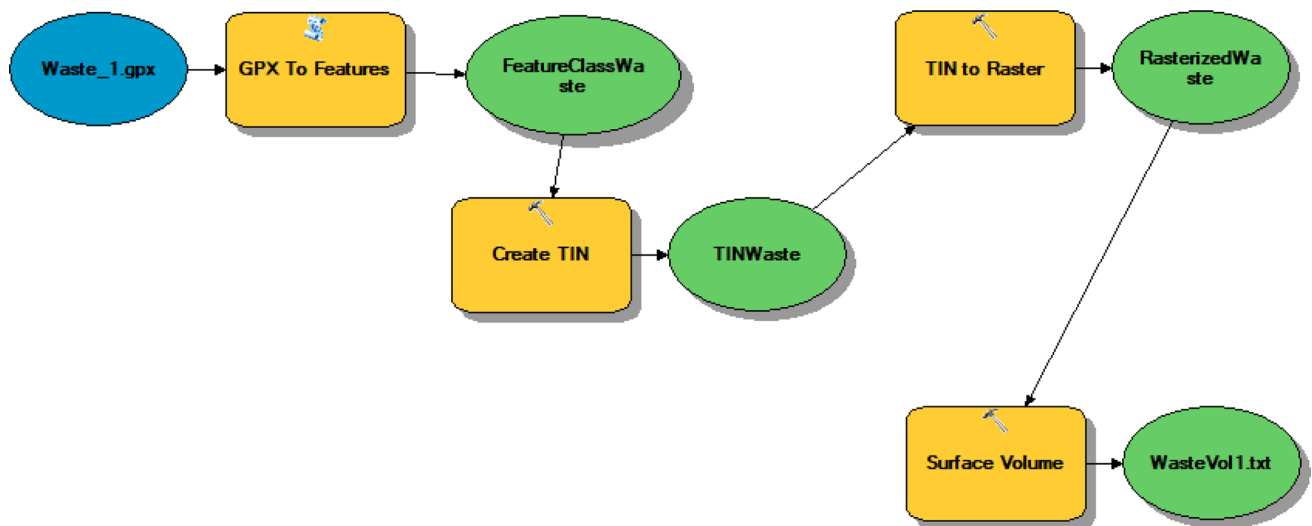


Fig. 13 Model workflow for volume computation in ArcGIS



Fig. 14 Mine wastes at Samrudha resources Mine; **a** Overburden material, **b** Waste dump, **c** Stockpiled iron ore fines and, **d** Waste rock dump

The waste dump and the overburdened materials cover a volume and area of 489,211.94 m³, and 84,500 m². This constitutes the highest amount of waste generated during stripping and mining operations. The wastes from the open pit and overburdened materials are dumped near the open-pit mine. On rare occasions, the waste and overburden are dumped away from the open-pit mine area. This is to reduce the mining cost, as revealed by the company. This waste generally results from blasting operations, stripping of gangue materials, and topsoil, which is heterogeneous to the geology of the ore.

The exposure of these solid wastes to the atmosphere and the environment may cause various impacts, such as acid drainage due to sulphide minerals (Almeida et al. 2018). There exist heavy metals concentrations in these mine wastes that pose an environmental concern (Cheneket 2018). This is why there is a need to map out the extents and the volumes to plan for various post-mining operations such as mine rehabilitation and plan monitoring activities. The quantifications are also essential to avert the anticipated environmental impacts. A mining company needs to know the approximate volumes and extents of mine waste they



Fig. 15 Overburden material at the sides of the active open pit

Table 4 Volume and areas of solid mine waste

| | |
|---|------------|
| Estimated volume of mine waste m ³ | 523,237.11 |
| Estimated area of solid mine waste m ² | 249,400 |

produce as they progressively carry out mining and processing operations. At times, this may prove to be a costly affair that results in these wastes' uncontrolled disposal. Studies done by Cheneket (2018) reveal that the disposal of mine wastes by Samrudha Resources Limited poses a grave danger to the community living around the mine as the soils are laced with heavy metals resulting from the mine waste. This information on volumes and areal coverage of these problematic solid mine wastes, which was missing, will help the company refocus on planning for waste disposal, treatment techniques, and some situations consider value addition and reusing.

Conclusion

Iron ore mining produces various mine wastes that may be toxic and harmful to humans and the resulting environment. By effectively applying GIS and remote sensing techniques to quantify the extent and volume of solid mine waste that are dynamic, the company now has the upper hand in monitoring the waste produced. This can come in handy to curb various environmental impacts associated with depositing the wastes into the environment. This method also provides a relatively cost-friendly yet fast and reliable way to monitor

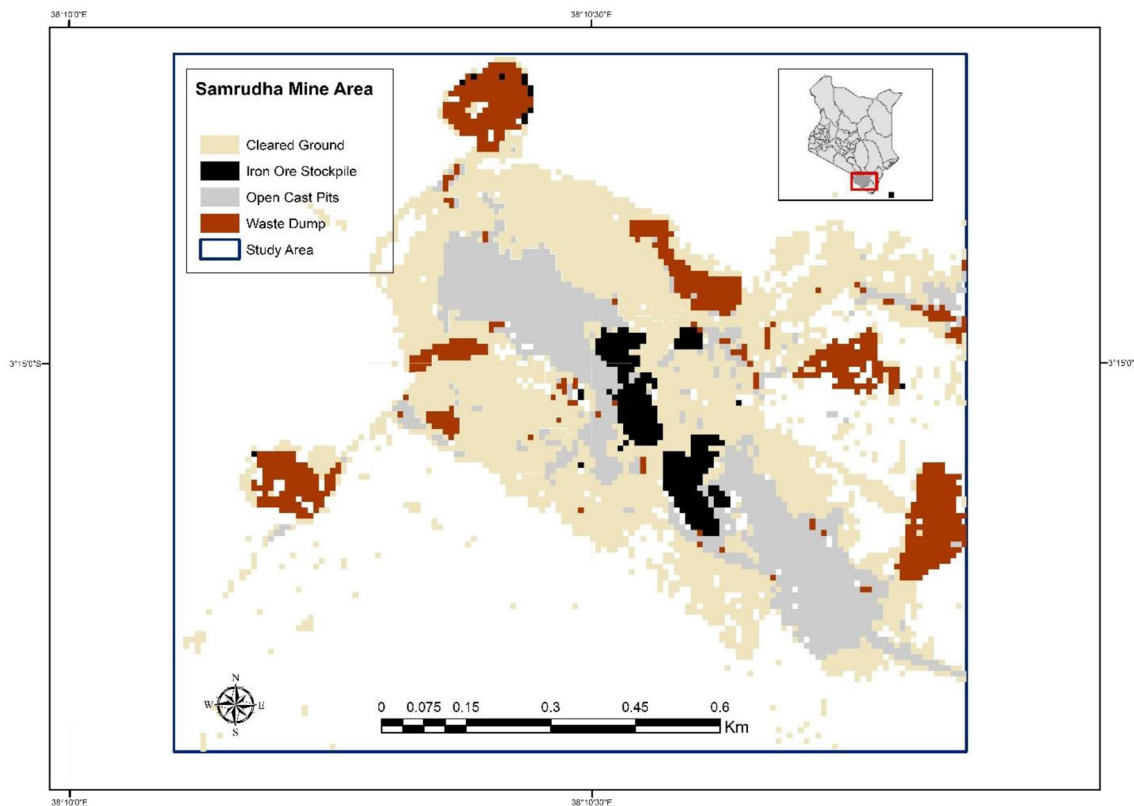


Fig. 16 Solid mine waste map

the environmental effects that these wastes may cause. The mining company can also effectively plan for the rehabilitation and restoration of some areas affected. It is important to note that though relatively expensive, UAV technology is faster and more accurate in surface differencing (Rahman et al. 2017). In future tool that integrates the dynamic volumes and areas of these solid wastes with real-time information for geochemistry and geochemical properties of the mine wastes need to be created to address the issue of environmental pollution of solid mine waste at any mine.

Acknowledgements I want to express my heartfelt gratitude to my Supervisors, Dr. Justin Maghanga and Dr Mary Nelima, for their support, encouragement, and advice during my research. I would also like to express my appreciation to the Kenyan German Centre for Mining, Environmental Engineering and Resource Management (CEMEREM) and DAAD for offering me a scholarship. In addition, I would like to extend thanks to colleagues who assisted with this research, especially TATAGIS Team, who provided relevant software and GPS for data collection and excellent processing and analysis advice.

Funding No funding was received for conducting this study.

Declaration

Conflict of interest The authors have no conflicts of interest to declare that are relevant to the content of this research.

References

- Adero NJ (2018) Redressing the nexus of human rights and mining in Kenya using geospatial modelling. In: 3rd PhD Conference—"The Social Responsibility of Science and Scientists" Organised by ProRat at Freiberg University of Mining and Technology, Germany, 6–7 June 2018, pp. 12–13
- Akoto R, Anning AK (2021) Heavy metal enrichment and potential ecological risks from different solid mine wastes at a mine site in Ghana. *Environ Adv* 3:100028. <https://doi.org/10.1016/j.envadv.2020.100028>
- Almeida CA, de Oliveira AF, Pacheco AA, Lopes RP, Neves AA, de Queiroz MELR (2018) Characterization and evaluation of sorption potential of the iron mine waste after Samarco dam disaster in Doce River basin—Brazil. *Chemosphere* 209:411–420. <https://doi.org/10.1016/j.chemosphere.2018.06.071>
- Bansah KJ, Dumakor-Dupey NK, Kansake BA, Assan E, Bekui P (2018) Socioeconomic and environmental assessment of informal artisanal and small-scale mining in Ghana. *J Clean Prod* 202:465–475. <https://doi.org/10.1016/j.jclepro.2018.08.150>
- Bhattacharjee A, Jensen-Butler C (2006) Estimation of spatial weights matrix in a spatial error model, with an application to diffusion in housing demand. *CRIEFF Discussion Papers* 0519:1–42
- Blight G (2011) Mine waste. *Waste*. <https://doi.org/10.1016/b978-0-12-381475-3.10005-1>
- Cheneket BK (2018) Impact of iron ore mining on heavy metal concentration in soils of Kishushe Area In Wundanyi, Taita Taveta County
- Elsaid O, Abdelkareem A (2018) Accuracy assessment of land use land cover in umabdalla natural reserved accuracy assessment of land use land cover in umabdalla natural reserved forest. *South Kordofan Sudan* 3(January):5–9
- Ha NT, Manley-Harris M, Pham TD, Hawes I (2020) A comparative assessment of ensemble-based machine learning and maximum likelihood methods for mapping seagrass using sentinel-2 imagery in Tauranga Harbor, New Zealand. *Remote Sens* 12(3):1–16. <https://doi.org/10.3390/rs12030355>
- Hale R, Sertel E, Musaoğlu N (2016) Assessment of classification accuracies of sentinel-2 and landsat-8 data for land cover/use mapping. *Int Arch Photogramm Remote Sens Spatial Inf Sci XLI(July):1055–1059*. <https://doi.org/10.5194/isprsarchives-XLI-B8-1055-2016>
- Hilson G, Hilson A, Maconachie R, McQuilken J, Goumandakoye H (2017) Artisanal and small-scale mining (ASM) in sub-Saharan Africa: re-conceptualizing formalization and 'illegal' activity. *Geoforum* 83(May):80–90. <https://doi.org/10.1016/j.geoforum.2017.05.004>
- Hosseini SAR, Gholami H, Esmaeilpoor Y (2019) Assessment of land use and land cover change detection by using remote sensing and gis techniques in the coastal deserts, South of Iran. *Int Arch Photogramm Remote Sens Spatial Inf Sci* 42(4/W18):489–492. <https://doi.org/10.5194/isprs-archi-ves-XLII-4-W18-489-2019>
- Jamali A (2019) A fit-for-purpose algorithm for environmental monitoring based on maximum likelihood, support vector machine and random forest. *Int Arch Photogramm Remote Sens Spatial Inf Sci* 42(3/W7):25–32. <https://doi.org/10.5194/isprs-archi-ves-XLII-3-W7-25-2019>
- Kevin K, Nthenge M (2020) Designing an efficient slurry transport system based on volumes extracted using uav-based photogrammetry. 1(december 2017):1–43
- Kuranichie FA (2015) Characterisation and applications of iron ore tailings in buildings and construction projects. 397. <http://ro.ecu.edu.au/theses/1685/>. Accessed 12 Jan 2021
- Leutner B, Horning N (2016) RStoolbox: tools for remote sensing data analysis. R Package version 0.1. 4. <http://CRAN.R-Project.Org/Package=RStoolbox>. Accessed 12 Jan 2021
- Lottermoser BG (2011) Mine wastes. *Waste*. <https://doi.org/10.1016/b978-0-12-381475-3.10005-1>
- Main-Knorn M, Pflug B, Louis J, Debaecker V, Müller-Wilm U, Gascon F (2017) Sen2Cor for Sentinel-2. *Image Signal Process Remote Sens* 1042704(October 2017):3. <https://doi.org/10.1117/12.2278218>
- Moraga J, Gurkan G (2020) Monitoring the impacts of a tailings dam failure using satellite images. *USSD 2020 Annual Conference*, pp 1–12
- Oдох B, Kenneth C, Kalu AU, Francis A (2017) Environmental impacts of mineral exploration in Nigeria and their phytoremediation strategies for sustainable ecosystem. Type: Double Blind Peer Rev Int Res J Publ: *Glob J Inc* 17(3).
- Oyedotun TDT (2020) Quantitative assessment of the drainage morphometric characteristics of Chaohu Lake Basin from SRTM DEM Data: a GIS-based approach. *Geol Ecol Landscapes*. <https://doi.org/10.1080/24749508.2020.1812147>
- Qu L, Chen Z, Li M, Zhi J, Wang H (2021) Accuracy improvements to pixel-based and object-based LULC classification with auxiliary datasets from google earth engine. *Remote Sens* 13(3):453. <https://doi.org/10.3390/rs13030453>
- Raeva PL, Filipova SL, Filipov DG (2016) Volume computation of a stockpile—a study case comparing GPS and uav measurements in an open pit quarry. *Int Arch Photogramm Remote Sens Spatial Inf Sci*. <https://doi.org/10.5194/isprsarchives-XLI-B1-999-2016>
- Rahman AAA, Maulud KNA, Mohd FA, Jaafar O, Tahar KN (2017) Volumetric calculation using low cost unmanned aerial vehicle (UAV) approach. *IOP Conf Ser*. <https://doi.org/10.1088/1757-899X/270/1/012032>

- Raju A (2020) Comparative study on methods of creating geodatabase using. 11(8):13–21. <https://doi.org/10.34218/IJARET.11.8.2020.003>
- Rwanga SS, Ndambuki JM (2017) Accuracy assessment of land use/land cover classification using remote sensing and GIS. *Int J Geosci* 08(04):611–622. <https://doi.org/10.4236/ijg.2017.84033>
- Sikaundi G (2015) Copper mining industry in Zambia. 1, 1–14. [https://unstats.un.org/unsd/environment/envpdf/UNSD_UNEP_ECA_Workshop/Session_08-5_Mining_in_Zambia_\(Zambia\).pdf](https://unstats.un.org/unsd/environment/envpdf/UNSD_UNEP_ECA_Workshop/Session_08-5_Mining_in_Zambia_(Zambia).pdf). Accessed 12 Jan 2021
- Tucci G, Gebbia A, Conti A, Fiorini L, Lubello C (2019) Monitoring and computation of the volumes of stockpiles of bulk material by means of UAV photogrammetric surveying. *Remote Sens.* <https://doi.org/10.3390/rs11121471>
- Verma P, Raghubanshi A, Srivastava PK, Raghubanshi AS (2020) Appraisal of kappa-based metrics and disagreement indices of accuracy assessment for parametric and nonparametric techniques used in LULC classification and change detection. *Model Earth Syst Environ* 6(2):1045–1059. <https://doi.org/10.1007/s40808-020-00740-x>
- Waweru M (2020) University of Nairobi Geological Setting and Mineralization of Iron Ore, Rare Earth Elements, and Associated Metals in Kithiori Area of Marimanti, Tharaka Nithi. The University of Nairobi.
- Werner TT, Bebbington A, Gregory G (2019) Assessing impacts of mining: recent contributions from GIS and remote sensing. *Extract Indus Soc* 6(3):993–1012. <https://doi.org/10.1016/j.exis.2019.06.011>

Publisher's Note Springer Nature remains neutral with regard to jurisdictional claims in published maps and institutional affiliations.

Terms and Conditions

Springer Nature journal content, brought to you courtesy of Springer Nature Customer Service Center GmbH (“Springer Nature”).

Springer Nature supports a reasonable amount of sharing of research papers by authors, subscribers and authorised users (“Users”), for small-scale personal, non-commercial use provided that all copyright, trade and service marks and other proprietary notices are maintained. By accessing, sharing, receiving or otherwise using the Springer Nature journal content you agree to these terms of use (“Terms”). For these purposes, Springer Nature considers academic use (by researchers and students) to be non-commercial.

These Terms are supplementary and will apply in addition to any applicable website terms and conditions, a relevant site licence or a personal subscription. These Terms will prevail over any conflict or ambiguity with regards to the relevant terms, a site licence or a personal subscription (to the extent of the conflict or ambiguity only). For Creative Commons-licensed articles, the terms of the Creative Commons license used will apply.

We collect and use personal data to provide access to the Springer Nature journal content. We may also use these personal data internally within ResearchGate and Springer Nature and as agreed share it, in an anonymised way, for purposes of tracking, analysis and reporting. We will not otherwise disclose your personal data outside the ResearchGate or the Springer Nature group of companies unless we have your permission as detailed in the Privacy Policy.

While Users may use the Springer Nature journal content for small scale, personal non-commercial use, it is important to note that Users may not:

1. use such content for the purpose of providing other users with access on a regular or large scale basis or as a means to circumvent access control;
2. use such content where to do so would be considered a criminal or statutory offence in any jurisdiction, or gives rise to civil liability, or is otherwise unlawful;
3. falsely or misleadingly imply or suggest endorsement, approval, sponsorship, or association unless explicitly agreed to by Springer Nature in writing;
4. use bots or other automated methods to access the content or redirect messages
5. override any security feature or exclusionary protocol; or
6. share the content in order to create substitute for Springer Nature products or services or a systematic database of Springer Nature journal content.

In line with the restriction against commercial use, Springer Nature does not permit the creation of a product or service that creates revenue, royalties, rent or income from our content or its inclusion as part of a paid for service or for other commercial gain. Springer Nature journal content cannot be used for inter-library loans and librarians may not upload Springer Nature journal content on a large scale into their, or any other, institutional repository.

These terms of use are reviewed regularly and may be amended at any time. Springer Nature is not obligated to publish any information or content on this website and may remove it or features or functionality at our sole discretion, at any time with or without notice. Springer Nature may revoke this licence to you at any time and remove access to any copies of the Springer Nature journal content which have been saved.

To the fullest extent permitted by law, Springer Nature makes no warranties, representations or guarantees to Users, either express or implied with respect to the Springer nature journal content and all parties disclaim and waive any implied warranties or warranties imposed by law, including merchantability or fitness for any particular purpose.

Please note that these rights do not automatically extend to content, data or other material published by Springer Nature that may be licensed from third parties.

If you would like to use or distribute our Springer Nature journal content to a wider audience or on a regular basis or in any other manner not expressly permitted by these Terms, please contact Springer Nature at

onlineservice@springernature.com

MAPPING AND CHARACTERIZATION OF SOLID IRON ORE MINING WASTES IN KISHUSHE AREA, TAITA TAVETA COUNTY, KENYA

ORIGINALITY REPORT

7%

SIMILARITY INDEX

5%

INTERNET SOURCES

3%

PUBLICATIONS

2%

STUDENT PAPERS

PRIMARY SOURCES

| | | |
|---|---|-----|
| 1 | erepository.uonbi.ac.ke:8080 Internet Source | 1% |
| 2 | etd.aau.edu.et Internet Source | 1% |
| 3 | "Mine Wastes", Springer Science and Business Media LLC, 2007 Publication | <1% |
| 4 | N. Haque, T. Norgate. "Life cycle assessment of iron ore mining and processing", Elsevier BV, 2015 Publication | <1% |
| 5 | Submitted to University of Alabama Student Paper | <1% |
| 6 | www.coursehero.com Internet Source | <1% |
| 7 | Mine Wastes, 2010. Publication | <1% |